1

Chemical Bonding and Molecular Structure

Introduction

In this chapter we consider *molecular structure* and the concepts of *chemical bonding* that are used to interpret molecular structure. We will also begin to see how information about molecular structure and ideas about bonds can be used to interpret and predict physical properties and chemical reactivity. *Structural formulas* are a key tool for describing both structure and reactivity. At a minimum, they indicate *molecular constitution* by specifying the *connectivity* among the atoms in the molecule. Structural formulas also give a rough indication of electron distribution by representing electron pairs in bonds by lines and unshared electrons as dots, although the latter are usually omitted in printed structures. The reader is undoubtedly familiar with structural formulas for molecules such as those shown in Scheme 1.1.

In quantitative terms, molecular structure specifies the relative position of all atoms in a molecule. These data provide the bond lengths and bond angles. There are a number of experimental means for precise determination of molecular structure, primarily based on spectroscopic and diffraction methods, and structural data are available for thousands of molecules. Structural information and interpretation is also provided by *computational chemistry*. In later sections of this chapter, we describe how molecular orbital theory and density functional theory can be applied to the calculation of molecular structure and properties.

The *distribution of electrons* is another element of molecular structure that is very important for understanding chemical reactivity. It is considerably more difficult to obtain experimental data on *electron density*, but fortunately, in recent years the rapid development of both structural theory and computational methods has allowed such calculations. We make use of computational electron density data in describing molecular structure, properties, and reactivity. In this chapter, we focus on the minimum energy structure of individual molecules. In Chapter 2, we consider other elements of molecular geometry, including dynamic processes involving *conformation*, that is, the variation of molecular shape as a result of bond rotation. In Chapter 3, we discuss

Scheme 1.1. Lewis Structures of Simple Molecules

Single Bonds

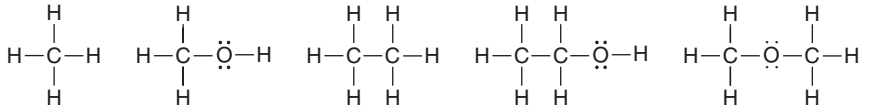

methane | methanol | ethane | ethanol | dimethyl ether

Double Bonds

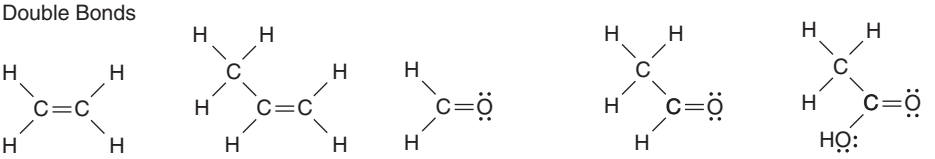

ethene (ethylene) | propene (propylene) | methanal (formaldehyde) | ethanal (acetaldehyde) | ethanoic acid (acetic acid)

Triple Bonds

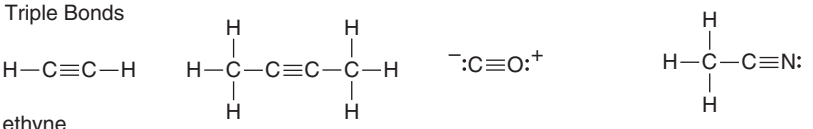

ethyne (acetylene) | 2-butyne | carbon monoxide | ethanecarbonitrile (acetonitrile)

how structure effects the energy of *transition structures* and *intermediates* in chemical reactions. The principal goal of this chapter is to discuss the concepts that chemists use to develop relationships between molecular structure and reactivity. These relationships have their foundation in the fundamental physical aspects of molecular structure, that is, nuclear position and electron density distribution. Structural concepts help us see, understand, and apply these relationships.

1.1. Description of Molecular Structure Using Valence Bond Concepts

Introductory courses in organic chemistry usually rely primarily on the valence bond description of molecular structure. Valence bond theory was the first structural theory applied to the empirical information about organic chemistry. During the second half of the nineteenth century, correct structural formulas were deduced for a wide variety of organic compounds. The concept of "valence" was recognized. That is, carbon almost always formed four bonds, nitrogen three, oxygen two, and the halogens one. From this information, chemists developed structural formulas such as those in Scheme 1.1. Kekule's structure for benzene, published in 1865, was a highlight of this period. The concept of *functional groups* was also developed. It was recognized that structural entities such as hydroxy (−OH), amino ($-NH_2$), carbonyl (C=O), and

carboxy (CO_2H) groups each had characteristic reactivity that was largely independent of the hydrocarbon portion of the molecule.

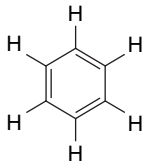

Kekule structure for benzene

These structural formulas were developed without detailed understanding of the nature of the *chemical bond* that is represented by the lines in the formulas. There was a key advance in the understanding of the origin of chemical bonds in 1916, when G.N. Lewis introduced the concept of electron-pair bonds and the "rule of 8" or *octet rule*, as we now know it. Lewis postulated that chemical bonds were the result of sharing of electron pairs by nuclei and that for the second-row atoms, boron through neon, the most stable structures have eight valence shell electrons.[1] Molecules with more than eight electrons at any atom are very unstable and usually dissociate, while those with fewer than eight electrons at any atom are usually highly reactive toward electron donors. The concept of bonds as electron pairs gave a fuller meaning to the traditional structural formulas, since the lines then specifically represent single, double, and triple bonds. The dots represent unshared electrons. Facility with Lewis structures as a tool for accounting for electrons, bonds, and charges is one of the fundamental skills developed in introductory organic chemistry.

Lewis structures, however, convey relatively little information about the details of molecular structure. We need other concepts to deduce information about relative atomic positions and, especially, electron distribution. *Valence bond theory* provides one approach to deeper understanding of molecular structure. Valence bond (VB) theory has its theoretical foundation in quantum mechanics calculations that demonstrated that electrons hold nuclei together, that is, form bonds, when shared by two nuclei. This fact was established in 1927 by calculations on the hydrogen molecule.[2] The results showed that an energy minimum occurs at a certain internuclear distance if the electrons are free to associate with either nucleus. Electron density accumulates between the two nuclei. This can be depicted as an electron density map for the hydrogen molecule, as shown in Figure 1.1a. The area of space occupied by electrons is referred to as an *orbital*. A fundamental concept of VB theory is that there is a concentration of electron density between atoms that are bonded to one another. Figure 1.1b shows that there is *electron density depletion* relative to spherical atoms outside of the hydrogen nuclei. Nonbonding electrons are also described by orbitals, which are typically more diffuse than bonding ones. The mathematical formulation of molecular structure by VB theory is also possible. Here, we emphasize qualitative concepts that provide insight into the relationship between molecular structure and properties and reactivity.

1. G. N. Lewis, *J. Am. Chem. Soc.*, **38**, 762 (1916).
2. W. Heitler and F. London, *Z. Phys.*, **44**, 455 (1927).

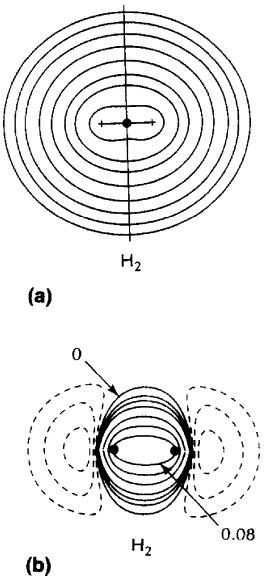

Fig. 1.1. Contour maps of (a) total electron density and (b) density difference relative to the spherical atoms for the H_2 molecule. Reproduced with permission from R. F. W. Bader, T. T. Nguyen, and Y. Tal, *Rep. Prog. Phys.*, **44**, 893 (1981).

1.1.1. Hybridization

Qualitative application of VB theory to molecules containing second-row elements such as carbon, nitrogen, and oxygen involves the concept of *hybridization*, which was developed by Linus Pauling.[3] The atomic orbitals of the second-row elements include the spherically symmetric 2*s* and the three 2*p* orbitals, which are oriented perpendicularly to one another. The combination of these atomic orbitals is equivalent to four sp^3 orbitals directed toward the corners of a tetrahedron. These are called *sp^3 hybrid orbitals*. In methane, for example, these orbitals overlap with hydrogen 1*s* orbitals to form σ bonds.

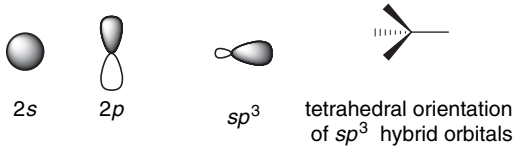

The valence bond description of methane, ammonia, and water predicts tetrahedral geometry. In methane, where the carbon valence is four, all the hybrid orbitals are involved in bonds to hydrogen. In ammonia and water, respectively, one and two nonbonding (unshared) pairs of electrons occupy the remaining orbitals. While methane

[3] L. Pauling, *J. Am. Chem. Soc.*, **53**, 1367 (1931).

is perfectly tetrahedral, the bond angles in ammonia and water are somewhat reduced. This suggests that the electron-electron repulsions between unshared pairs are greater than for electrons in bonds to hydrogen. In other words, the unshared pairs occupy somewhat larger orbitals. This is reasonable, since these electrons are not attracted by hydrogen nuclei.

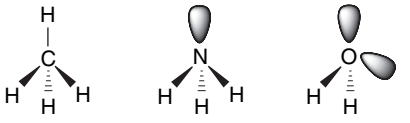

The hybridization concept can be readily applied to molecules with double and triple bonds, such as those shown in Scheme 1.1. Second-row elements are described as having sp^2 or sp orbitals, resulting from hybridization of the s orbital with two or one p orbitals, respectively. The double and triple bonds are conceived as arising from the overlap of the unhybridized p orbitals on adjacent atoms. These bonds have a nodal plane and are called π bonds. Because the overlap is not as effective as for sp^3 orbitals, these bonds are somewhat weaker than σ bonds.


trigonal orientation
of sp^2 hybrid orbitals


digonal orientation
of *sp* hybrid orbitals

The prototypical hydrocarbon examples of sp^2 and sp hybridization are ethene and ethyne, respectively. The total electron density between the carbon atoms in these molecules is the sum from the π and σ bonds. For ethene, the electron density is somewhat elliptical, because the π component is not cylindrically symmetrical. For ethyne, the combination of the two π bonds restores cylindrical symmetry. The electron density contours for ethene are depicted in Figure 1.2, which shows the highest density near the nuclei, but with net accumulation of electron density between the carbon and hydrogen atoms.

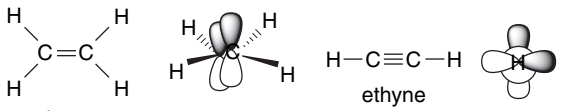

The hybridization concept also encompasses empty antibonding orbitals, which are designated by an asterisk (*). These orbitals have nodes between the bound atoms. As discussed in Section 1.1.8, σ^* and π^* orbitals can interact with filled orbitals and contribute to the ground state structure of the molecule. These empty orbitals are also

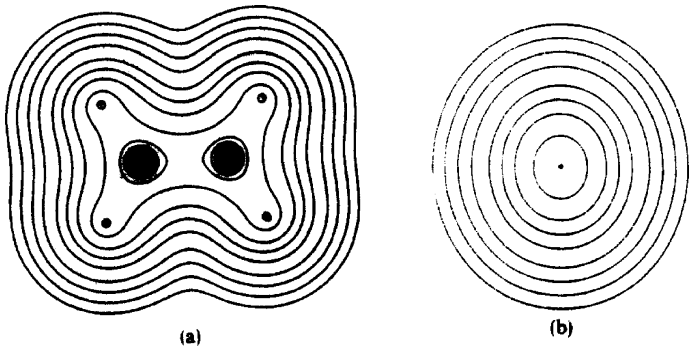

Fig. 1.2. (a) Contour map of electron density in the plane of the ethene molecule. (b) Contour map of electron density perpendicular to the plane of the ethene molecule at the midpoint of the C=C bond. Reproduced with permission from R. F. W. Bader, T. T. Nguyen-Dang, and Y. Tal, *Rep. Prog. Phys.*, **44**, 893 (1981).

of importance in terms of reactivity, particularly with electron-donating *nucleophilic* reagents, since it is the empty antibonding orbitals that interact most strongly with approaching nucleophiles.

The hybridization concept indicates some additional aspects of molecular structure. The tetrahedral, trigonal, and digonal natures of sp^3, sp^2, and *sp* carbon atoms provide an approximation of bond angles. The idea that π bonds are formed by the overlap of *p* orbitals puts some geometrical constraints on structure. Ethene, for example, is planar to maximize *p*-orbital overlap. Allene, on the other hand, must have the terminal CH_2 groups rotated by 90° to accommodate two π bonds at the central *sp* carbon.

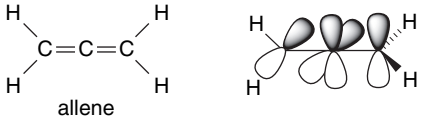

It is important to remember that hybridization is a *description* of the observed molecular geometry and electron density. Hybridization does not *cause* a molecule to have a particular shape. Rather, the molecule adopts a particular shape because it maximizes bonding interactions and minimizes electron-electron and other repulsive interactions. We use the hybridization concept to recognize similarities in structure that have their origin in fundamental forces within the molecules. The concept of hybridization helps us to see how molecular structure is influenced by the number of ligands and electrons at a particular atom.

It is worth noting at this point that a particular hybridization scheme *does not provide a unique description of molecular structure*. The same fundamental conclusions about geometry and electron density are reached if ethene and ethyne are described in terms of sp^3 hybridization. In this approach, the double bond in ethene is thought of as arising from two overlapping sp^3 orbitals. The two bonds are equivalent and are called *bent bonds*. This bonding arrangement also predicts a planar geometry and elliptical electron distribution, and in fact, this description is mathematically equivalent to the sp^2 hybridization description. Similarly, ethyne can be thought of as arising by the sharing of three sp^3 hybrid orbitals. The fundamental point is that there is a single real molecular structure defined by atomic positions and electron density. Orbitals partition the electron density in specific ways, and it is the *sum of the orbital contributions that describes the structure*.

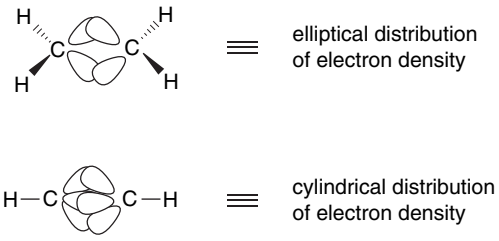

1.1.2. The Origin of Electron-Electron Repulsion

We have already assumed that electron pairs, whether in bonds or as nonbonding pairs, repel other electron pairs. This is manifested in the tetrahedral and trigonal geometry of tetravalent and trivalent carbon compounds. These geometries correspond to maximum separation of the electron-pair bonds. Part of this repulsion is electrostatic, but there is another important factor. The *Pauli exclusion principle* states that only two electrons can occupy the same point in space and that they must have opposite spin quantum numbers. Equivalent orbitals therefore maintain maximum separation, as found in the sp^3, sp^2, and sp hybridization for tetra-, tri-, and divalent compounds of the second-row elements. The combination of Pauli exclusion and electrostatic repulsion leads to the *valence shell electron-pair repulsion rule* (VSEPR), which states that bonds and unshared electron pairs assume the orientation that permits maximum separation.

An important illustration of the importance of the Pauli exclusion principle is seen in the O_2 molecule. If we were to describe O_2 using either the sp^2 hybridization or bent bond model, we would expect a double bond with all the electrons paired. In fact, O_2 is *paramagnetic*, with two unpaired electrons, and yet it does have a double bond. If we ask how electrons would be distributed to maintain maximum separation, we arrive at two tetrahedral arrays, with the tetrahedra offset by the maximum amount.[4] Electronic spin can be represented as x and o. The structure still has four bonding electrons between the oxygen atoms, that is, a double bond. It also obeys the octet rule for each oxygen and correctly predicts that two of the electrons are unpaired.

[4.] J. W. Linnett, *The Electronic Structure of Molecules*, Methren Co. LTD, London, 1964, pp. 37–42; R. J. Gillespie and P. L. A. Popelier, *Chemical Bonding and Molecular Geometry*, Oxford University Press, New York, 2001, pp 102–103.

This structure minimizes electron-electron repulsions and obeys the Pauli principle by maximizing the separation of electrons having the same spin.

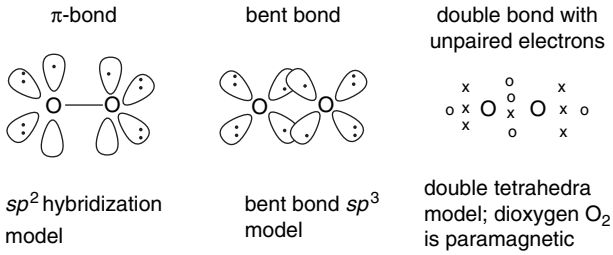

A similar representation of N_2 with offset of the tetrahedral of electrons correctly describes the molecule as having a triple bond, but it is diamagnetic, since there are equal numbers of electrons of each spin. For ethane, all the electrons are bonding and are attracted toward the hydrogen nuclei, and the tetrahedra of electrons of opposite spin both occupy a region of space directed toward a hydrogen nucleus.

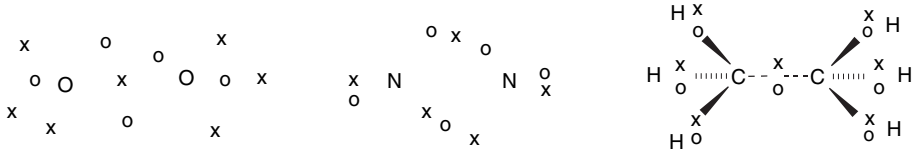

For most of the molecules and reactions we want to consider, the Pauling hybridization scheme provides an effective structural framework, and we use VB theory to describe most of the reactions and properties of organic compounds. However, we have to keep in mind that it is *neither a unique nor a complete description of electron density*, and we will find cases where we need to invoke additional ideas. In particular, we discuss *molecular orbital theory* and *density functional theory*, which are other ways of describing molecular structure and electron distribution.

1.1.3. Electronegativity and Polarity

The VB concept of electron-pair bonds recognizes that the sharing of electrons by the nuclei of two different elements is unequal. Pauling defined the concept of unequal sharing in terms of *electronegativity*,[5] defining the term as "the power of an atom in a molecule to attract electrons to itself." Electronegativity depends on the number of protons in the nucleus and is therefore closely associated with position in the periodic table. The metals on the left of the periodic table are the least electronegative elements, whereas the halogens on the right have the highest electronegativity in each row. Electronegativity decreases going down the periodic table for both metals and nonmetals.

The physical origin of these electronegativity trends is *nuclear screening*. As the atomic number increases from lithium to fluorine, the nuclear charge increases, as does

[5] L. Pauling, *J. Am. Chem. Soc.*, **54**, 3570 (1932).

the number of electrons. Each successive electron "feels" a larger nuclear charge. This charge is partially screened by the additional electron density as the shell is filled. However, the screening, on average, is less effective for each electron that is added. As a result, an electron in fluorine is subject to a greater effective nuclear charge than one in an atom on the left in the periodic table. As each successive shell is filled, the electrons in the valence shell "feel" the effective nuclear charge as screened by the filled inner shells. This screening is more effective as successive shells are filled and the outer valence shell electrons are held less tightly going down the periodic table. As we discuss later, the "size" of an atom also changes in response to the nuclear charge. Going across the periodic table in any row, the atoms become *smaller* as the shell is filled because of the higher effective nuclear charge. Pauling devised a numerical scale for electronegativity, based on empirical interpretation of energies of bonds and relating specifically to electron sharing in covalent bonds, that has remained in use for many years. Several approaches have been designed to define electronegativity in terms of other atomic properties. Allred and Rochow defined electronegativity in terms of the electrostatic attraction by the effective nuclear charge Z_{eff}[6]:

$$\chi_{\text{AR}} = \frac{0.3590 Z_{\text{eff}}}{r^2} + 0.744 \tag{1.1}$$

where r is the covalent radius in Å. This definition is based on the concept of nuclear screening described above. Another definition of electronegativity is based explicitly on the relation between the number of valence shell electrons, n, and the effective atomic radius r:[7]

$$V = n/r \tag{1.2}$$

As we will see shortly, covalent and atomic radii are not absolutely measurable quantities and require definition.

Mulliken found that there is a relationship between *ionization potential* (IP) and *electron affinity* (EA) and defined electronegativity χ as the average of those terms:[8]

$$\chi_{\text{abs}} = \frac{\text{IP} + \text{EA}}{2} \tag{1.3}$$

This formulation, which turns out to have a theoretical justification in density functional theory, is sometimes referred to as *absolute electronegativity* and is expressed in units of eV.

A more recent formulation of electronegativity, derived from the basic principles of atomic structure, has led to a *spectroscopic scale for electronegativity*.[9] In this formulation, the electronegativity is defined as the average energy of a valence electron in an atom. The lower the average energy, the greater the electron-attracting power (electronegativity) of the atom. The formulation is

$$\chi_{\text{spec}} = \frac{(a\text{IP}_s + b\text{IP}_p)}{a + b} \tag{1.4}$$

6. A. L. Allred and E. G. Rochow, *J. Inorg. Nucl. Chem.*, **5**, 264 (1958).
7. Y.-R. Luo and S. W. Benson, *Acc. Chem. Res.*, **25**, 375 (1992).
8. R. S. Mulliken, *J. Chem. Phys.*, **2**, 782 (1934); R. S. Mulliken, *J. Chem. Phys.*, **3**, 573 (1935).
9. L. C. Allen, *J. Am. Chem. Soc.*, **111**, 9003 (1989); L. C. Allen, *Int. J. Quantum Chem.*, **49**, 253 (1994); J. B. Mann, T. L. Meek, and L. C. Allen, *J. Am. Chem. Soc.*, **122**, 2780 (2000).

where IP_s and IP_p are the ionization potentials of the *s* and *p* electrons and *a* and *b* are the number of *s* and *p* electrons, respectively.

The values on this scale correlate well with the Pauling and Allred-Rochow scales. One feature of this scale is that the IP values can be measured accurately so that electronegativity becomes an *experimentally measured* quantity. When the same concepts are applied to atoms in molecules, the atom undergoes an electronegativity adjustment that can be related to the energy of its orbitals (as expressed by molecular orbital theory). The average adjusted energy of an electron is called the *energy index* (EI). The EI values of two bound atoms provide a measure of bond polarity called the *bond polarity index*[10] (BPI), formulated as

$$\mathrm{BPI_{AB}} = (\mathrm{EI_A} - \mathrm{EI_A}^{\mathrm{ref}}) - (\mathrm{EI_B} - \mathrm{EI_B}^{\mathrm{ref}}) \tag{1.5}$$

where $\mathrm{EI}^{\mathrm{ref}}$ are parameters of A−A and B−B bonds.

These approaches, along with several others, give electronegativity scales that are in good relative agreement in assessing the electron-attracting power of the elements. Each scale is based on fundamental atomic properties. However, they are in different units and therefore not directly comparable. Table 1.1 gives the values assigned by some of the electronegativity scales. The numerical values are scaled to the original Pauling range. At this point, we wish to emphasize the broad consistency of the values, not the differences. We use the *order of the electronegativity of the elements* in a qualitative way, primarily when discussing *bond polarity*. It should be noted, however, that the concept of electronegativity has evolved from an empirical scale to one with specific physical meaning. We pursue the relationship between these scales further in Topic 1.5.3.

The most obvious consequence of differential electronegativity is that covalent bonds between different elements are *polar*. Each atom bears a partial charge reflecting the relative electronegativity of the two elements sharing the bond. These charges can be estimated, and the values found for BF_3, CF_4, and NF_3 are shown below.[11] Note that the negative charge on fluorine becomes smaller as the electronegativity of the central atom increases.

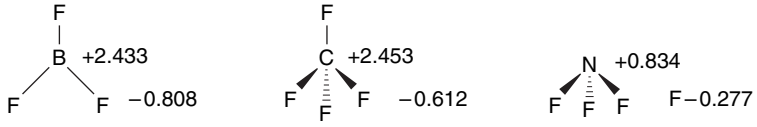

The individual polar bonds contribute to the polarity of the overall molecule. The overall molecular polarity is expressed as the dipole moment. For the three molecules shown, the overall molecular dipole moment is 0 for BF_3 (planar) and CF_4 (tetrahedral), because of the symmetry of the molecules, but NF_3 has a dipole moment of 0.235 D, since the molecule is pyramidal.[12]

[10] L. C. Allen, D. A. Egolf, E. T. Knight, and C. Liang, *J. Phys. Chem.*, **94**, 5603 (1990); L. C. Allen, *Can. J. Chem.*, **70**, 631 (1992).

[11] R. J. Gillespie and P. L. A. Popelier, *Chemical Bonding and Molecular Geometry*, Oxford University Press, New York, 2001, p. 47.

[12] Dipole moments are frequently expressed in Debye (D) units; $1\,\mathrm{D} = 3.335641 \times 10^{-30}\,\mathrm{C\ m}$ in SI units.

Table 1.1. Electronegativity Scales[a]

Atom	Original Pauling[b]	Modified Pauling[c]	Allred-Rochow[d]	Luo-Benson[e]	Mulliken[f]	Allen[g]
H	2.1	2.20	2.20		2.17	2.30
Li	1.0	0.98	0.97	0.93	0.91	0.91
Be	1.5	1.57	1.47	1.39	1.45	1.58
B	2.0	2.04	2.01	1.93	1.88	2.05
C	2.5	2.55	2.50	2.45	2.45	2.54
N	3.0	3.04	3.07	2.96	2.93	3.07
O	3.5	3.44	3.50	3.45	3.61	3.61
F	4.0	3.98	4.10	4.07	4.14	4.19
Na	0.9	0.93	1.01	0.90	0.86	0.87
Mg	1.2	1.31	1.23	1.20	1.21	1.29
Al	1.5	1.61	1.47	1.50	1.62	1.61
Si	1.8	1.90	1.74	1.84	2.12	1.92
P	2.1	2.19	2.06	2.23	2.46	2.25
S	2.5	2.58	2.44	2.65	2.64	2.59
Cl	3.0	3.16	2.83	3.09	3.05	2.87
Ge	1.8	2.01	2.02	1.79	2.14	1.99
As	2.0	2.18	2.20	2.11	2.25	2.21
Se	2.4	2.55	2.48	2.43	2.46	2.42
Br	2.8	2.96	2.74	2.77	2.83	2.69
Sn	1.8	1.96	1.72	1.64	2.12	1.82
I	2.5	2.66	2.21	2.47	2.57	2.36

a. All numerical values are scaled to the original Pauling scale.
b. L. Pauling, *The Nature of the Chemical Bond*, 3rd Edition, Cornell University Press, Ithaca, NY, 1960.
c. A. L. Allred , *J. Inorg. Nucl. Chem.*, **17**, 215 (1961).
d. A. L. Allred and E.G. Rochow, *J. Inorg. Nucl. Chem.*, **5**, 264 (1958).
e. Y. R. Luo and S.W. Benson, *Acc. Chem. Res.*, **25**, 375 (1992).
f. D. Bergman and J. Hinze, *Angew. Chem. Int. Ed. Engl.*, **35**, 150 (1996).
g. L. C. Allen, *Int. J. Quantum Chem.*, **49**, 253 (1994).

1.1.4. Electronegativity Equalization

The concept of *electronegativity equalization* was introduced by R. T. Sanderson.[13] The idea is implicit in the concept of a molecule as consisting of nuclei embedded in an electronic cloud and leads to the conclusion that the electron density will reach an equilibrium state in which there is no net force on the electrons. The idea of electronegativity equalization finds a theoretical foundation in *density functional theory* (see Section 1.3). Several numerical schemes have been developed for the assignment of charges based on the idea that electronegativity equalization must be achieved. Sanderson's initial approach averaged all atoms of a single element, e.g., carbon, in a molecule and did not distinguish among them. This limitation was addressed by Hercules and co-workers,[14] who assigned electronegativity values called SR′ values to specific groups within a molecule. For example, the methyl and ethyl groups, respectively, were derived from the number of C and H atoms in the group:

$$SR'_{CH3} = (SR_C \times SR_H{}^3)^{1/4} \tag{1.6}$$

$$SR'_{C2H5} = [(SR_C \times SR_H{}^2)(SR_C \times SR_H{}^3)^{1/4}]^{1/4} \tag{1.7}$$

13. R. T. Sanderson, *Chemical Bonds and Bond Energies*, Academic Press, New York, 1976; R. T. Sanderson, *Polar Covalence*, Academic Press, New York, 1983.
14. J. C. Carver, R. C. Gray, and D. M. Hercules, *J. Am. Chem. Soc.*, **96**, 6851 (1974).

This approach was extended by M. Sastry to a variety of organic compounds.[15] For example, the charges calculated for the carbon atoms in $CF_3CO_2C_2H_5$ are as shown below. We see that the carbon of the methyl group carries a small negative charge, whereas the carbons bound to more electronegative elements are positive.

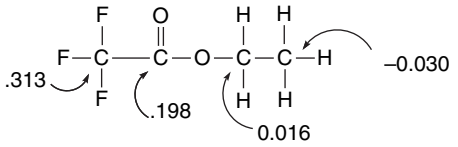

The calculated charge on carbon for a number of organic molecules showed good correlation with the core atomic binding energies, as measured by X-ray photoemission spectroscopy. We discuss other methods of assigning charges to atoms based on computational chemistry in Section 1.4. We also find that all these methods are in some sense arbitrary divisions of molecules. The concept of electronegativity equalization is important, however. It tells us that electron density shifts in response to bonding between atoms of different electronegativity. This is the basis of *polar substituent effects*. Furthermore, as the data above for ethyl trifluoroacetate suggest, a highly electronegative substituent induces a net positive charge on carbon, as in the CF_3 and C=O carbons in ethyl trifluoroacetate. Electronegativity differences are the origin of *polar bonds*, but electronegativity equalization suggests that there will also be an *inductive effect*, that is, the propagation of changes in electron distribution to adjacent atoms.

1.1.5. Differential Electronegativity of Carbon Atoms

Although carbon is assigned a single numerical value in the Pauling electronegativity scale, its effective electronegativity depends on its hybridization. The qualitative relationship is that carbon electronegativity toward other bound atoms increases with the extent of *s* character in the bond, i.e., $sp^3 < sp^2 < sp$. Based on the atomic radii approach, the carbon atoms in methane, benzene, ethene, and ethyne have electronegativity in the ratio 1:1.08:1.15:1.28. A scale based on bond polarity measures gives values of 2.14, 2.34, and 2.52 for sp^3, sp^2, and *sp* carbons, respectively.[16] A scale based on NMR coupling constants gives values of 1.07 for methyl, 1.61 for ethenyl, and 3.37 for ethynyl.[17] If we use the density functional theory definition of electronegativity (see Topic 1.5.1) the values assigned to methyl, ethyl, ethenyl, and ethynyl are 5.12, 4.42, 5.18, and 8.21, respectively.[18] Note that by this measure methyl is significantly more electronegative than ethyl. With an *atoms in molecules* approach (see Section 1.4.3), the numbers assigned are methyl 6.84; ethenyl 7.10, and ethynyl 8.23.[19] Table 1.2 converts each of these scales to a relative scale with methyl equal to 1. Note that the various definitions *do not* reach a numerical consensus on the relative electronegativity of sp^3, sp^2, and *sp* carbon, although the order is consistent. We are

15. M. Sastry, *J. Electron Spectros.*, **85**, 167 (1997).
16. N. Inamoto and S. Masuda, *Chem. Lett.*, 1003, 1007 (1982).
17. S. Marriott, W. F. Reynolds, R. W. Taft, and R. D. Topsom, *J. Org. Chem.*, **49**, 959 (1984).
18. F. De Proft, W. Langenaeker, and P. Geerlings, *J. Phys. Chem.*, **97**, 1826, (1995).
19. S. Hati and D. Datta, *J. Comput. Chem.*, **13**, 912 (1992).

Table 1.2. Ratio of Electronegativity for Carbon of Different Hybridization

Comparison	Methyl	Ethenyl	Ethynyl
Atomic radii	1.0	1.15	1.28
Bond polarity	1.0	1.09	1.18
NMR coupling	1.0	1.50	3.15
Density function theory	1.0	1.01	1.60
Atoms in molecules	1.0	1.04	1.20

not so concerned with the precise number, but rather with the trend of increasing electronegativity $sp^3 < sp^2 < sp$. It is also important to note that the range of carbon electronegativities is close to that of hydrogen. While sp^3 carbon and hydrogen are similar in electronegativity, sp^2 and sp carbon are more electronegative than hydrogen.

If we compare the pK_a values of propanoic acid (4.87), propenoic acid (4.25), and propynoic acid (1.84), we get some indication that the hybridization of carbon does exert a substantial polar effect. The acidity increases with the electronegativity of the carbon group.

$$CH_3CH_2CO_2H \qquad CH_2{=}CHCO_2H \qquad HC{\equiv}CCO_2H$$

Orbitals of different hybridization on the same carbon are also thought of as having different electronegativities. For example, in strained hydrocarbons such as cyclopropane the C–H bonds are more acidic than normal. This is attributed to the additional *s* character of the C–H bonds, which compensates for the added *p* character of the strained C–C bonds.[20]

It is also possible to assign electronegativity values to groups. For alkyl groups the numbers are: CH_3, 2.52; C_2H_5, 2.46; $(CH_3)_2CH$, 2.41; $(CH_3)_3C$, 2.38; C_6H_5, 2.55, $CH_2{=}CH$, 2.55; $HC{\equiv}C$, 2.79.[21] The order is in accord with the general trend that *more-substituted alkyl groups are slightly better electron donors than methyl groups*. The increased electronegativity of sp^2 and sp carbons is also evident. These values are based on bond energy data by a relationship first explored by Pauling and subsequently developed by many other investigators. The original Pauling expression is

$$D[A-B] = 1/2(D[A-A] + D[B-B]) + 23(\Delta\chi)^2 \tag{1.8}$$

where $\Delta\chi$ is the difference in electronegativity of A and B.

Thus the bond strength (in kcal/mol) can be approximated as the average of the two corresponding homonuclear bonds and an increment that increases with the difference in electronegativity. For any bond, application of this equation suggests a "covalent" and "polar" term. The results for the series CH_3F, CH_3OH, CH_3NH_2, and CH_3CH_3 is shown below.

[20] J. N. Shoolery, *J. Chem. Phys.*, **31**, 1427 (1959); N. Muller and D. E. Pritchard, *J. Chem. Phys.*, **31**, 1471 (1959); K. B. Wiberg, R. F. W. Bader, and C. D. H. Lau, *J. Am. Chem. Soc.*, **109**, 1001 (1987).

[21] N. Matsunaga, D. W. Rogers, and A. A. Zavitsas, *J. Org.,Chem.*, **68**, 3158 (2003).

	D(A – A)	χ	$(\Delta\chi)^2$	Covalent	Polar	% Covalent	% Polar
CH_3	89.8	2.525					
–F	38.0	3.938	1.189	63.90	27.35	70	30
–OH	56.1	3.500	0.987	72.95	22.70	76	24
$-NH_2$	61.1	3.071	0.749	75.45	17.23	81	19
$-CH_3$	89.8	2.525	0.000	89.8	0.0	100	0

An important qualitative result emerges from these numbers. *Bond strength is increased by electronegativity differences*. This is illustrated, for example, by the strength of the bonds of fluorine with the other second-row elements.

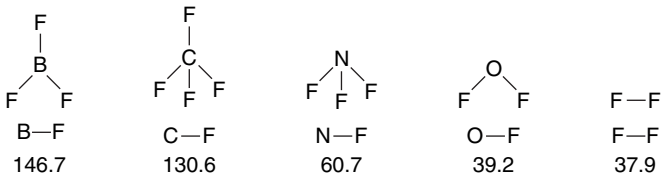

1.1.6. Polarizability, Hardness, and Softness

The interaction of valence shell electrons with the nucleus and intervening filled shells also affects the *polarizability* of the valence shell electrons. Polarizability can be described in terms of *hardness* and *softness*. A relatively large atom or ion with a small effective nuclear charge is relatively easily distorted (polarized) by an external charge and is called *soft*. A more compact electron distribution resulting from a higher net nuclear charge and less effective screening is called *hard*. The hard-soft-acid-base (HSAB) theory of stability and reactivity, introduced by Pearson,[22] has been extensively applied to qualitative reactivity trends,[23] and has been theoretically justified.[24] The qualitative expression of HSAB is that hard-hard and soft-soft reaction partners are preferred to hard-soft combinations. As for electronegativity, numerical scales of hardness and softness have been devised. One definition, like the Mulliken definition of absolute electronegativity, is based on ionization potential and electron affinity:

$$\text{Hardness} = \eta = \tfrac{1}{2}(\text{IP} - \text{EA}) \quad \text{and} \quad \text{Softness} = \sigma = 1/\eta \sim 2(\text{IP} - \text{EA}) \qquad (1.9)$$

Hardness increases with electronegativity and with positive charge. Thus, for the halogens the order is $F^- > Cl^- > Br^- > I^-$, and for second-row anions, $F^- > HO^- > H_2N^- > H_3C^-$. For cations, hardness decreases with size and increases with positive charge, so that $H^+ > Li^+ > Na^+ > K^+$. The proton, lacking any electrons, is infinitely hard. In solution it does not exist as an independent entity but contributes to the hardness of some protonated species. Metal ion hardness increases with oxidation state as the electron cloud contracts with the removal of each successive electron. All these as

[22] R. G. Pearson and J. Songstad, *J. Am. Chem. Soc.*, **89**, 1827 (1967); R. G. Pearson, *J. Chem. Educ.*, **45**, 581, 643 (1968).

[23] R. G. Pearson, *Inorg. Chim. Acta*, **240**, 93 (1995).

[24] P. K. Chattaraj, H. Lee, and R. G. Parr, *J. Am. Chem. Soc.*, **113**, 1855 (1991).

well as other hardness/softness relationships are consistent with the idea that hardness and softness are manifestations of the influence of nuclear charge on polarizability.

For polyatomic molecules and ions, hardness and softness are closely related to the HOMO and LUMO energies, which are analogous to the IP and EA values for atoms. The larger the HOMO-LUMO gap, the greater the hardness. Numerically, hardness is approximately equal to half the energy gap, as defined above for atoms. In general, chemical reactivity increases as LUMO energies are lower and HOMO energies are higher. The implication is that softer chemical species, those with smaller HOMO-LUMO gaps, tend to be more reactive than harder ones. In qualitative terms, this can be described as the ability of nucleophiles or bases to donate electrons more readily to electrophiles or acids and begin the process of bond formation. Interactions between harder chemical entities are more likely to be dominated by electrostatic interactions. Table 1.3 gives hardness values for some atoms and small molecules and ions. Note some of the trends for cations and anions. The smaller Li^+, Mg^{2+}, and Na^+ ions are harder than the heavier ions such as Cu^+, Hg^{2+}, and Pd^{2+}. The hydride ion is quite hard, second only to fluoride. The increasing hardness in the series $CH_3^- < NH_2^- < OH^- < F^-$ is of considerable importance and, in particular, correlates with nucleophilicity, which is in the order $CH_3^- > NH_2^- > OH^- > F^-$.

Figure 1.3 shows the IP-EA gap (2η) for several neutral atoms and radicals. Note that there is a correlation with electronegativity and position in the periodic table. The halogen anions and radicals become progressively softer from fluorine to iodine. Across the second row, softness decreases from carbon to fluorine. The cyanide ion is a relatively soft species.

The HSAB theory provides a useful precept for understanding Lewis acid-base interactions in that hard acids prefer hard bases and soft acids prefer soft bases. The principle can be applied to chemical equilibria in the form of the *principle of maximum hardness*,[25] which states that "molecules arrange themselves so as to

Table 1.3. Hardness of Some Atoms, Acids, and Bases[a]

Atom	η	Cations	η	Anions	η
H	6.4	H^+		H^-	6.8
Li	2.4	Li^+	35.1	F^-	7.0
C	5.0	Mg^{2+}	32.5	Cl^-	4.7
N	7.3	Na^+	21.1	Br^-	4.2
O	6.1	Ca^{2+}	19.7	I^-	3.7
F	7.0	Al^{3+}	45.8	CH_3^-	4.0
Na	2.3	Cu^+	6.3	NH_2^-	5.3
Si	3.4	Cu^{2+}	8.3	OH^-	5.6
P	4.9	Fe^{2+}	7.3	SH^-	4.1
S	4.1	Fe^{3+}	13.1	CN^-	5.3
Cl	4.7	Hg^{2+}	7.7		
		Pb^{2+}	8.5		
		Pd^{2+}	6.8		

a. From R. G. Parr and R. G. Pearson, *J. Am. Chem. Soc.*, **105**, 7512 (1983).

25. R. G. Pearson, *Acc. Chem. Res.*, **26**, 250 (1993); R. G. Parr and Z. Zhou, *Acc. Chem. Res.*, **26**, 256 (1993); R. G. Pearson, *J. Org. Chem.*, **54**, 1423 (1989); R. G. Parr and J. L. Gazquez, *J. Phys. Chem.*, **97**, 3939 (1993).

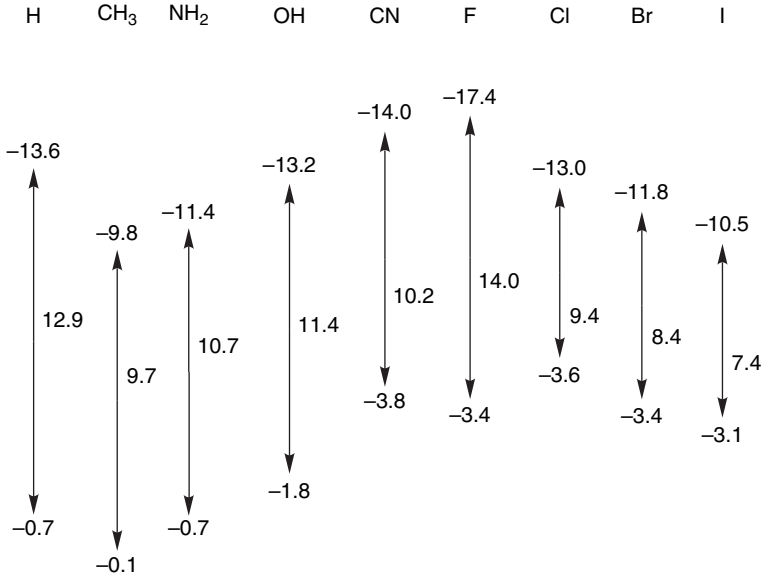

Fig. 1.3. Ionization (IP) and electron affinity (EA) gaps in eV for neutral atoms and radicals. Adapted from R. G. Pearson, *J. Am. Chem. Soc.*, **110**, 7684 (1988).

be as hard as possible." Expressed in terms of reaction energetics, ΔE is usually negative for

$$\mathrm{h{-}s + h{-}s \leftrightharpoons h{-}h + s{-}s}$$

The hard-hard interactions are dominated by electrostatic attraction, whereas soft-soft interactions are dominated by mutual polarization.[26] Electronegativity and hardness determine the extent of electron transfer between two molecular fragments in a reaction. This can be approximated numerically by the expression

$$\Delta N = \frac{\chi_x - \chi_y}{2(\eta_x + \eta_y)} \tag{1.10}$$

where χ is absolute electronegativity and η is hardness for the reacting species. For example, we can calculate the degree of electron transfer for each of the four halogen atoms reacting with the methyl radical to form the corresponding methyl halide.

$$\mathrm{X\cdot + CH_3\cdot \rightarrow CH_3X}$$

X·	χ_x	η_x	ΔN	η_{CH3X}
F·	10.4	7.0	0.23	9.4
Cl·	8.3	4.7	0.17	7.5
Br·	7.6	4.2	0.14	5.8
I·	6.8	3.7	0.10	4.7

[26] R. G. Pearson, *J. Am. Chem. Soc.*, **85**, 3533 (l963); T. L. Ho, *Hard and Soft Acids and Bases in Organic Chemistry*, Academic Press, New York, 1977; W. B. Jensen, *The Lewis Acid-Base Concept*, Wiley-Interscience, New York, 1980, Chap. 8.

According to this analysis, the C−X bond is successively both more polar and harder in the order I < Br < Cl < F. This result is in agreement with both the properties and reactivities of the methyl halides. When bonds are compared, reacting pairs of greater hardness result in a larger net charge transfer, which adds an increment to the exothermicity of bond formation. That is, bonds formed between two hard atoms or groups are stronger than those between two soft atoms or groups.[27] This is an example of a general relationship that recognizes that there is an increment to bond strength resulting from added ionic character.[28]

Polarizability measures the response of an ion or molecule to an electric field and is expressed in units of volume, typically 10^{-24} cm^3 or Å^3. Polarizability increases with atomic or ionic radius; it depends on the effectiveness of nuclear screening and increases as each valence shell is filled. Table 1.4 gives the polarizability values for the second-row atoms and some ions, molecules, and hydrocarbons. Methane is the least polarizable hydrocarbon and polarity increases with size. Polarizability is also affected by hybridization, with ethane > ethene > ethyne and propane > propene > propyne.

It should be noted that polarizability is *directional*, as illustrated in Scheme 1.2 for the methyl halides and halogenated benzenes.

Polarizability is related to the *refractive index* (n) of organic molecules, which was one of the first physical properties to be carefully studied and related to molecular structure.[29] As early as the 1880s, it was recognized that the value of the refractive index can be calculated as the sum of atomic components. Values for various groups were established and revised.[30] It was noted that some compounds, in particular compounds with conjugated bonds, had higher ("exalted") polarizability. Polarizability is also directly related to the dipole moment *induced by an electric field*. The greater the polarizability of a molecule, the larger the induced dipole.

Table 1.4. Polarizability of Some Atoms, Ions, and Molecules[a]

Atoms		Ions		Molecules		Hydrocarbons	
H	0.67			H_2O	1.45	CH_4	2.59
Li	24.3			N_2	1.74	C_2H_6	4.47
Be	5.6			CO	1.95	$CH_2{=}CH_2$	4.25
B	3.0			NH_3	2.81	HC≡CH	3.93
C	1.8			CO_2	2.91	C_3H_8	6.29
N	1.1			BF_3	3.31	$CH_3CH{=}CH_2$	6.26
O	0.8					$CH_3C{\equiv}CH$	6.18
F	0.06	F^-	1.2			n-C_4H_{10}	8.20
Ne	1.4	Na^+	0.9			i-C_4H_{10}	8.14
Cl	2.2	Cl^-	3			n-C_5H_{12}	9.99
Ar	3.6	K^+	2.3			Neopentane	10.20
Br	3.1	Br^-	4.5			n-C_6H_{14}	11.9
Kr	4.8					Cyclohexane	10.9
I	5.3	I^-	7			C_6H_6	10.3
Xe	6.9						

a. T. M. Miller, in *Handbook of Chemistry and Physics*, 83rd Edition, pp. 10-163–10-177, 2002.
b. A. Dalgano, *Adv. Phys.*, **11**, 281 (1962), as quoted by R. J. W. Le Fevre, *Adv. Phys. Org. Chem.*, **3**, 1 (1965).

27. P. K. Chattaraj, A. Cedillo, R. G. Parr, and E.M. Arnett, *J. Org. Chem.*, **60**, 4707 (1995).
28. P. R. Reddy, T. V. R. Rao, and R. Viswanath, *J. Am. Chem. Soc.*, **111**, 2914 (1989).
29. R. J. W. Le Fevre, *Adv. Phys. Org. Chem.*, **3**, 1 (1965).
30. K. von Auwers, *Chem. Ber.*, **68**, 1635 (1935); A. I. Vogel, *J. Chem. Soc.*, 1842 (1948); J. W. Brühl, *Liebigs Ann.Chem.*, **235**, 1 (1986); J. W. Brühl, *Liebigs Ann.Chem.*, **236**, 233 (1986).

Scheme 1.2. Molecular Polarizability[a]

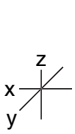

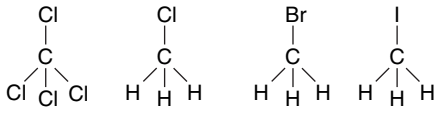

	CCl_4	$CHCl_3$	CH_3Br	CH_3I
x	1.026	.411	.499	.657
y	1.026	.411	.499	.657
z	1.026	.509	.656	.872

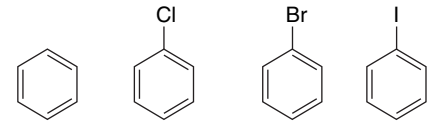

		C_6H_5Cl	C_6H_5Br	C_6H_5I
x	1.12	1.255	1.301	1.588
y	.736	.821	.892	.996
z	1.12	1.478	1.683	1.971

a. From R J. W. Le Fevre, *Adv. Phys. Org. Chem.*, **3**, 1 (1965).

The concepts of electronegativity, polarizability, hardness, and softness are all interrelated. For the kind of qualitative applications we make in discussing reactivity, the concept that initial interactions between reacting molecules can be dominated by either partial electron transfer and bond formation (soft reactants) or by electrostatic interaction (hard reactants) is an important generalization.

1.1.7. Resonance and Conjugation

Qualitative application of VB theory makes use of the concept of *resonance* to relate structural formulas to the description of molecular structure and electron distribution. The case of benzene is a familiar and striking example. Two equivalent Lewis structures can be drawn, but the actual structure is the average of these two *resonance structures*. The double-headed arrow is used to specify a resonance relationship.

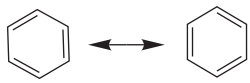

What structural information does this symbolism convey? Resonance structures imply that the true molecular structure is a weighted average of the individual structures. In the case of benzene, since the two structures are equivalent, each contributes equally. The *resonance hybrid* structure for benzene indicates hexagonal geometry and that the bond lengths are intermediate between a double and a single bond, since a bond order of 1.5 results from the average of the two structures. The actual structure of benzene is in accord with these expectations. It is perfectly hexagonal in shape and the carbon-carbon bond length is 1.40 Å. On the other hand, naphthalene, with three neutral resonance structures, shows bond length variation in accord with the predicted 1.67 and 1.33 bond orders.

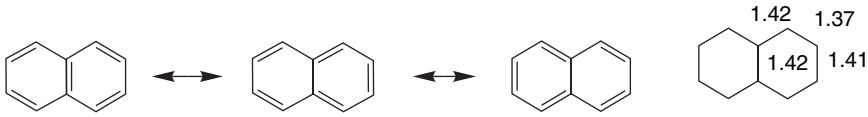

Another important property of benzene is its thermodynamic stability, which is greater than expected for either of the two resonance structures. It is much more stable than noncyclic polyenes of similar structure, such as 1,3,5-hexatriene. What is the origin of this additional stability, which is often called *resonance stabilization or resonance energy*? The resonance structures imply that the π electron density in benzene is equally distributed between the sets of adjacent carbon atoms. This is not the case in acyclic polyenes. The electrons are evenly spread over the benzene ring, but in the polyene they are more concentrated between alternating pairs of carbon atoms. Average electron-electron repulsion is reduced in benzene. The difference in energy is called the *delocalization energy*. The resonance structures for benzene describe a particularly favorable bonding arrangement that leads to greater thermodynamic stability. In keeping with our emphasis on structural theory as a means of describing molecular properties, resonance *describes*, *but does not cause*, the extra stability.

Figure 1.4 shows electron density contours for benzene and 1,3,5-hexatriene. Note that the contours show completely uniform electron density distribution in benzene, but significant concentration between atoms 1,2; 3,4; and 5,6 in hexatriene, as was argued qualitatively above.

Resonance is a very useful concept and can be applied to many other molecules. Resonance is associated with delocalization of electrons and is a feature of *conjugated systems*, which have alternating double bonds that permit overlap between adjacent π bonds. This permits delocalization of electron density and usually leads to stabilization of the molecule. We will give some additional examples shortly.

We can summarize the applicability of the concept of resonance as follows:

1. When alternative Lewis structures can be written for a molecule and they differ only in the assignment of electrons among the nuclei, with nuclear positions being constant, then the molecule is not completely represented by a single Lewis structure, but has weighted properties of all the alternative Lewis structures.
2. Resonance structures are restricted to the maximum number of valence electrons that is appropriate for each atom: two for hydrogen and eight for second-row elements.

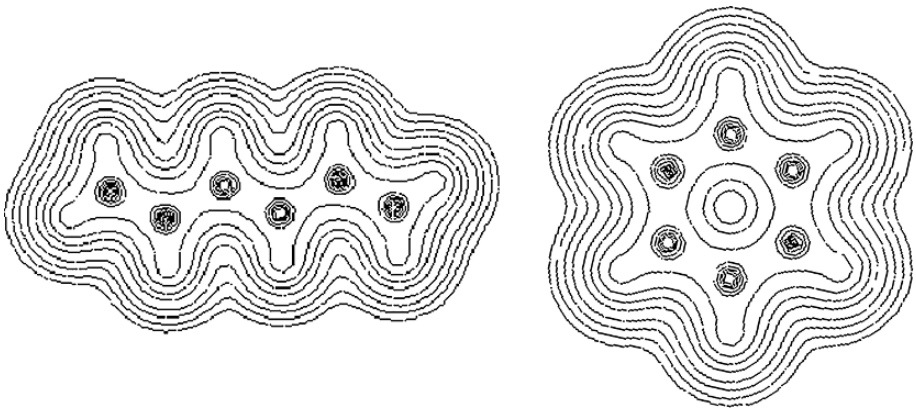

Fig. 1.4. Contour maps of electron density for 1,3,5-hexatriene and benzene in the planes of the molecules. Electron density was calculated at the HF/6-311G level. Electron density plots were created by applying the AIM2000 program; F.Biegler-Koenig, J.Shoenbohm and D.Dayles, *J. Compt. Chem*., **22**, 545-559 (2001).

3. The more stable Lewis structures make the largest contribution to the weighted composite structure. Structures that have the following features are more stable and make the largest contribution: (a) maximum number of bonds, (b) minimum separation of opposite charges, and (c) charge distribution that is consistent with relative electronegativity.

Resonance structures are used to convey the structural and electron distribution consequences of conjugation and delocalization. Let us look specifically at 1,3-butadiene, 1,3,5-hexatriene, prop-2-enal (acrolein), methoxyethene (methyl vinyl ether), and ethenamine (vinylamine) to illustrate how resonance can help us understand electron distribution and reactivity. The hybridization picture for 1,3-butadiene suggests that there can be overlap of the *p* orbitals. Thermodynamic analysis (see Section 3.1.2.3) indicates that there is a net stabilization of about 3–4 kcal/mol, relative to two isolated double bonds. The electron density profile in Figure 1.5 shows some enhancement of π-electron density between C(2) and C(3).

Resonance structures portray increased electron density between C(2) and C(3), but only in structures that have fewer bonds and unfavorable charge separation.

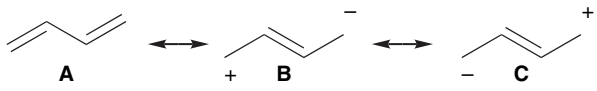

In the diagram above there are two identical structures having opposite charge distributions and there is no net separation of charge. The importance of resonance structures to the composite structure increases with the stability of the individual structures, so structures **B** and **C** are less important than **A**, as they have separation of charge and only one rather than two π bonds. By applying resonance criteria 3a and 3b, we conclude that these two structures contribute less stabilization to butadiene than the two equivalent benzene resonance structures. Therefore, we expect the enhancement of electron density between C(2) and C(3) to be small.

For propenal (acrolein), one uncharged and two charged structures analogous to 1,3-butadiene can be drawn. In this case, the two charged structures are not equivalent.

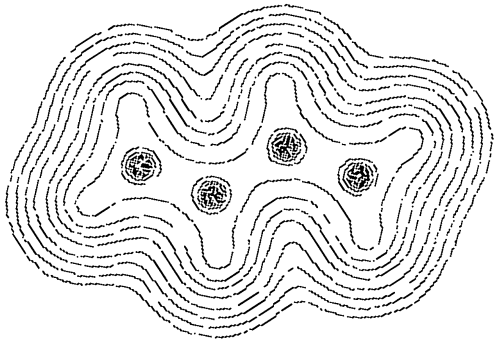

Fig. 1.5. Contour map of electron density for 1,3-butadiene in the plane of the molecule. Electron density was calculated at the HF/6-311G level. Electron density plots were created by applying the AIM2000 program; F.Biegler-Koenig, J.Shoenbohm and D.Dayles, *J. Compt. Chem*., **22**, 545-559 (2001).

Structure **B** is a better structure than **C** because it places the negative charge on a more electronegative element, oxygen (resonance criteria 3c). Structure **D** accounts for the polarity of the C=O bond. The real molecular structure should then reflect the character of **A** > **B** ~ **D** > **C** ~ **E**. The composite structure can be qualitatively depicted by indicating weak partial bonding between C(1) and C(2) and partial positive charges at C(1) and C(3).

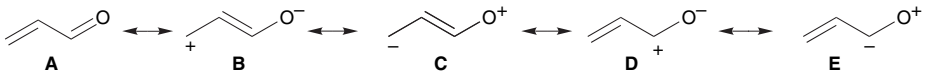

The electronic distributions for butadiene and propenal have been calculated using molecular orbital methods and are shown below.[31] Butadiene shows significantly greater negative charge at the terminal carbons. In propenal there is a large charge distortion at the carbonyl group and a decrease in the electron density at the terminal carbon C(3).

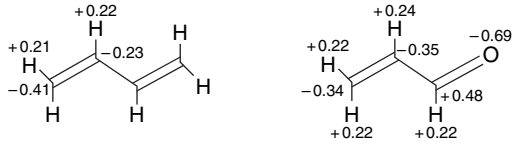

The chemical reactivity of propenal is representative of α,β-*unsaturated carbonyl compounds*. The conjugation between a carbon-carbon double bond and a carbonyl group leads to characteristic reactivity, which includes reduced reactivity of the carbon-carbon double bond toward electrophiles and enhanced susceptibility to the addition of nucleophilic reagents at the β carbon. The anion formed by addition is a delocalized *enolate*, with the negative charge shared by oxygen and carbon. The topic of nucleophilic addition to enals and enones is considered further in Section 2.6, Part B.

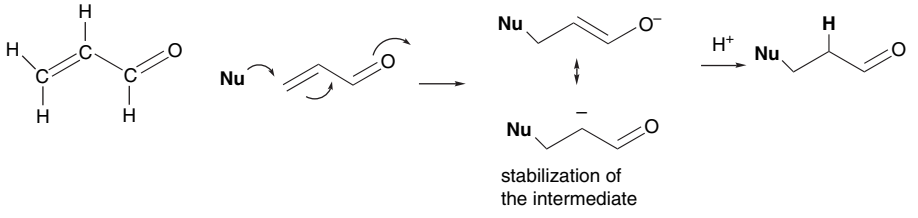

Methoxyethene (methyl vinyl ether) is the prototype of another important class of compounds, the *vinyl ethers*, which have an alkoxy substituent attached directly to a double bond. Such compounds have important applications in synthesis, and the characteristic reactivity is toward electrophilic attack at the β-carbon.

[31] M. A. McAllister and T. T. Tidwell, *J. Org. Chem.*, **59**, 4506 (1994).

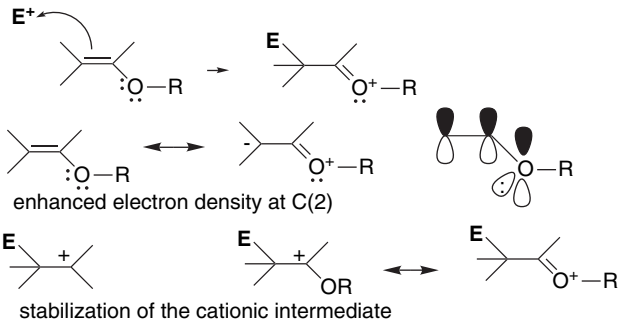

Why does an alkoxy group enhance reactivity and direct the electrophile to the β position? A resonance structure can be drawn that shows an oxygen unshared pair in conjugation with the double bond. More importantly, the same conjugation strongly stabilizes the cation formed by electrophilic attack. This conjugation provides an additional covalent bond in the intermediate and is strongly stabilizing (resonance criterion 3a). Taking the ethyl cation for comparison, there is a stabilization of nearly 30 kcal, according to PM3 MO semiempirical computations (see Section 1.2.2).[32] Stabilization relative to the methyl cation is as follows:

CH_3^+	$CH_3CH_2^+$	$CH_3CH{=}O^+R$	$CH_3CH{=}N^+H_2$
0	29.0 kcal/mol	57.6 kcal/mol	80.2 kcal/mol

Vinyl amines (also called enamines) are even more reactive than vinyl ethers toward electrophiles. The qualitative nature of the conjugation is the same as in vinyl ethers, both for the neutral vinyl amine and for the cationic intermediate. However, nitrogen is an even better electron donor than oxygen, so the stabilizing effect is stronger. The stabilization for the cation is calculated to be around 80 kcal/mol relative to the methyl cation.

These molecules, propenal, methoxyethene, and etheneamine, show how we can apply VB theory and resonance to questions of reactivity. We looked at how structure and conjugation affect *electron density* and *bond formation* in both the reactant and the intermediate. When VB theory indicates that the particular disposition of function groups will change the electron distribution relative to an unsubstituted molecule, we can expect to see those differences reflected in altered reactivity. For propenal, the *electron withdrawal* by the formyl group causes decreased reactivity toward electrophiles and increased reactivity toward nucleophiles. For methoxyethene and ethenamine, the *electron release* of the substituents is reflected by increased reactivity toward electrophiles with strong *selectivity* for the β-carbon.

1.1.8. Hyperconjugation

All the examples of resonance cited in the previous section dealt with conjugation through π bonds. VB theory also incorporates the concept of hyperconjugation, which is the idea that there can be electronic interactions between σ and σ* bonds and between σ and π* bonds. In alkenes such as propene or 2-methylpropene, the electron-releasing effect of the methyl substituents can be represented by hyperconjugated

[32] A. M. El-Nahas and T. Clark, *J. Org. Chem.*, **60**, 8023 (1995).

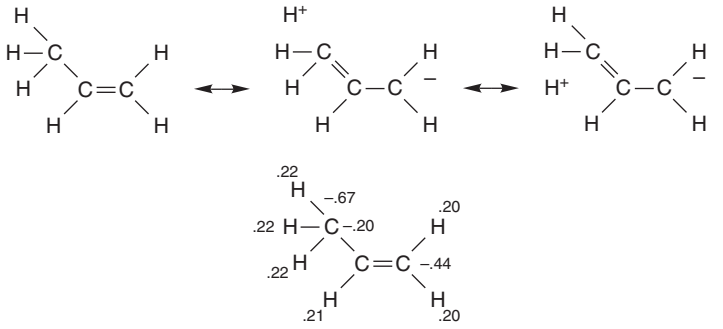

Fig. 1.6. Electron density distribution for propene.

(no-bond) resonance structures. The implication of these resonance structures is that some electron density is transferred from the C−H σ bond to the empty π^* orbital. This is in accord with the calculated electron density distribution for propene shown in Figure 1.6. Carbon-1, which is negatively charged in the resonance structure, has a higher electron density than carbon-2, even though the latter carries the methyl substituent.

There is also hyperconjugation *across* the double bond. Indeed, this interaction may be even stronger because the double bond is shorter than a corresponding single bond, permitting better orbital overlap.[33] Because these resonance structures show equivalent compensating charge transfer, there is no net charge separation, but structural features, such as bond length, and spectroscopic properties are affected.

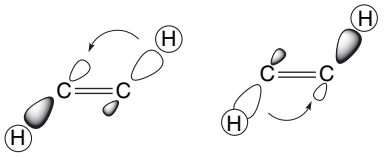

Hyperconjugation also can describe the electron-releasing effect of alkyl groups on aromatic rings.

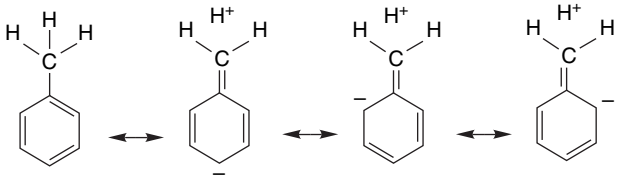

While part of the electron-releasing effect of alkyl groups toward double bonds and aromatic rings can be attributed to the electronegativity difference between sp^3 and sp^2 carbon, the fact that the β-carbon of alkenes and the *ortho* and *para* positions of aromatic rings are selectively affected indicates a resonance component.

[33] I. V. Alabugin and T. A. Zeidan, *J. Am. Chem. Soc.*, **124**, 3175 (2002).

Heteroatoms with unshared electron pairs can also interact with adjacent σ* bonds. For example, oxygen and nitrogen substituents substantially weaken an adjacent (geminal) C−H bond.

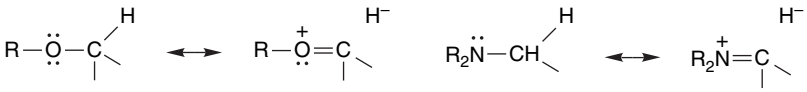

This interaction is readily apparent in spectroscopic properties of amines. The C−H bond that is antiperiplanar to a nitrogen unshared electron pair is lengthened and weakened.[34] Absorptions for C−H bonds that are *anti* to nitrogen nonbonded pairs are shifted in both IR and NMR spectra. The C−H vibration is at higher frequency (lower bond energy) and the ^{1}H signal is at higher field (increased electron density), as implied by the resonance structures. There is a *stereoelectronic* component in hyperconjugation. The optimal alignment is for the σ C−H bond that donates electrons to be aligned with the σ* orbital. The heteroatom bond-weakening effect is at a maximum when the electron pair is antiperiplanar to the C−H bond, since this is the optimal alignment for the overlap of the *n* and σ* orbitals (see Topic 1.2 for further discussion).

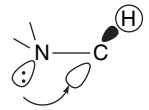

Population of σ* orbital
weakens anti C—H bond

1.1.9. Covalent and van der Waals Radii of Atoms

Covalent and van der Waals radii are other fundamental properties of atoms in molecules that are influenced by nuclear charge and electron distribution. A glance at a molecular model or graphic suggests that most atoms have several different dimensions. There is the distance between each bound atom and also a dimension in any direction in which the atom in not bonded to another atom. The former distance, divided between the two bonded atoms, is called the *covalent radius*. The nonbonded dimension of an atom or group in a molecule is called the *van der Waals radius*. This is the distance at which nonbonded atoms begin to experience mutual repulsion. Just short of this distance, the interatomic forces are weakly attractive and are referred to as *dispersion* or *London* forces and are attributed to mutual *polarization* of atoms.

There are several definitions and values assigned to covalent radii. Pauling created an early scale using bond lengths in simple homonuclear compounds as the starting point. An extended version of this scale is listed as "covalent" in Table 1.5. A related, but more comprehensive, approach is to examine structural data to determine covalent radii that best correlate with observed bond distances. This approach was developed by Slater.[35] An extensive tabulation of bond lengths derived from structural data was published in 1987.[36] These values are labeled "structural" in Table 1.5. A set of

[34] A. Pross, L. Radom, and N. V. Riggs, *J. Am. Chem. Soc.*, **102**, 2253 (1980).
[35] J. C. Slater, *J. Chem. Phys.*, **39**, 3199 (1964); J. C. Slater, *Quantum Theory of Molecules and Solids,* McGraw-Hill, New York, 1965, Vol. 2.
[36] F. H. Allen, O. Kennard, D. G. Watson, L. Brammer, A. G. Opren and R. Taylor, *J. Chem. Soc., Perkin Trans. 2*, Supplement S1–S19 (1987).

Table 1.5. Covalent Radii in Å

	Covalent[a]	Structural[b]	Alcock[c]	Carbon[d]
H	0.37	0.25	0.30	0.327
Li	1.34	1.45		1.219
Be	0.90	1.05	1.06	0.911
B	0.82	0.85	0.83	0.793
C (sp^3)	0.77	0.70	0.77	0.766
C (sp^2)	0.67			
C (sp)	0.60			
N	0.75	0.65	0.70	0.699
O	0.73	0.60	0.66	0.658
F	0.71	0.50	0.62	0.633
Al	1.18	1.25	1.18	1.199
Si	1.11	1.10	1.09	1.123
P	1.06	1.00	1.09	1.110
S	1.02	1.00	1.05	1.071
Cl	0.99	1.00	1.02	1.039
Se	1.19	1.15	1.20	1.201
Br	1.14	1.15	1.20	1.201
I	1.33	1.4	1.40	1.397

a. L. E. Sutton, ed., *Tables of Interatomic Distances and Configuration in Molecules and Ions*, Suppl., 1956–1959, Chemical Society Special Publication No. 18, 1965.
b. J. C. Slater, *J. Chem. Phys.*, **39**, 3199 (1964).
c. N. W. Alcock, *Bonding and Structure*, Ellis Horwood, Chichester, 1990.
d. C. H. Suresh and N. Koga, *J. Phys. Chem. A*, **105**, 5940 (2001).

numbers that may be particularly appropriate for organic compounds was introduced by Alcock, who examined carbon compounds and subtracted the carbon covalent radii to obtain the covalent radii of the bound atoms.[37] This definition was subsequently applied to a larger number of compounds using computational bond length data.[38] These values are listed as "carbon" in Table 1.5. The covalent radii given for sp^3, sp^2, and sp carbon are half of the corresponding C−C bond lengths of 1.55, 1.34, and 1.20 Å. Note that the covalent radii shorten somewhat going to the right in the periodic table. This trend reflects the greater nuclear charge and the harder character of the atoms on the right and is caused by the same electronic shielding effect that leads to decreased polarizability, as discussed in Section 1.1.6. Covalent radii, of course, increase going down the periodic table.

Van der Waals radii also require definition. There is no point at which an atom ends; rather the electron density simply decreases to an infinitesimal value as the distance from the nucleus increases. There are several approaches to assigning van der Waals radii. A set of numbers originally suggested by Pauling was refined and extended by Bondi.[39] These values were developed from nonbonded contacts in crystal structures and other experimental measures of minimum intermolecular contact. A new set of data of this type, derived from a much larger structural database, was compiled somewhat more recently.[40] The latter values were derived from a search of nearly 30,000 crystal structures. Table 1.6 gives both sets of radii.

37. N. W. Alcock, *Bonding and Structure*, Ellis Horwood, Chichester, 1990.
38. C. H. Suresh and N. Koga, *J. Phys. Chem. A*, **105**, 5940 (2001).
39. A. Bondi, *J. Phys. Chem.*, **68**, 441 (1964).
40. R. S. Rowland and R. Taylor, *J. Phys. Chem.*, **100**, 7384 (1996).

Table 1.6. Van der Waals Radii in Å

	Bondi[a]	Structural[b]
H	1.20	1.09
C	1.70	1.75
N	1.55	1.61
O	1.52	1.56
F	1.47	1.44
S	1.80	1.79
Cl	1.75	1.74
Br	1.85	1.85
I	1.98	2.00

a. A. Bondi, *J. Phys. Chem.*, **68**, 441 (1964).
b. R. S. Rowland and R. Taylor, *J. Phys. Chem.*, **100**, 7384 (1996).

Van der Waals dimensions are especially significant in attempts to specify the "size" of molecules, for example, in computational programs that attempt to "fit" molecules into biological receptor sites. In the next chapter, we discuss the effects of van der Waals interactions on molecular shape (conformation). These effects can be quantified by various *force fields* that compute the repulsive energy that molecules experience as *nonbonded repulsion*.

1.2. Molecular Orbital Theory and Methods

Molecular orbital (MO) theory is an alternative way of describing molecular structure and electron density. The fundamental premise of MO theory is that the orbitals used to describe the molecule are not necessarily associated with particular bonds between the atoms but can encompass all the atoms of the molecule. The properties of the molecule are described by the sum of the contributions of all orbitals having electrons. There are also empty orbitals, which are usually at positive (i.e., antibonding) energies. The theoretical foundation of MO theory lies in quantum mechanics and, in particular, the Schrödinger equation, which relates the total energy of the molecule to a wave function describing the electronic configuration:

$$E = \int \psi H \psi d\tau \qquad \text{when} \qquad \int \psi^2 d\tau = 1 \tag{1.11}$$

where H is a Hamiltonian operator.

The individual MOs are described as linear combinations of the atomic orbitals $\{\varphi_x\}$ (LCAO):

$$\psi_\rho = c_{1\rho}\varphi_1 + c_{2\rho}\varphi_2 + c_{3\rho}\varphi_3 \ldots c_{n\rho}\varphi_n \tag{1.12}$$

The atomic orbitals that are used constitute the *basis set* and a minimum basis set for compounds of second-row elements is made up of the $2s$, $2p_x$, $2p_y$, and $2p_z$ orbitals of each atom, along with the $1s$ orbitals of the hydrogen atoms. In MO calculations, an initial molecular structure and a set of approximate MOs are chosen and the molecular energy is calculated. Iterative cycles of calculation of a self-consistent electrical field (SCF) and geometry optimization are then repeated until a minimization

of total energy is reached. It is not possible to carry out these calculations exactly, so various approximations are made and/or parameters introduced. Particular sets of approximations and parameters characterize the various MO methods. We discuss some of these methods shortly.

The output of an MO calculation includes atomic positions and the fractional contribution of each basis set orbital to each MO, that is, the values of $c_{\kappa\rho}$. The energy of each MO is calculated, and the total binding energy of the molecule is the sum of the binding energies of the filled MOs:

$$E = \Sigma f_{ii} + h_{ii} \tag{1.13}$$

The electronic charge at any particular atom can be calculated by the equation

$$q_r = \Sigma n_j {c_{jr}}^2 \tag{1.14}$$

where c_{jr} is the contribution of the atom to each occupied orbital. Thus, MO calculations give us information about molecular structure (from the nuclear positions), energy (from the total binding energy), and electron density (from the atomic populations).

The extent of approximation and parameterization varies with the different MO methods. As computer power has expanded, it has become possible to do MO calculations on larger molecules and with larger basis sets and fewer approximations and parameters. The accuracy with which calculations can predict structure, energy, and electron density has improved as better means of dealing with the various approximations have been developed. In the succeeding sections, we discuss three kinds of MO calculations: (1) the Hückel MO method, (2) semiempirical methods, and (3) ab initio methods, and give examples of the application of each of these approaches.

1.2.1. The Hückel MO Method

The Hückel MO (HMO) method was very important in introducing the concepts of MO theory into organic chemistry. The range of molecules that the method can treat is quite limited and the approximations are severe, but it does provide insight into a number of issues concerning structure and reactivity. Furthermore, the mathematical formulation is simple enough that it can be used to illustrate the nature of the calculations. The HMO method is restricted to planar conjugated systems such as polyenes and aromatic compounds. The primary simplification is that only the $2p_z$ orbitals are included in the construction of the HMOs. The justification is that many of the properties of conjugated molecules are governed by the π orbitals that arise from the p_z atomic orbitals. A further approximation of the HMO calculations is that only adjacent p_z orbitals interact. This allows construction of mathematical formulations for the π MOs for such systems as linear and branched-chain polyenes, cyclic polyenes, and fused-ring polyenes. For conjugated linear polyenes such as 1,3,5-hexatriene, the energy levels are given by the equation

$$E = \alpha + m_j\beta \tag{1.15}$$

where $m_j = 2\cos(j\pi/n+1)$ for $j = 1, 2, 3, \ldots, n$, with n being the number of carbon atoms in the conjugated polyene.

The quantity α is called the *Coulomb integral*; it represents the binding of an electron in a $2p_z$ orbital and is considered to be constant for all sp^2 carbon atoms. The

quantity β is called the *resonance integral* and represents the energy of an electron distributed over two or more overlapping $2p_z$ orbitals. For linear polyenes, this equation generates a set of HMOs distributed symmetrically relative to the energy α associated with an isolated $2p_z$ orbital. The contribution of each atomic orbital to each HMO is described by a coefficient:

$$\boldsymbol{C}_{rj} = \left(\frac{2}{n+1}\right)^{1/2} \sin\left(\frac{rj\pi}{n+1}\right) \tag{1.16}$$

Figure 1.7 gives the resulting HMOs for $n = 2$ to $n = 7$. Table 1.7 gives the coefficients for the HMOs of 1,3,5-hexatriene. From these coefficients, the overall shape of the orbitals can be deduced and, in particular, the location of nodes is determined. Nodes represent an antibonding contribution to the total energy of a particular orbital. Orbitals with more nodes than bonding interactions are *antibonding* and are above the reference α energy level. The spacing between orbitals decreases with the length of the polyene chain, and as a result, the gap between the HOMO and LUMO decreases as the conjugated chain lengthens.

These coefficients give rise to the pictorial representation of the 1,3,5-hexatriene molecular orbitals shown in Figure 1.8. Note in particular the increase in the energy of the orbital as the number of nodes goes from 0 to 5. The magnitude of each atomic coefficient indicates the relative contribution at that atom to the MO. In ψ_1, for example, the central atoms C(3) and C(4) have larger coefficients than the terminal atoms C(1) and C(6), whereas for ψ_3 the terminal carbons have the largest coefficients.

The equation for the HMOs of completely conjugated monocyclic polyenes is

$$E = \alpha + m_j\beta \tag{1.17}$$

where $m_j = 2\cos(2j\pi/n)$ for $j = 0, \pm1, \pm2, \ldots (n-1)/2$ for $n =$ odd and $(n/2)$ for $n =$ even. This gives rise to the HMO diagrams shown in Figure 1.9 for cyclic polyenes with $n = 3$ to $n = 7$. Table 1.8 gives the atomic coefficients for benzene, $n = 6$, and Figure 1.10 gives pictorial representations of the MOs.

There is an easy way to remember the pattern of MOs for monocyclic systems. Figure 1.11 shows Frost's circle.[41] A polygon corresponding to the ring is inscribed

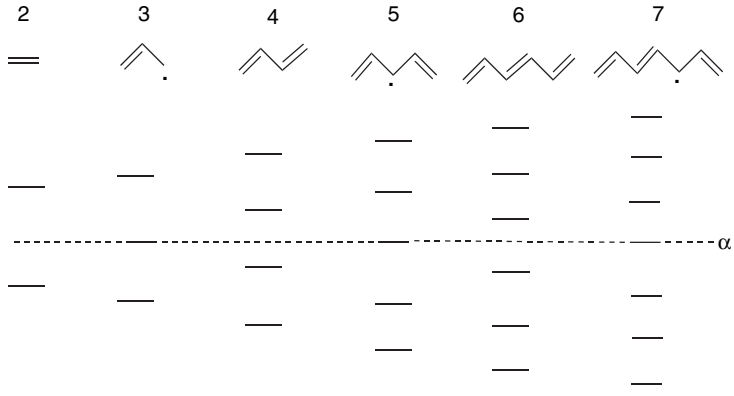

Fig. 1.7. HMO orbital diagram for polyenes $n = 2$ to $n = 7$.

[41] A. A. Frost and B. Musulin, *J. Chem. Phys.*, **21**, 572 (1953).

Table 1.7. Energy Levels and Atomic Coefficients for HMOs of 1,3,5-Hexatriene

π orbital m_j		c_1	c_2	c_3	c_4	c_5	c_6
Ψ_1	1.802	0.2319	0.4179	0.5211	0.5211	0.4179	0.2319
Ψ_2	1.247	0.4179	0.5211	0.2319	−0.2319	−0.5211	−0.4179
Ψ_3	0.445	0.5211	0.2319	−0.4179	−0.4179	0.2319	0.5211
Ψ_4	−0.445	0.5211	−0.2319	−0.4179	0.4179	0.2319	−0.5211
Ψ_5	−1.247	0.4179	−0.5211	0.2319	0.2319	−0.5211	0.4179
Ψ_6	−1.802	0.2319	−0.4179	0.5211	−0.5211	0.4179	−0.2319

in a circle with one point of the polygon at the bottom. The MO pattern corresponds to each point of contact of the polygon and circle. If the circle is given a radius of 2β, the point of contact gives the coefficient of β in the expression for the energy of the MO. Compilations of HMO energy levels and atomic coefficients are available for a number of conjugated systems.[42]

What do we learn about molecules such as 1,3,5-hexatriene and benzene from the HMO description of the π orbitals?

1. *The frontier MOs are identified and described.* The frontier orbitals are the *highest occupied* MO (HOMO) and the *lowest unoccupied* MO (LUMO). These orbitals are intimately involved in chemical reactivity, because they are the most available to electrophiles and nucleophiles, respectively. From the atomic coefficients, which can be represented graphically, we see the symmetry and relative atomic contribution

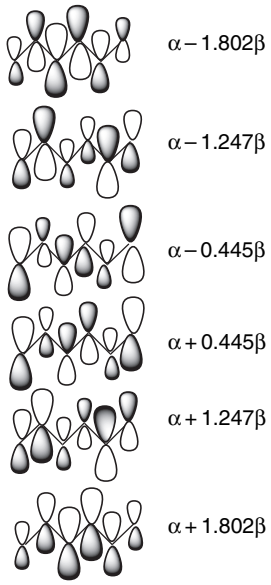

Fig. 1.8. π Molecular orbitals for 1,3,5-hexatriene.

[42] E. Heilbronner and P. A. Straub, *Hückel Molecular Orbitals*, Springer Verlag, New York, 1966; C. A. Coulson, A. Streitwieser, Jr., and J. I. Brauman, *Dictionary of π-Electron Calculations*, W H. Freeman, San Francisco, 1965.

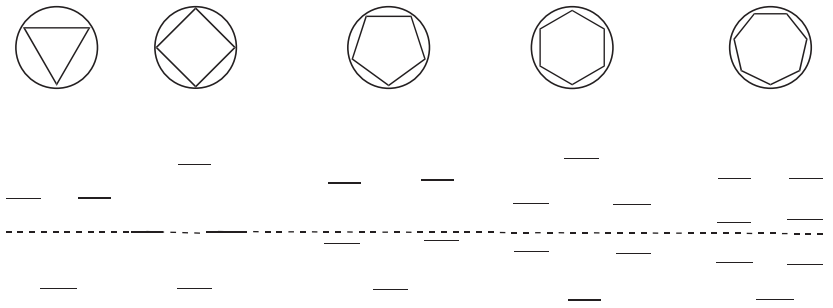

Fig. 1.9. HMO energy levels for cyclic polyene $n = 3$ to $n = 7$.

of the orbitals. Reaction is facilitated by large overlap of interacting orbitals, so we expect reactions to involve atoms with large orbital coefficients.

2. *The HOMO-LUMO gap is approximated.* Remember that for atoms, radicals, and ions, hardness and softness are defined in relation to the electron affinity (EA) and ionization potential (IP) (see Section 1.1.6). The energies of the HOMO and LUMO are indicators of the IP and EA, respectively, of the molecules. The HOMO-LUMO gap is an indicator of the reactivity of the molecules in terms of hardness or softness. The smaller the gap, the softer the molecule.

3. *The overall stabilization of the molecule as the result of conjugation is estimated.* Remember from the resonance concept in VB theory that conjugation is generally associated with additional stabilization (see Section 1.1.7). In HMO theory this stabilization is expressed as the difference between the energy of the conjugated system and the same number of isolated double bonds. The energy of an isolated double bond in the HMO method is equal to $2\alpha + 2\beta$, so for 1,3,5-hexatriene, a stabilization of 0.988β is computed. For benzene, the computed stabilization is 2β:

$$\text{Three isolated double bonds} = 3(2\alpha + 2\beta) = 6\alpha + 6\beta$$
$$\text{Hexatriene} = 2(\alpha + 1.802\beta) + 2(\alpha + 1.247\beta) + 2(\alpha + 0.445\beta) = 6\alpha + 6.988\beta$$
$$\text{Stabilization} = (6\alpha + 6.988\beta) - (6\alpha + 6\beta) = 0.988\beta$$
$$\text{Benzene} = 2(\alpha + 2\beta) + 2(\alpha + \beta) + 2(\alpha + \beta) = 6\alpha + 8\beta$$
$$\text{Stabilization} = (6\alpha + 8\beta) - (6\alpha + 6\beta) = 2.0\beta$$

Let us consider the significance of this stabilization, which is sometimes called the *delocalization energy* (DE). The stabilization results from the removal of the restriction that the π electrons be localized between two particular atoms. Comparison of the DE of 1,3,5-hexatriene and benzene would suggest that the triene is stabilized by almost half the extent of benzene, but *thermodynamic comparisons do*

Table 1.8. Energy Levels and Coefficients for HMOs of Benzene

π-orbital	m_j	c_1	c_2	c_3	c_4	c_5	c_6
Ψ_1	2.000	0.4083	0.4083	0.4083	0.4083	0.4083	0.4083
Ψ_2	1.000	0.0000	0.5000	0.5000	0.0000	−0.5000	−0.5000
Ψ_3	1.000	0.5774	0.2887	−0.2887	−0.5774	−0.2887	0.2887
Ψ_4	−1.000	0.0000	−0.5000	−0.5000	0.0000	0.5000	−0.5000
Ψ_5	−1.000	0.5774	−0.2887	0.2887	−0.5774	−0.2887	0.2887
Ψ_6	−2.000	−0.4083	−0.4083	−0.4083	−0.4083	−0.4083	−0.4083

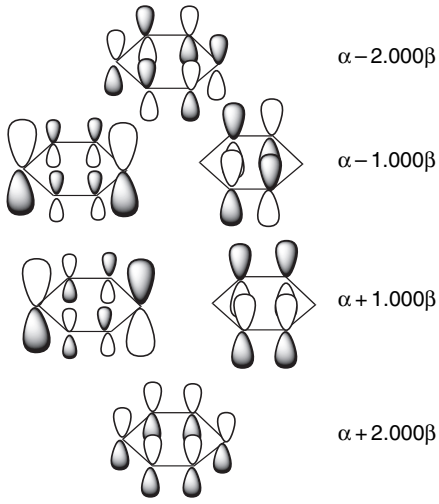

Fig. 1.10. π Molecular orbitals for benzene.

not support this result (see Section 3.1.1). Relative to three ethene double bonds, 1,3,5-hexatriene is stabilized by about 8 kcal,[43] whereas for benzene the stabilization is around 30 kcal/mol. Furthermore, the HMO DE for polycyclic aromatic hydrocarbons such as anthracene and phenanthrene continues to increase with molecular size. This is contrary to chemical reactivity and thermodynamic data, which suggest that on a per atom basis, benzene represents the optimum in stabilization. Thus, the absolute value of the DE does not seem to be a reliable indicator of stabilization.

On the other hand, the *difference in stabilization* between acyclic and cyclic polyenes turns out to be a very useful indicator of the extra stabilization associated with cyclic systems. This extra stabilization or *aromaticity* is well represented by the difference in the DE of the cyclic compound and the polyene having the same number of conjugated double bonds.[44] For 1,3,5-hexatriene and benzene, this difference is 1.012β. For comparison of molecules of different sizes, the total stabilization energy is divided by the number of π electrons.[45] We will see in Chapter 9 that this value gives a very useful estimate of the stability of cyclic conjugated systems.

For monocyclic conjugated polyenes, high stabilization is found for systems with $(4n+2)$ π electrons but not for systems with $(4n)$ π electrons. The relationship is formulated as *Hückel's rule*, which states that completely conjugated planar hydrocarbons are strongly stabilized (aromatic) when they have $(4n+2)$ π electrons. Benzene (6 π electrons) is aromatic but cyclobutadiene (4 π electrons) and cyclooctatetraene (8 π electrons) are not.

Fig. 1.11. Frost's circle mnenomic for HMOs of cyclic polyenes.

43. W. Fang and D. W. Rogers, *J. Org. Chem.*, **57**, 2294 (1992).
44. M. J. S. Dewar and C. de Llano, *J. Am. Chem. Soc.*, **91**, 789 (1969).
45. B. A. Hess, Jr., and L. J. Schaad, Jr., *J. Am. Chem. Soc.*, **93**, 305, 2413 (1971).

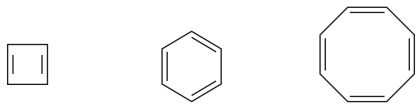

Hückel's rule also pertains to charged cyclic conjugated systems. The cyclopropenyl (2 π electrons), cyclopentadienyl anion (6 π electrons), and cycloheptatrienyl (tropylium) cation (6 π electrons) are examples of stabilized systems. We say much more about the relationship between MO configuration and aromaticity in Chapter 9.

1.2.2. Semiempirical MO Methods

Beginning in the 1960s, various more elaborate MO methods were developed and applied to organic molecules. Among those that are historically significant are extended Hückel theory (EHT),[46] complete neglect of differential overlap (CNDO),[47] and modified neglect of differential overlap (MNDO).[48] In contrast to HMO theory, these methods include all the valence shell electrons in the calculation. Each of these methods incorporates various approximations and parameters. The parameters are assigned values based on maximizing the agreement for a set of small molecules. The CNDO findings were calibrated with higher-level computational results, while MNDO was calibrated to experimental stability data. These parameters are then employed for computations on more complex molecules. The output provides molecular geometry, atomic coefficients, and orbital energies. Each method had both strengths and limitations with respect to the range of molecules and properties that could be adequately described. At the present time, the leading semiempirical methods, called AM1[49] and PM3,[50] are incorporated into various MO computational programs and are widely employed in the interpretation of structure and reactivity. In Section 1.2.6, we illustrate some of the problems that can be addressed using these methods.

1.2.3. Ab Initio Methods

Ab initio computations are based on iterative calculations of a self-consistent electronic field (SCF), as is the case in the semiempirical methods just described, but do not use experimental data to calibrate quantities that appear in the calculations. These methods are much more computationally demanding than semiempirical methods, but their reliability and range of applicability has improved greatly as more powerful computers have permitted more sophisticated approaches and have enabled handling of more complex molecules. The computations are carried out by successive series of calculations minimizing the energy of the electron distribution and the molecular geometry. The cycle of the calculations is repeated until there is no further improvement (convergence).

46. R. Hoffmann, *J. Chem. Phys.*, **39**, 1397 (1963).
47. J. A. Pople and G. A. Segal, *J. Chem. Phys.*, **44**, 3289 (1966).
48. M. J. S. Dewar and W. Thiel, *J. Am. Chem. Soc.*, **99**, 4907 (1977).
49. M. J. S. Dewar, E. G. Zoebisch, E. F. Healy, and J. P. Stewart. *J. Am. Chem. Soc.*, **109**, 3902 (1985).
50. J. P. Stewart, *J. Comput. Chem.*, **10**, 209, 221 (1989).

Specific ab initio methods are characterized by the form of the wave function and the nature of the basis set functions that are used. The most common form of the wave function is the single determinant of molecular orbitals expressed as a linear combination of basis functions, as is the case with semiempirical calculations. We describe alternatives later in this section. Early calculations were often done with Slater functions, designated STO for Slater-type orbitals. Currently most computations are done with Gaussian basis functions, designated by GTOs. A fairly accurate representation of a single STO requires three or more GTOs. This is illustrated in Figure 1.12, which compares the forms for one, two, and three GTOs. At the present time most basis sets use a six-Gaussian representation, usually designated 6G. The weighting coefficients for the N components of a STO-NG representation are not changed in the course of a SCF calculation.

A basis set is a collection of basis functions. For carbon, nitrogen, and oxygen compounds, a minimum basis set is composed of a 1s function for each hydrogen and 1s, 2s, and three 2p functions for each of the second-row atoms. More extensive and flexible sets of basis functions are in wide use. These basis sets may have two or more components in the outer shell, which are called *split-valence* sets. Basis sets may include p functions on hydrogen and/or d and f functions on the other atoms. These are called *polarization functions*. The basis sets may also include *diffuse functions*, which extend farther from the nuclear center. Split-valence bases allow description of tighter or looser electron distributions on atoms in differing environments. Polarization permits changes in orbital shapes and shifts in the center of charge. Diffuse functions allow improved description of the outer reaches of the electron distribution.

Pople developed a system of abbreviations that indicates the composition of the basis sets used in ab initio calculations. The series of digits that follows the designation 3G or 6G indicates the number of Gaussian functions used for each successive shell. The combination of Gaussian functions serves to improve the relationship between electron distribution and distance from the nucleus. Polarization functions incorporate additional orbitals, such as p for hydrogen and d and/or f for second-row atoms. This permits changes in orbital shapes and separation of the centers of charge. The inclusion of d and f orbitals is indicated by the asterisk (*). One asterisk signifies d orbitals on second-row elements; two asterisks means that p orbitals on hydrogen are also included. If diffuse orbitals are used they are designated by a plus sign (+), and the

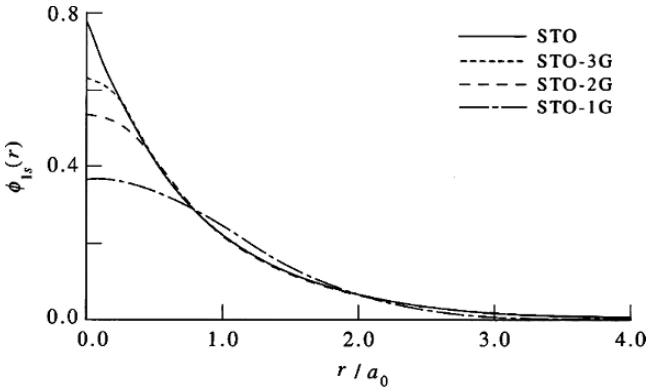

Fig. 1.12. Comparison of electron distribution for STO, G, 2G, and 3G expressions of orbitals.

designation double plus (++) means that diffuse orbitals are present on both hydrogen and the second-row elements. Split-valence sets are indicated by a sequence defining the number of Gaussians in each component. Split-valence orbitals are designated by primes, so that a system of three Gaussian orbitals would be designated by single, double, and triple primes ($'$, $''$, and $'''$). For example 6-311 + G(d, p) conveys the following information:

- 6: Core basis functions are represented as a single STO-6G expression.
- 311: The valence set is described by three sets of STO-NG functions; each set includes an s orbital and three p orbitals. In the 6-311+G(d) basis there are three such sets. One is composed of three Gaussians (STO-3G expression of one s-type and three p-type forms) and the other two are represented by a single Gaussian (STO-1G) representation of the s-p manifold. The collection of components of the split-valence representation can be designated by a series of primes.
- +: A STO-1G diffuse s-p manifold is included in the basis set for each nonhydrogen atom; ++ implies that diffuse functions are also included for the hydrogen atoms.
- p: A set of p functions placed on each nonhydrogen atom and specifies the composition.
- d: A set of STO-1G d-functions is placed on each nonhydrogen atom for which d functions are not used in the ground state configuration. If d functions are so used, polarization is effected by a manifold of f functions.

The composition of several basis sets is given in Table 1.9.

An important distinguishing feature among ab initio calculations is the extent to which they deal with *electron correlation*. Correlation is defined as the difference between the exact energy of a molecular system and the best energy obtainable by a SCF calculation in which the wave function is represented by a single determinant. In single-determinant calculations, we consider that each electron experiences an averaged electrostatic repulsion defined by the total charge distribution, a *mean field* approximation. These are called *Hartree-Fock* (HF) calculations. Correlation corrections arise from fluctuations of the charge distribution. Correlations energies can be estimated by including effects of admixtures of excited states into the Hartree-Fock determinant.

Table 1.9. Abbreviations Describing Gaussian Basis Sets[a]

Designation	H	C	Functions on second-row atoms
3-21G	2	9	$1s'$; $2s'$, 3 $2p'$; $2s'''$, 3 $2p''$
3-21+G	2	13	$1s'$; $2s'$, 3 $2p'$; $2s''$, 3 $2p''$; $2s$+, 3 $2p$+
6-31G* or 6-31G(d)	2	15	$1s$; $2s'$, 3 $2p'$; $2s''$, 3 $2p''$; 5 $3d$
6-31G** or 6-31(d,p)	5	18	$1s$; $2s'$, 3 $2p'$; $2s''$, 3 $2p''$; $2s'''$; 3 $2p'''$; 5 $3d$
6-31+G* or 6-31+(d)	3	19	$1s$; $2s'$, 3 $2p'$; $2s''$, 3 $2p''$; 5 $3d$; $2s$+, 3 $2p$+
6-311G** or 6-311(d,p)	6	18	$1s$; $2s'$, 3 $2p'$; $2s''$, 3 $2p''$; $2s'''$; 3 $2p'''$; 5 $3d$
6-311G(df,p)	6	25	$1s$; $2s'$, 3 $2p'$; $2s''$, 3 $2p$; $2s'''$; 3 $2p'''$; 5 $3d$; 7 $4f$
6-311G(3df,3pd)	17	35	$1s$; $2s'$, 3 $2p'$; $2s''$, 3 $2p''$; $2s'''$ 3p'''; 5 $3d$, 7 $4f$

a. From E. Lewars, *Computational Chemistry*, Kluwer Academic Publishers, Boston, 2003, pp. 225–229.

This may be accomplished by perturbation methods such as *Moeller-Plesset* (MP)[51] or by including excited state determinants in the wave equation as in *configurational interaction* (CISD)[52] calculations. The excited states have electrons in different orbitals and reduced electron-electron repulsions.

The output of ab initio calculations is analogous to that from HMO and semiempirical methods. The atomic coordinates at the minimum energy are computed. The individual MOs are assigned energies and atomic orbital contributions. The total molecular energy is calculated by summation over the occupied orbitals. Several schemes for apportioning charge among atoms are also available in these programs. These methods are discussed in Section 1.4. In Section 1.2.6, we illustrate some of the applications of ab initio calculations. In the material in the remainder of the book, we frequently include the results of computational studies, generally indicating the type of calculation that is used. The convention is to list the treatment of correlation, e.g., HF, MP2, CISDT, followed by the basis set used. Many studies do calculations at several levels. For example, geometry can be minimized with one basis set and then energy computed with a more demanding correlation calculation or basis set. This is indicated by giving the basis set used for the energy calculation followed by parallel lines (//) and the basis set used for the geometry calculation. In general, we give the designation of the computation used for the energy calculation. The information in Scheme 1.3 provides basic information about the nature of the calculation and describes the characteristics of some of the most frequently used methods.

1.2.4. Pictorial Representation of MOs for Molecules

The VB description of molecules provides very useful generalizations about molecular structure and properties. Approximate molecular geometry arises from hybridization concepts, and qualitative information about electron distribution can be deduced by applying the concepts of polarity and resonance. In this section we consider how we can arrive at similar impressions about molecules by using the underlying principles of MO theory in a qualitative way. To begin, it is important to remember some fundamental relationships of quantum mechanics that are incorporated into MO theory. The *Aufbau principle* and the *Pauli exclusion principle*, tell us that electrons occupy the MOs of lowest energy and that any MO can have only two electrons, one of each spin. The MOs must also conform to molecular symmetry. Any element of symmetry that is present in a molecule must also be present in *all the corresponding MOs*. Each MO must be either *symmetric* or *antisymmetric* with respect to each element of molecular symmetry. To illustrate, the π MOs of *s-cis*-1,3-butadiene in Figure 1.13 can be classified with respect to the plane of symmetry that dissects the molecule between C(2) and C(3). The symmetric orbitals are identical (exact reflections) with respect to this plane, whereas the antisymmetric orbitals are identical in shape but

[51] W. J. Hehre, L. Radom, P. v. R. Schleyer, and J. A. Pople, *Ab Initio Molecular Orbital Theory*, Wiley-Interscience, New York, 1986, pp. 38–40; A. Bondi, *J. Phys. Chem.*, **68**, 441 (1964); R. S. Rowland and R. Taylor, *J. Phys. Chem.*, **100**, 7384 (1996); M. J. S. Dewar and C. de Llano, *J. Am. Chem. Soc.*, **91**, 789 (1969); R. Hoffmann, *J. Chem. Phys.*, **39**, 1397 (1963); J. A. Pople and G. A. Segal, *J. Chem. Phys.*, **44**, 3289 (1966); M. J. S. Dewar and W. Thiel, *J. Am. Chem. Soc.*, **99**, 4907 (1977);. M. J. S. Dewar, E. G. Zoebisch, E. F. Healy, and J. P. Stewart. *J. Am. Chem. Soc.*, **109**, 3902 (1985); J. P. Stewart, *J. Comput. Chem.*, **10**, 209, 221 (1989); ; J. A. Pople, M. Head-Gordon, and K. Raghavachari, *J. Phys. Chem.*, **87**, 5968 (1987).

[52] J. A. Pople, M. Head-Gordon, and K. Raghavachari, *J. Phys. Chem.*, **87**, 5968 (1987).

Scheme 1.3. Characteristics of ab Initio MO Methods

STO-3G. STO-3G is a minimum basis set consisting of 1*s* orbitals for hydrogen and 2*s* and 2*p* orbitals for second-row elements, described by Gaussian functions.

Split-Valence Gaussian Orbitals. (3-21G, 4-31G, 6-31G) Split-valence orbitals are described by two or more Gaussian functions. Also in this category are Dunning-Huzinaga orbitals.

Polarized Orbitals. These basis sets add further orbitals, such as *p* for hydrogen and *d* for carbon that allow for change of shape and separation of centers of charge. Numbers in front of the *d*, *f* designations indicate inclusion of multiple orbitals of each type. For example, 6-311(2*df*, 2*pd*) orbitals have two *d* functions and one *f* function on second-row elements and two *p* functions and one *d* function on hydrogen.

Diffuse Basis Sets. (6-31+G*, 6-31++G*) Diffuse basis sets include expanded orbitals that are used for molecules with relatively loosely bound electrons, such as anions and excited states. 6-31+G* have diffuse *p* orbitals on second-row elements. 6-31++G* orbitals have diffuse orbitals on both second-row elements and hydrogen.

Correlation Calculations

MP2, MP4. MP (Moeller-Plesset) calculations treat correlation by a perturbation method based on adding excited state character. MP2 includes a contribution from the interaction of doubly excited states with the ground state. MP4 includes, single, double, and quadruple excited states in the calculation.

CISD. CISD (configuration interaction, single double) are LCAO expressions that treat configuration interactions by including one or two excited states. The designations CISDT and CISDTQ expand this to three and four excitations, respectively.

CAS-SCF. CAS-SCF (complete active space self-consistent field) calculations select the chemically most significant electrons and orbitals and apply configuration interactions to this set.

Composite Calculations

G1, G2, G2(MP2), and G3 are composite computations using the 6-311G** basis set and MP2/6-31G* geometry optimization. The protocols are designed for efficient calculation of energies and electronic properties. The G2 method calculates electron correlation at the MP4 level, while G2(MP2) correlation calculations are at the MP2 level. A scaling factor derived from a series of calibration molecules is applied to energies.

CBS. CBS protocols include CBS-4, CBS-Q, and CBS-APNO. The objectives are the same as for G1 and G2. The final energy calculation (for CBS-Q) is at the MP4(SQD)/6-31G(*d*, *p*) level, with a correction for higher-order correlation. A scaling factor is applied for energy calculations.

References to Scheme 1.3

STO-3G: W. J. Hehre, R. F. Stewart, and J. A. Pople, *J. Phys. Chem.*, **51**, 2657 (1969).

3-21G, 4-21G, and 6-31G: R. Ditchfield, W. J. Hehre, and J. A. Pople, *J. Chem. Phys.*, **54**, 724 (1971); W. J. Hehre and W. A. Lathan, *J. Chem. Phys.*, **56**, 5255 (1972); W. J. Hehre, R. Ditchfield, and J. A. Pople, *J. Chem. Phys.*, **56**, 2257 (1972); M. M. Francl, W. J. Pietro, W. J. Hehre, J. S. Binkley, M. S. Gordon, D. J. DeFrees, and J. A. Pople, *J. Chem. Phys.*, **77**, 3654 (1982).

Dunning-Huzinaga Orbitals: T. H. Dunning, Jr., and P. J. Hay, in *Modern Theoretical Chemistry*, Vol. 3, H. F. Schaefer, ed., Plenum Publishing, New York, 1977, pp 1–27.

MP: J. S. Binkley and J. A. Pople, *Int. J. Quantum Chem.*, **9**, 229 (1975).

G1, G2, G3: J. A. Pople, M. Head-Gordon, D. J. Fox, K. Raghavachari, and L. A. Curtiss, *J. Chem. Phys.*, **90**, 5622 (1989); L. A. Curtiss, C. Jones, G. W. Trucks, K. Raghavachari, and J. A. Pople, *J. Chem. Phys.*, **93**, 2537 (1990); L. A. Curtiss, K. Raghavachari, G. W. Tucks, and J. A. Pople, *J. Chem. Phys.*, **94**, 7221 (1991); L. A. Curtiss, K. Raghavachari, and J. A. Pople, *J. Chem. Phys.*, **98**, 1293 (1993); M. Head-Gordon, *J. Chem. Phys.*, **100**, 13213 (1996); L. A. Curtiss and K. Raghavachari, *Theor. Chem. Acc.*, **108**, 61 (2002).

CBS-Q: J. W. Ochterski, G. A. Petersson, and J. A. Montgomery, *J. Chem. Phys.*, **104**, 2598 (1996); G. A. Petersson, *Computational Thermochemistry,* ACS Symposium Series, Vol, 677, pp 237–266 (1998).

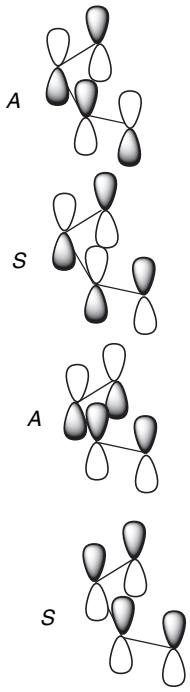

Fig. 1.13. Symmetry characteristics of butadiene HMOs with respect to a plane bisecting the molecule in the *s-cis* conformation perpendicular to the plane of the molecule.

change phase at all locations. Although these formal symmetry restrictions can ignore nonconjugated substituents, the symmetry pattern of the MOs must conform to the symmetry of the conjugated system.

What do the MOs of other small molecules look like? Let us consider methane. A convenient frame of reference is a cube with the four hydrogens at alternate corners and the carbon at the center. This orientation of the molecule reveals that methane possesses three twofold symmetry axes, one each along the x, y, and z axes. There are also planes of symmetry diagonally across the cube. Because of this molecular symmetry, the MOs of methane must possess symmetry with respect of these same axes. There are two possibilities: the orbital may be unchanged by 180° rotation about the axis (symmetric), or it may be transformed into an orbital of identical shape but opposite phase by the symmetry operation (antisymmetric). The minimum basis set orbitals are the hydrogen 1s and the carbon $2s, 2p_x, 2p_y$, and $2p_z$ atomic orbitals. The combinations that are either symmetric or antisymmetric with respect to the diagonal planes of symmetry are shown in Figure 1.14. These give rise to four bonding MOs. One has no nodes and bonds between all the atoms. The other three consist of two boomerang-shaped lobes, with a node at carbon corresponding to the node in the basis set p orbital.

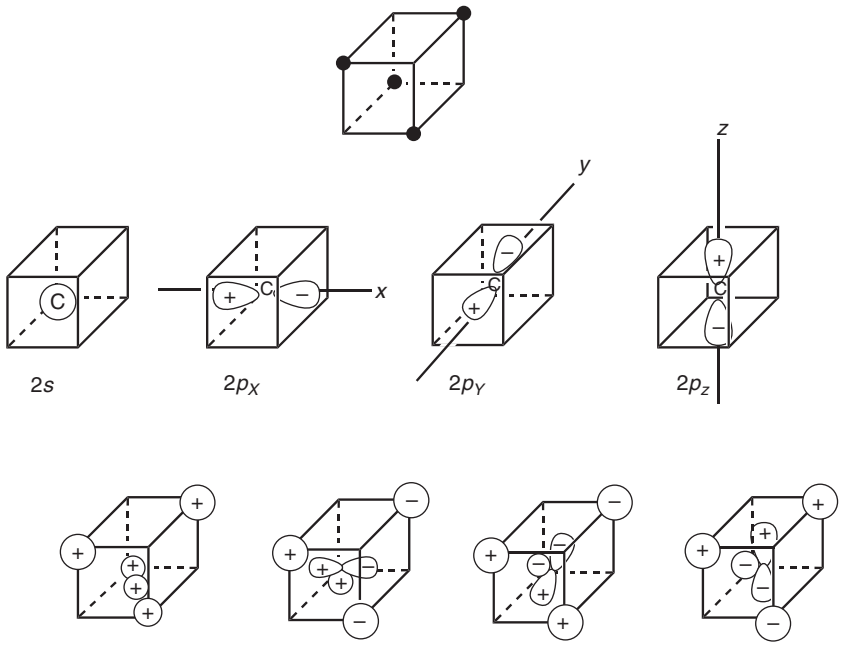

Fig. 1.14. Combinations of atomic orbitals leading to the methane molecular orbitals.

The carbon 2*s* orbital is symmetric with respect to each axis but the three 2*p* orbitals are each antisymmetric to two of the axes and symmetric with respect to one. The combinations that give rise to molecular orbitals that meet these symmetry requirements are shown in the lower part of Figure 1.14. The bonding combination of the carbon 2*s* orbital with the four 1*s* hydrogen orbitals leads to a molecular orbital that encompasses the entire molecule and has no nodes. Each of the MOs derived from a carbon 2*p* orbital has a node at carbon. The three combinations are equivalent, but higher in energy than the MO with no nodes. The four antibonding orbitals arise from similar combinations, but with the carbon and hydrogen orbitals having opposite phases in the region of overlap. Thus the molecular orbital diagram arising from these considerations shows one bonding MO with no nodes and three degenerate (having the same energy) MOs with one node. The diagram is given in Figure 1.15.

There is experimental support for this MO pattern. The ESCA spectrum of methane is illustrated in Figure 1.16. It shows two peaks for valence electrons at 12.7 and 23.0 eV, in addition to the band for the core electron at 291.0 eV.[53] Each band

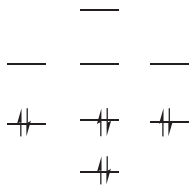

Fig. 1.15. Molecular orbital diagram for methane.

[53] U. Gelius, in *Electron Spectroscopy*, D. A. Shirley, ed., American Elsevier, New York, 1972, pp. 311–344.

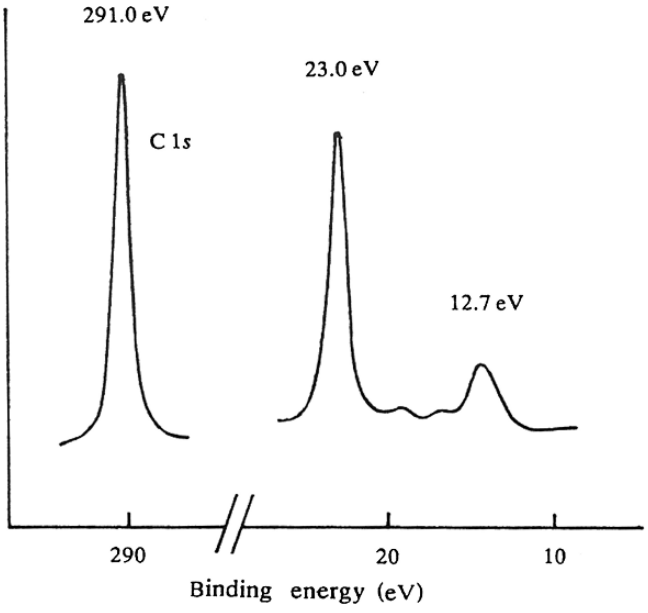

Fig. 1.16. ESCA spectrum of methane.

corresponds to the binding energy for the removal of a particular electron, not the successive removal of one, two, and three electrons. The presence of two bands in the valence region is consistent with the existence of two different molecular orbitals in methane.

The construction of the MOs of ethene is similar to the process used for methane, but the total number of atomic orbitals is greater: twelve instead of eight. We must first define the symmetry of ethene, which is known from experiment to be a planar molecule.

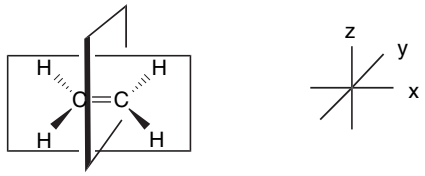

This geometry possesses three important elements of symmetry, the molecular plane and two planes that bisect the molecule. All MOs must be either symmetric or antisymmetric with respect to each of these symmetry planes. With the axes defined as in the diagram above, the orbitals arising from carbon $2p_z$ have a node in the molecular plane. These are the π and π^* orbitals. Because the two p_z atomic orbitals are perpendicular (orthogonal) to all the other atomic orbitals and the other orbitals lie in the nodal plane of the p_z orbitals, there is no interaction of the p_z with the other C and H atomic orbitals. The π orbital is symmetric with respect to both the x-z plane and the y-z plane. It is antisymmetric with respect to the molecular (x-y) plane. On the other hand, π^* is antisymmetric with respect to the y-z plane.

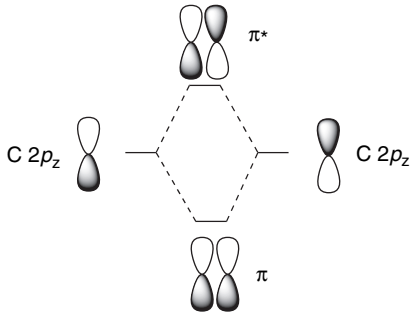

The orbitals that remain are the four hydrogen 1*s*, two carbon 1*s*, and four carbon 2*p* orbitals. All lie in the molecular plane. The combinations using the carbon 2*s* and hydrogen 1*s* orbitals can take only two forms that meet the molecular symmetry requirements. One, σ, is bonding between all atoms, whereas σ* is antibonding between all nearest-neighbor atoms. No other combination corresponds to the symmetry of the ethene molecule.

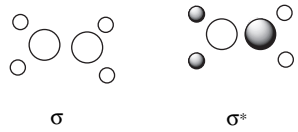

Let us next consider the interaction of $2p_y$ with the four hydrogen 1*s* orbitals. There are four possibilities that conform to the molecular symmetry.

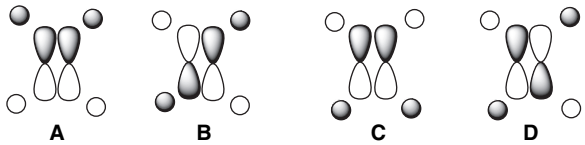

Orbital **A** is bonding between all nearest-neighbor atoms, whereas **B** is bonding within the CH_2 units but antibonding with respect to the two carbons. The orbital labeled **C** is C−C bonding but antibonding with respect to the hydrogens. Finally, orbital **D** is antibonding with respect to all nearest-neighbor atoms. Similarly, the $2p_x$ orbitals must be considered. Again, four possible combinations arise. Note that the nature of the overlap of the $2p_x$ orbitals is different from the $2p_y$ case, so the two sets of MOs have different energies.

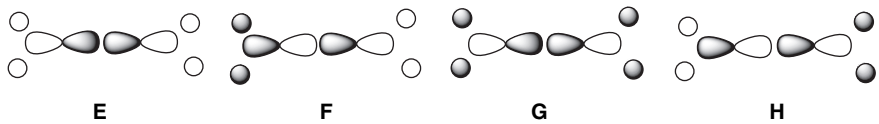

The final problem in construction of a qualitative MO diagram for ethene is the relative placement of the orbitals. There are some useful guidelines. The relationship between the relative energy and the number of nodes has already been mentioned. The more nodes, the higher the energy of the orbital. Since π-type interactions are normally weaker than σ-type, we expect the separation between σ and σ* to be greater than between π and π*. Within the sets

ABCD and **EFGH** we can order **A** < **B** < **C** < **D** and **E** < **F** < **G** < **H** on the basis that C–H bonding interactions outweigh C–C antibonding interactions arising from weaker *p*-*p* overlaps. Placement of the set **ABCD** in relation to **EFGH** is not qualitatively obvious. Calculations give the results shown in Figure 1.17.[54] Pictorial representations of the orbitals are given in Figure 1.18.

The kinds of qualitative considerations that we used to construct the ethene MO diagram do not give any indication of how much each atomic orbital contributes to the individual MOs. This information is obtained from the coefficients provided by the MO calculation. Without these coefficients we cannot specify the shapes of the MOs very precisely. However, the qualitative ideas do permit conclusions about the *symmetry* of the orbitals. As will be seen in Chapter 10, just knowing the symmetry of the MOs provides very useful insight into many chemical reactions.

1.2.5. Qualitative Application of MO Theory to Reactivity: Perturbational MO Theory and Frontier Orbitals

The construction of MO diagrams under the guidance of the general principles and symmetry restrictions that we have outlined can lead to useful insights into molecular structure. Now we want to consider how these concepts can be related to reactivity. In valence bond terminology, structure is related to reactivity in terms of the electronic nature of the substituents. The impact of polar and resonance effects on the electron

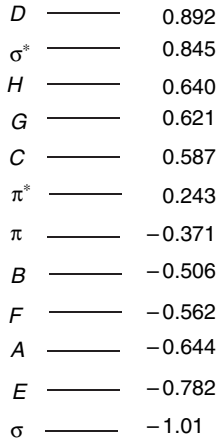

Fig. 1.17. Ethene molecular orbital energy levels. Energies are in atomic units. From W. L. Jorgensen and L. Salem, *The Organic Chemists Book of Orbitals*, Academic Press, New York, 1973.

54. W. L. Jorgensen and L. Salem, *The Organic Chemist's Book of Orbitals*, Academic Press, New York, 1973.

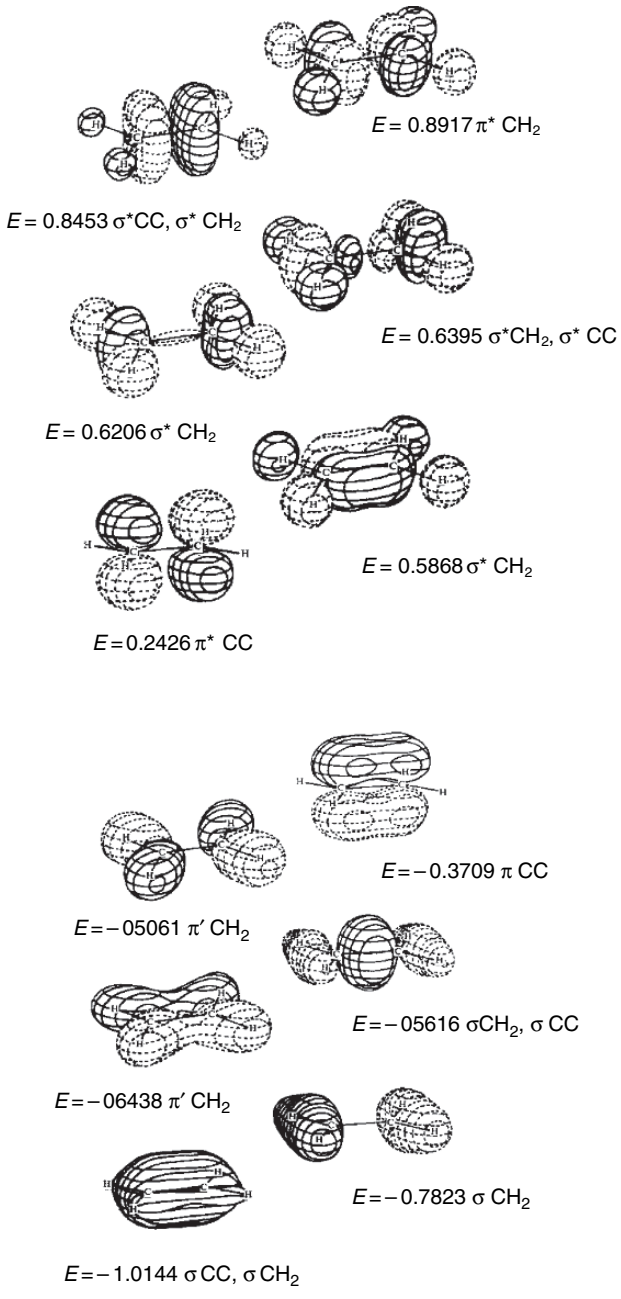

Fig. 1.18. Pictorial representation of ethene MOs. Reproduced with permission from W. L. Jorgensen and L. Salem, *The Organic Chemist's Book of Orbitals*, Academic Press, New York, 1973.

distribution and stability of reactants, transition structures, intermediates, and products is assessed and used to predict changes in reactivity. In MO theory, reactivity is related to the relative energies and shapes of the orbitals that are involved as the reactants are transformed into products. Reactions that can take place through relatively stable

intermediates and transition structures are more favorable than reactions that involve less stable ones. The *symmetry of the molecular orbitals* is a particularly important feature of many analyses of reactivity based on MO theory. The shapes of orbitals also affect the energy of reaction processes. Orbital shapes are defined by the atomic coefficients. The strongest interactions (bonding when the interacting orbitals have the same phase) occur when the orbitals have high coefficients on those atoms that undergo bond formation.

The qualitative description of reactivity in molecular orbital terms begins with a basic understanding of the MOs of the reacting systems. At this point we have developed a familiarity with the MOs of ethene and conjugated unsaturated systems from the discussion of HMO theory and the construction of the ethene MOs from atomic orbitals. To apply these ideas to new systems, we have to be able to understand how a change in structure will affect the MOs. One approach is called *perturbation molecular orbital theory* or PMO for short.[55] The system under analysis is compared to another related system for which the MO pattern is known. In PMO theory, the MO characteristics of the new system are deduced by analyzing how the change in structure affects the MO pattern. The type of changes that can be handled in a qualitative way include substitution of atoms by other elements, with the resulting change in electronegativity, as well as changes in connectivity that alter the pattern of direct orbital overlap. The fundamental thesis of PMO theory is that the resulting changes in the MO energies are relatively small and can be treated as adjustments (perturbations) on the original MO system.

Another aspect of qualitative application of MO theory is the analysis of interactions of the orbitals in reacting molecules. As molecules approach one another and reaction proceeds there is a mutual perturbation of the orbitals. This process continues until the reaction is complete and the product (or intermediate in a multistep reaction) is formed. The concept of *frontier orbital control* proposes that the most important interactions are between a particular pair of orbitals.[56] These orbitals are the highest filled orbital of one reactant (the HOMO) and the lowest unfilled (LUMO) orbital of the other reactant. We concentrate attention on these two orbitals because they are the closest in energy. A basic postulate of PMO theory is that *interactions are strongest between orbitals that are close in energy*. Frontier orbital theory proposes that these strong initial interactions guide the course of the reaction as it proceeds to completion. A further general feature of MO theory is that only MOs of matching symmetry can interact and lead to bond formation. Thus, analysis of a prospective reaction path focuses attention on the *relative energy* and *symmetry* of the frontier orbitals.

These ideas can be illustrated by looking at some simple cases. Let us consider the fact that the double bonds of ethene and formaldehyde have quite different chemical reactivities. Formaldehyde reacts readily with nucleophiles, whereas ethene does not. The π bond in ethene is more reactive toward electrophiles than the formaldehyde C=O π bond. We have already described the ethene MOs in Figures 1.17 and 1.18. How do those of formaldehyde differ? In the first place, the higher atomic number of

[55] C. A. Coulson and H. C. Longuet-Higgins, *Proc. R. Soc. London Ser. A*, **192**, 16 (1947); L. Salem, *J. Am .Chem. Soc.*, **90**, 543, 553 (1968); M. J. S. Dewar and R. C. Dougherty, *The PMO Theory of Organic Chemistry*, Plenum Press, New York, 1975; G. Klopman, *Chemical Reactivity and Reaction Paths*, Wiley-Interscience, New York, 1974, Chap. 4.

[56] K. Fukui, *Acc. Chem. Res.*, **4**, 57 (1971); I. Fleming, *Frontier Orbital and Organic Chemical Reactions*, Wiley, New York, 1976; L. Salem, *Electrons in Chemical Reactions*, Wiley, New York, 1982, Chap. 6.

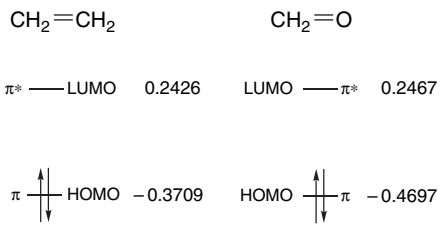

Fig. 1.19. Relative energy of the π and π^* orbitals in ethene and formaldehyde. Energies values in au are from W. L. Jorgensen and L. Salem, *The Organic Chemists Book of Orbitals*, Academic Press, New York, 1973.

oxygen provides two additional electrons, so that in place of the CH_2 group of ethene, the oxygen of formaldehyde has two pairs of nonbonding electrons. This introduces an additional aspect to the reactivity of formaldehyde. The oxygen atom can form a bond with a proton or a Lewis acid, which increases the effective electronegativity of the oxygen.

Another key change has to do with the frontier orbitals, the π (HOMO) and π^* (LUMO) orbitals. These are illustrated in Figure 1.19. One significant difference between the two molecules is the lower energy of the π and π^* orbitals in formaldehyde. These are lower in energy than the corresponding ethene orbitals because they are derived in part from the lower-lying (more electronegative) $2p_z$ orbital of oxygen. Because of its lower energy, the π^* orbital is a better acceptor of electrons from the HOMO of any attacking nucleophile than is the LUMO of ethene. We also see why ethene is more reactive to electrophiles than formaldehyde. In electrophilic attack, the HOMO acts as an electron donor to the approaching electrophile. In this case, because the HOMO of ethene lies higher in energy than the HOMO of formaldehyde, the electrons are more easily attracted by the approaching electrophile. The unequal electronegativities of the oxygen and carbon atoms also distort electron distribution in the π molecular orbital. In contrast to the symmetrical distribution in ethene, the formaldehyde π MO has a higher atomic coefficient at oxygen. This results in a net positive charge on the carbon atom, which is favorable for an approach by a nucleophile. One method of charge assignment (see Section 1.4.1) estimates that the π orbital has about 1.2 electrons associated with oxygen and 0.8 electrons associated with carbon, placing a positive charge of $+0.2e$ on carbon. This is balanced by a greater density of the LUMO on the carbon atom.

One principle of PMO theory is that the degree of perturbation is a function of the degree of overlap of the orbitals. Thus in the qualitative application of MO theory, it is important to consider the shape of the orbitals (as indicated quantitatively by their atomic coefficients) and the proximity that can be achieved by the orbitals within the limits of the geometry of the reacting molecules. Secondly, the strength of an interaction depends on the relative energy of the orbitals. The closer in energy, the greater the mutual perturbation of the orbitals. This principle, if used in conjunction with reliable estimates of relative orbital energies, can be of value in predicting the relative importance of various possible interactions.

Let us illustrate these ideas by returning to the comparisons of the reactivity of ethene and formaldehyde toward a nucleophilic species and an electrophilic species.

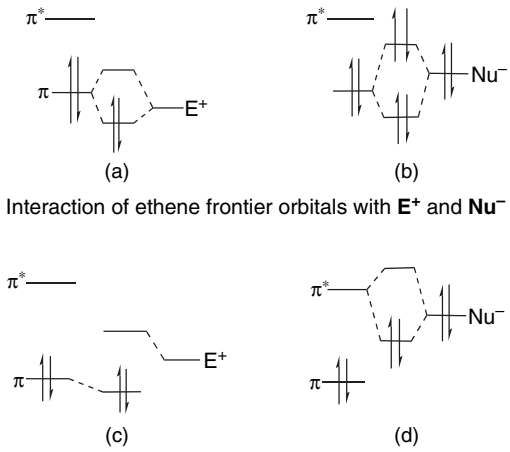

Fig. 1.20. PMO description of interaction of ethylene and formaldehyde with an electrophile ($\mathbf{E}^+$) and a nucleophile ($\mathbf{Nu}^-$).

The perturbations that arise as a nucleophile and an electrophile approach are sketched in Figure 1.20.

The electrophilic species $\mathbf{E}^+$ must have a low-lying empty orbital. The strongest interaction will be with the ethene π orbital and this leads to a stabilizing effect on the complex since the electrons are located in an orbital that is stabilized (Figure 1.20a). The same electrophilic species would lie further from the π orbital of formaldehyde since the formaldehyde orbitals are shifted to lower energy. As a result the mutual interaction with the formaldehyde HOMO will be weaker than in the case of ethene (Figure 1.20c). The conclusion is that an electrophile will undergo a greater stabilizing attraction on approaching ethene than it will on approaching formaldehyde. In the case of $\mathbf{Nu}^-$, a strong bonding interaction with π^* of formaldehyde is possible (Figure 1.20d). In the case of ethene, the strongest interaction is with the HOMO of the nucleophile, but this is a destabilizing interaction since both orbitals are filled and the lowering of one orbital is canceled by the raising of the other (Figure 1.20b). Thus we conclude that a nucleophile with a high-lying HOMO will interact more favorably with formaldehyde than with ethene.

The representations of nucleophilic attack on formaldehyde as involving the carbonyl LUMO and electrophilic attack on ethene as involving the HOMO also make a prediction about the trajectory of the approach of the reagents. The highest LUMO density is on carbon and it is oriented somewhat away from the oxygen. On the other hand, the ethene HOMO is the π orbital, which has maximum density at the midpoint above and below the molecular plane. Calculations of the preferred direction of attack of electrophilic and nucleophilic reagents are in accord with this representation, as shown below.[57]

[57] H. B. Bürgi, J. D. Dunitz, J. M. Lehn, and G. Wipff, *Tetrahedron*, **30**, 1563 (1974); H. B. Bürgi, J. M. Lehn, and G. Wipff, *J. Am. Chem. Soc.*, **96**, 1956 (1974); K. N. Houk, M. N. Paddon-Row, N. G. Rondan, Y.D. Wu, F. K. Brown, D. C. Spellmeyer, J. T. Metz, Y. Li, and R. J. Loncarich, *Science*, **231**, 1108 (1986).

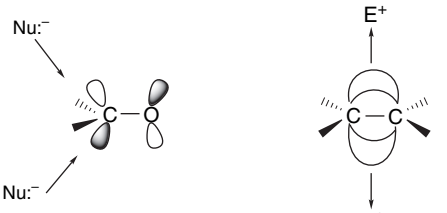

Preferred trajectory for nucleophilic attack.

Preferred trajectory for electrophilic attack.

The ideas of PMO theory can also be used to describe substituent effects. Let us consider, for example, the effect of a π-donor substituent and a π-acceptor substituent on the MO levels and reactivity of substituted ethenes. We can take the amino group as an example of a π-donor substituent. The nitrogen atom adds one additional $2p_z$ orbital and two electrons to the π system. The overall shape of the π orbitals for ethenamine is very similar to those of an allyl anion. The highest charge density is on the terminal atoms, i.e, the nitrogen atom and the ß-carbon, because the HOMO has a node at the center carbon. The HOMO in ethenamine resembles ψ_2 of the allyl anion and is higher in energy than the HOMO of ethene. It is not as high as the allyl ψ_2 because ethenamine is neutral rather than anionic and because of the greater electronegativity of the nitrogen atom. Thus we expect ethenamine, with its higher-energy HOMO, to be more reactive toward electrophiles than ethene. Furthermore, the HOMO has the highest coefficient on the terminal atoms so we expect an electrophile to become bonded to the ß-carbon or nitrogen, but not to the α-carbon. The LUMO corresponds to the higher-energy ψ_3 of the allyl anion, so we expect ethenamine to be even less reactive toward nucleophiles than is ethene.

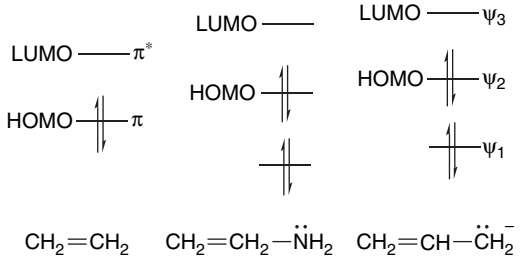

π MO energy levels for ethene with a π-donor substituent

An example of a π-acceptor group is the formyl group as in propenal (acrolein).

$$CH_2 = CHCH = O$$

In this case, the π MOs resemble those of butadiene. Relative to butadiene, however, the propenal orbitals lie somewhat lower in energy because of the more electronegative oxygen atom. This factor also increases the electron density at oxygen at the expense of carbon.

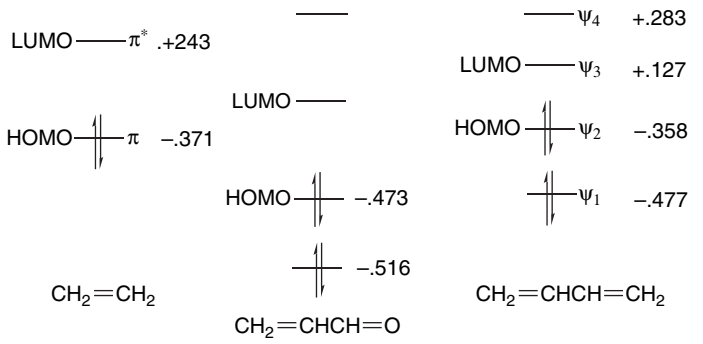

π MO energy levels in au for ethylene with a π-acceptor substituent. From Ref 54.

The LUMO, which is the frontier orbital in reactions with nucleophiles, has a larger coefficient on the ß-carbon atom, whereas the two occupied orbitals are distorted in such a way as to have larger coefficients on the oxygen. The overall effect is that the LUMO is relatively low lying and has a high coefficient on the ß-carbon atom. Frontier orbital theory therefore predicts that nucleophiles will react preferentially at the ß-carbon atom.

MO orbital calculations at the HF/6-31G** level have been done on both propenal and ethenamine. The resulting MOs were used to calculate charge distributions. Figure 1.21 gives the electron densities calculated for butadiene, propenal, and aminoethyene.[58] We see that the C(3) in propenal has a less negative charge than the terminal carbons in butadiene. On the other hand, C(2), the β-carbon in ethenamine, is more negative.

The MO approach gives the same qualitative picture of the substituent effect as described by resonance structures. The amino group is pictured by resonance as an electron donor, indicating a buildup of electron density at the ß-carbon, whereas the formyl group is an electron acceptor and diminishes electron density at the ß-carbon.

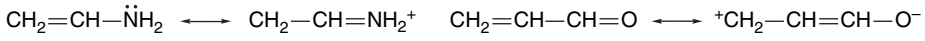

The chemical reactivity of these two substituted ethenes is in agreement with the MO and resonance descriptions. Amino-substituted alkenes, known as enamines, are very reactive toward electrophilic species and it is the ß-carbon that is the site of attack. For example, enamines are protonated on the ß-carbon. Propenal is an electrophilic alkene, as predicted, and the nucleophile attacks the ß-carbon.

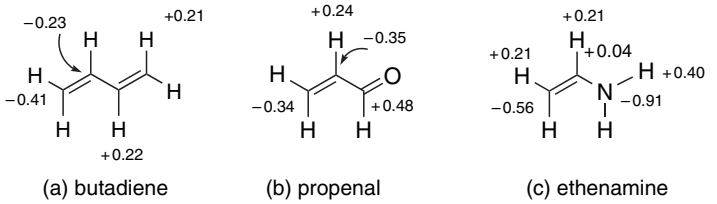

Fig. 1.21. Charge distribution in butadiene, acrolein, and aminoethylene based on HF/6-31G* calculations. From *J. Org. Chem.*, **59**, 4506 (1994).

58. M. A. McAllister and T. T. Tidwell, *J. Org. Chem.*, **59**, 4506 (1994).

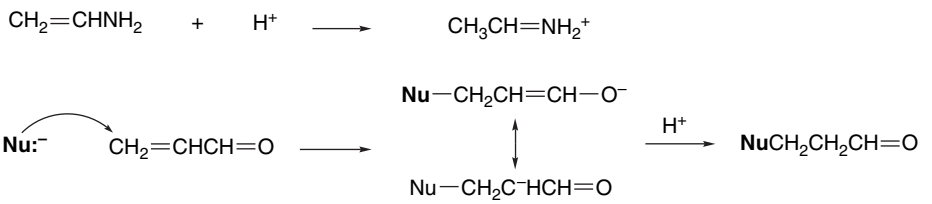

Frontier orbital theory also provides the framework for analysis of the effect that the orbital symmetry has on reactivity. One of the basic tenets of PMO theory is that the symmetries of two orbitals must match to permit a strong interaction between them. This symmetry requirement, used in the context of frontier orbital theory, can be a very powerful tool for predicting reactivity. As an example, let us examine the approach of an allyl cation and an ethene molecule and ask whether the following reaction is likely to occur:

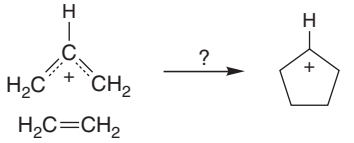

The positively charged allyl cation would be the electron acceptor in any initial interaction with ethene. Therefore to consider this reaction in terms of frontier orbital theory, the question we have to ask is: "Do the ethene HOMO and allyl cation LUMO interact favorably as the reactants approach one another?" The orbitals that are involved are shown in Figure 1.22. If we assume that a symmetrical approach is necessary to simultaneously form the two new bonds, we see that the symmetries of the two orbitals do not match. Any bonding interaction developing at one end is canceled by an antibonding interaction at the other end. The conclusion drawn from this analysis is that this particular reaction process is not favorable. We would need to consider other modes of approach to examine the problem more thoroughly, but this analysis

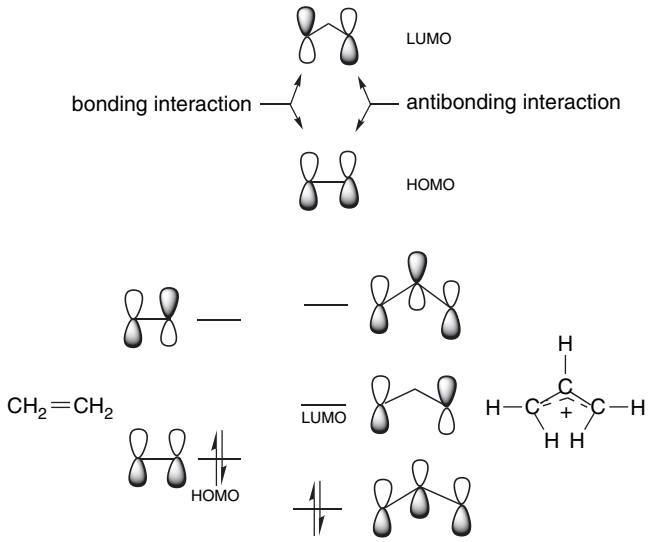

Fig. 1.22. MOs for ethene and allyl cation.

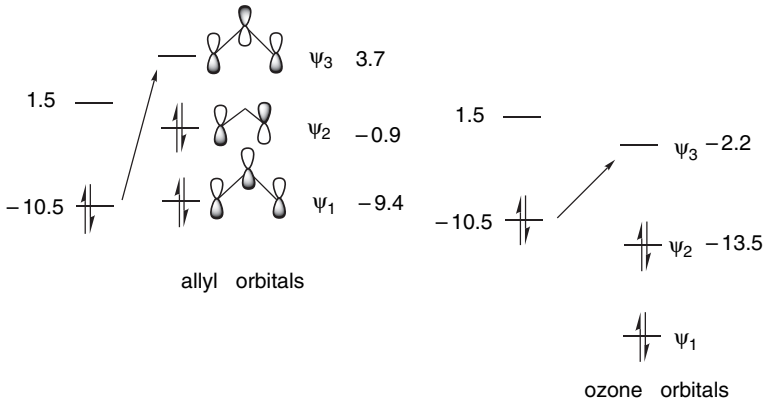

Fig. 1.23. Comparison of FMO interactions of ethene with an allyl anion and ozone.

indicates that simultaneous (concerted) bond formation between ethene and an allyl cation to form a cyclopentyl cation will not occur.

Another case where orbital symmetry provides a useful insight is ozonolysis, which proceeds through a 1,2,3-trioxolane intermediate to a 1,2,4-trioxolane (ozonide) product.

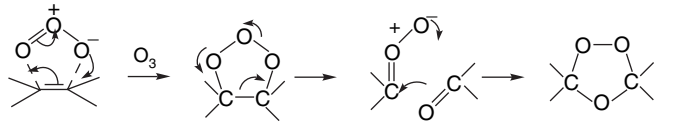

Each step in this reaction sequence is a *concerted reaction* and therefore requires matching of orbital symmetry. The first step is a *cycloaddition reaction*, the second is a *cycloreversion*, and the third is another cycloaddition.[59] Furthermore, because of the electronegative character of O_3 relative to a C=C double bond, we anticipate that O_3 will furnish the LUMO and the alkene the HOMO. The π orbitals of ozone are analogous to those of an allyl anion, although much lower in energy, and contain four π electrons. We see that concerted bond formation is possible. Because of the large shift in the placement of the orbitals, the strongest interaction is between the ethene HOMO and the O_3 LUMO. The approximate energies (eV) shown in Figure 1.23 are from CNDO calculations.[60]

In contrast to the reaction of ethene with ozone, which is very fast, the reaction with an allyl anion itself is not observed, even though the reaction does meet the symmetry requirement.

A major factor is the absence of an electrophilic component, that is, a species with a low-lying LUMO. The energy of ψ_3 for of allyl anion lies well above the π orbital of ethene.[61]

[59] R. C. Kuczkowski, *Chem. Soc. Rev.*, **21**, 79 (1992).
[60] K. N. Houk, J. Sims, C. R. Watts, and L. J. Luskus, *J. Am. Chem. Soc.*, **95**, 7301 (1973).
[61] R. R. Sauers, *Tetrahedron Lett.*, **37**, 7679 (1996).

The concepts of PMO and frontier orbital theory can be related to the characteristics of hard-hard and soft-soft reactions. Recall that hard-hard reactions are governed by electrostatic attractions, whereas soft-soft reactions are characterized by partial bond formation. The hard-hard case in general applies to situations in which there is a large separation between the HOMO and LUMO orbitals. Under these conditions the stabilization of the orbitals is small and the electrostatic terms are dominant. In soft-soft reactions, the HOMO and LUMO are close together, and the perturbational stabilization is large.

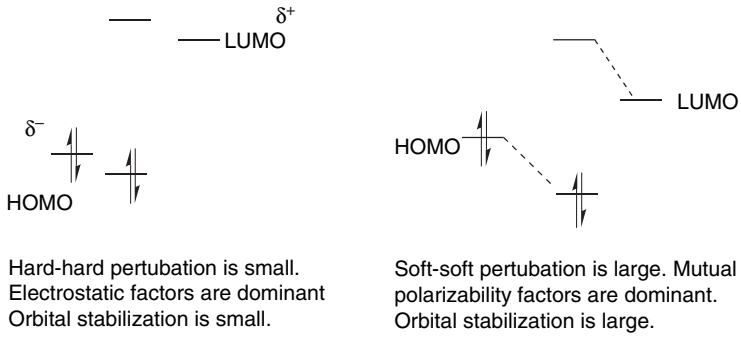

Hard-hard pertubation is small. Electrostatic factors are dominant Orbital stabilization is small.

Soft-soft pertubation is large. Mutual polarizability factors are dominant. Orbital stabilization is large.

1.2.6. Numerical Application of MO Theory

Molecular orbital computations are currently used extensively for calculation of a range of molecular properties. The energy minimization process can provide detailed information about the most stable structure of the molecule. The total binding energy can be related to thermodynamic definitions of molecular energy. The calculations also provide the total electron density distribution, and properties that depend on electron distribution, such as dipole moments, can be obtained. The spatial distribution of orbitals, especially the HOMO and LUMO, provides the basis for reactivity assessment. We illustrate some of these applications below. In Chapter 3 we show how MO calculations can be applied to intermediates and transitions structures and thus help define reaction mechanisms. Numerical calculation of spectroscopic features including electronic, vibrational, and rotational energy levels, as well as NMR spectra is also possible.

Most MO calculations pertain to the *gas phase*. The effect of solvent can be probed by examining the effect of the dielectric constant on the structure and energy of molecules. The most common treatment of solvation effects is by one of several *continuum models*, which describe the change in energy as a result of *macroscopic solvation effects*. They describe averaged effects of the solvent, rather than specific interactions. The calculations require information about the shape of the molecule and its charge distribution, which are available from the MO computation. The molecule is represented as a surface reflecting van der Waal radii and point charges corresponding to charge separation. The solvent is characterized by a dielectric constant chosen to correspond to the solvent of interest. The calculations take into account electrostatic, polarization, and repulsive interactions with the solvent. A commonly used procedure is the polarizable continuum model (PCM).[62] The application of a solvation model

[62] J. Tomasi and M. Persico, *Chem. Rev.*, **94**, 2027 (1994); V. Barone, M. Cossi, and J. Tomasi, *J. Phys. Chem.*, **107**, 3210 (1997).

can adjust the relative energy of molecules. Species with substantial charge separation will be stabilized most strongly.

Current ab initio methods give computed molecular structures that are in excellent agreement with experimental results. Quite good agreement is obtained using relatively small basis sets, without the need for correlation corrections. Scheme 1.4 compares the bond lengths for some small compounds calculated at the MP2/6-31G* level with experimental values.

Quite good energy comparisons can also be obtained. The MO calculations pertain to a rigid molecule at 0 K, so corrections for zero-point energy and temperature effects must be made for comparison with thermodynamic data (see Section 3.1). The various computational methods differ in their scope of application and reliability. All give good results for most small hydrocarbons. A particularly challenging area is small ring compounds and other strained molecules. Table 1.10 gives some data comparing agreement for some small hydrocarbons and also for some strained molecules.

A common numerical application of MO calculations is to compare the stability of related compounds. For example, in the discussion of both resonance and qualitative MO theory, we stated that "stabilization" results from attachment of conjugating substituents to double bonds. We might ask, "How much stabilization?" One way to answer this question is to compare the total energy of the two compounds, but since they are not isomers, simple numerical comparison is not feasible. We discuss various ways to make the comparison, and some of the pitfalls, in Chapter 3, but one method is to use *isodesmic reactions.* These are hypothetical reactions in which *the number of each kind of bond is the same on each side of the equation*. For the case of substituents on double bonds the isodesmic reaction below estimates the added stabilization, since it is balanced with respect to bond types. Any extra stabilization owing to substituents will appear as an energy difference.

$$CH_3CH_2-H+CH_2=CH-X \longrightarrow CH_3CH_2-X+CH_2=CH-H \quad E = \text{stabilization}$$

Scheme 1.4. Comparison of Computed and Experimental Bond Lengths[a]

(Upper number is MP2/6-31G* computed bond length. Lower number is experimental value.)

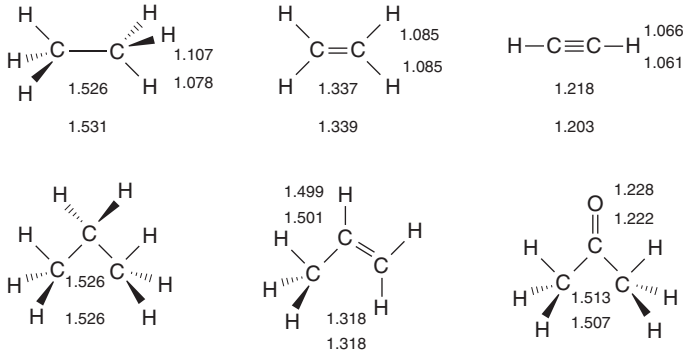

a. From E. Lewars, *Computational Chemistry*, Kluwer Academic Publishers, Boston 2003, pp. 255–260.

Table 1.10. Comparison of Differences in kcal/mol between Computed and Experimental ΔH_f for Some Hydrocarbons

	MNDO[a]	AM1[b]	PM3[c]	HF/6-31G*[a]	G2[d]
Methane	5.9	9.0	4.9	−0.5	0.7
Ethane	0.3	2.6	2.1	0.9	−0.2
Butane	0.7	−0.7	1.3	−0.8	−0.6
Pentane	0.7	−2.8	0.6	−0.5	
Cyclopentane	−11.9	−10.4	−5.6	4.0	−0.4
Cyclohexane	−5.3	−9.0	−1.5	3.1	3.9
Cyclopropane					−1.6
Cyclobutane					−1.5
Bicyclo[1.1.0]butane					−1.5
Bicyclo[2.2.1]heptane	2.1	−2.0	−1.3	8.8	
Bicyclo[2.2.2]octane	−2.2	−11.9	−3.7	10.7	
Ethene	3.1	4.0	4.2	−2.4	0.3
Allene	−1.6	0.6	1.5	−6.8	0.0[e]
1,3-Butadiene	2.7	3.6	5.0	−2.9	0.5[f]
Benzene	1.5	2.2	3.6		4.0[g]

a. M. J. S. Dewar, E. G. Zoebisch, E. F. Healy, and J. J. P. Stewart, *J. Am. Chem. Soc.*, **107**, 3902 (1985).
b. M. J. S. Dewar and D. M. Storch, *J. Am. Chem. Soc.*, **107**, 3898 (1985).
c. J. J. P. Stewart, *J. Comput. Chem.*, **10**, 221 (1989).
d. J. A. Pople, M. Head-Gordon, D. J. Fox, K. Raghavachari, and L. A. Curtiss, *J. Chem. Phys.*, **90**, 5622 (1989); L. A. Curtiss, K. Raghavachari, G. W. Trucks, and J. A. Pople, *J. Chem. Phys.*, **94**, 7221 (1991); L. A. Curtiss, K. Raghavachari, P. C. Redfern, and J. Pople, *J. Phys. Chem.*, **106**, 1063 (1997).
e. D. W. Rogers and F. W. McLafferty, *J. Phys. Chem.*, **99**, 1375 (1993).
f. M. N. Glukhovtsev and S. Laiter, *Theor. Chim. Acta*, **92**, 327 (1995).
g. A. Nicolaides and L. Radom, *J. Phys. Chem.*, **98**, 3092 (1994).

The results using HF/4-31G[63] and HF/6-31G**[64] for some common substituents are given below. They indicate that both electron-donating groups, such as amino and methoxy, and electron-withdrawing groups, such as formyl and cyano, have a stabilizing effect on double bonds. This is consistent with the implication of resonance that there is a stabilizing interaction as a result of electron delocalization.

Stabilization (kcal/mol)

Substituent	HF/4-31G	HF/6-31G**
CH_3	3.2	3.05
NH_2	11.2	7.20
OH	6.6	6.43
OCH_3	6.1	
F		0.99
Cl		−0.54
CH=O	4.5	
CN	2.4	
CF_3	−2.5	

The dipole moments of molecules depend on both the molecular dimensions and the electron distribution. For example, *Z*-1,2-dichloroethene has a dipole moment of 1.90 D, whereas, owing to its symmetrical structure, the *E* isomer has no molecular dipole.

63. A. Greenberg and T. A. Stevenson, *J. Am. Chem. Soc.*, **107**, 3488 (1985).
64. K. B. Wiberg and K. E. Laidig, *J. Org. Chem.,* **57**, 5092 (1992).

Table 1.11. Comparison of Computed and Experimental Molecular Dipoles[a]

	HF/6-31G*	MP2/6-31G*	Experimental
$CH_3C{\equiv}CH$	0.64	0.66	0.75
CH_3OCH_3	1.48	1.60	1.30
CH_3OH	1.87	1.95	1.70
CH_3Cl	2.25	2.21	1.87
$(CH_3)_2SO$	4.50	4.63	3.96

a. From E. Lewars, *Computational Chemistry*, Kluwer Academic Publishers, Boston, 2003, pp 296–300.

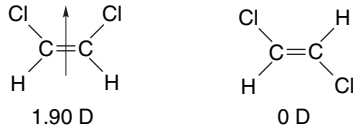

MO calculations of molecular dipoles involves summing the electron distribution in the filled orbitals. Although calculating the order correctly, both HF/6-31G* and MP2/6-31G* calculations seem to overestimate the dipole moments of small polar molecules (Table 1.11).

MO calculations can also be applied to reactions. The effect of substituents on the acidity (pK_a) of carboxylic acids is a well-studied area experimentally. Shields and co-workers used several of the ab initio protocols to calculate the aqueous acidity of some substituted carboxylic acids relative to acetic acid,[65] which represented quite a challenging test of theory. The dissociation of a carboxylic acid involves formation of ions, and solvation is a major component of the free energy change. Furthermore, solvation introduces both enthalpy and entropy components. The calculations were approached using a thermodynamic cycle that includes the energies of solvation of the neutral acids and the anion. Since the calculation is relative to acetic acid, the energy of solvation of the proton cancels out.

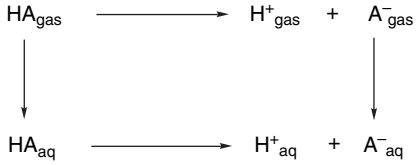

Calculated Solvation Energies CPCM/HF/6-31+G(*d*) (kcal/mol)

X-CO_2H	HA	Exp	A^-	Experimental
H	−8.23		−77.10	
CH_3	−7.86	−6.69	−77.58	−77
$ClCH_2$	−10.61		−70.57	
$NCCH_2$	−14.52		−69.99	
$(CH_3)_3C$	−6.70		−72.42	

65. A. M. Toth, M. D. Liptak, D. L. Phillips, and G. C. Shields, *J. Chem. Phys.*, **114**, 4595 (2001).

Table 1.12. Calculated pK_a Relative to Acetic Acid[a]

X-CO_2H	CBS-4	CBS-QB3	G-2	G2(MP2)	G3	Experimental
H	2.46	3.10	3.83	3.88	4.02	3.75
CH_3[b]	[4.75]	[4.75]	[4.75]	[4.75]	[4.75]	4.75
$ClCH_2$	3.30	2.92	3.37	3.37	3.18	2.85
$NCCH_2$	1.38	1.90	2.31	2.32	1.90	2.45
$(CH_3)_3C$	5.08	4.75	6.28	6.24	6.20	5.03

a. CPCM/HF/6-31+G(*d*) continuum solvent model
b. Reference standard.

The differences in ionization energies are only a small fraction (1–5 kcal/mol) of the total gas phase ionization energies (325–350 kcal/mol), and the solvation terms for the anions are quite large (70–80 kcal/mol). The results from CBS-4, CBS-QB3, G2, G2(MP), and G3, along with the experimental results are shown in Table 1.12. The calculation reproduces the electron-withdrawing and acid-strengthening effect of substituents such as Cl and CN and the acid-weakening effect of the *t*-butyl group. The mean errors ranged between 0.4 and 1.2 kcal/mol for the various methods.

1.3. Electron Density Functionals

Another means of calculating molecular properties is based on *density functional theory* (DFT),[66] which focuses on the total electron density of a molecule. The introduction of efficient versions of density functional theory in the 1990s profoundly altered computational chemistry. Computational study of medium-sized organic and organometallic systems is currently dominated by density functional methods. DFT methods are founded on a theorem by Hohenberg and Kohn that states that the exact energy for a ground state system is defined entirely by the electron density and the functional of that density that links it to the energy.[67] This means that the density functional contains all the information on electron correlation. The invention of useful approximations to the functional has made DFT powerful and popular.

DFT calculations describe the electron density ρ at a point in a particular field, designated $n(\mathbf{r})$. The external potential operating on this field, symbolized by $\upsilon(\mathbf{r})$, is generated by the atomic nuclei. The electron distribution is specified by $\rho(\mathbf{r})$, which is the measure of electron density per unit volume at any point **r**. Integration over space provides the information needed to describe the structure and electron distribution of molecules. The calculation involves the construction of an expression for the electron density. The energy of the system is expressed by the Kohn-sham equation.[68]

$$E = T + \nu_{en} + J_{ee} + \nu_{xc} \tag{1.18}$$

where T is the kinetic energy, υ_{en} and J_{ee} are electrostatic electron-nuclear and electron-electron interactions, respectively, and υ_{xc} are electron correlation and exchange effects.

The energy function F contains terms for kinetic energy, electrostatic interactions, and exchange and correlation energy:

66. R. G. Parr and W. Yang, *Density Functional Theory of Atoms and Molecules*, Oxford University Press, Oxford, 1989; W. Kohn, A. D. Becke, and R. G. Parr, *J. Phys. Chem.*, **100**, 12974 (1996).
67. P. Hohenberg and W. Kohn, *Phys. Rev. A*, **136**, 864 (1964); M. Levy, *Proc. Natl. Acad. Sci. USA*, **76**, 6062 (1979).
68. W. Kohn and L. J. Shan *Phys. Rev. A,* **140**, 1133 (1965).

$$F[n(\mathbf{r})] = T_s[n(\mathbf{r})] + 1/2 \int \frac{n(\mathbf{r})n(\mathbf{r})}{|r - r'|} dr dr' + E_{xc}[n(\mathbf{r})] \tag{1.19}$$

The energy of the system is given by integration:

$$E = \sum_{1}^{0} \varepsilon_j - \frac{1}{2} \int \frac{n(\mathbf{r})n(\mathbf{r}')}{|r - r'|} dr dr' - \int \nu_{xc}(\mathbf{r})n(\mathbf{r})dr + E_{xc}[n(\mathbf{r})] \tag{1.20}$$

In principle, these equations provide an exact description of the energy, but the value $E_{xc}[n(\mathbf{r})]$ is not known. Although $E_{xc}[n(\mathbf{r})]$ cannot be formulated exactly, Kohn and Sham developed equations that isolate this term:

$$h_i^{KS}\chi_i = \varepsilon_i \chi_i$$

$$h_i^{KS} = -\frac{1}{2}\nabla_i^2 - \sum \frac{Z_A}{|r_i - R_A|} + \int \frac{\rho(r')}{|r_i - r'_i|} dr' + V_{XC}[\rho]$$

Various approximations have been developed and calibrated by comparison with experimental data and MO calculations. The strategy used is to collect the terms that can be calculated exactly and parameterize the remaining terms. Parameters in the proposed functionals are generally selected by optimizing the method's description of properties of a training set of molecular data. The methods used most frequently in organic chemistry were developed by A. D. Becke.[69] Lee, Yang, and Parr[70] (LYP) developed a correlation functional by a fit to exact helium atom results. Combining such "pure DFT" functionals with the Hartree-Fock form of the exchange is the basis for the hybrid methods. Becke's hybrid exchange functional called "B3," combined with the LYP correlation functional, is the most widely applied of the many possible choices of exchange and correlation functionals. This is called the B3LYP method. Much of the mechanics for solution of the Kohn-Sham equations is analogous to what is used for solution of the SCF (Hartree-Fock) equations and employs the same basis sets. That is, a guess is made at the orbitals; an approximation to the Kohn-Sham Hamiltonian h_i^{KS} is then reconstructed using the guess. Revised orbitals are recovered from the Kohn-Sham equations, the Hamiltonian is reconstructed, and the process continued until it converges.

DFT computations can be done with less computer time than the most advanced ab initio MO methods. As a result, there has been extensive use of B3LYP and other DFT methods in organic chemistry. As with MO calculations, the minimum energy geometry and total energy are calculated. Other properties that depend on electronic distribution, such as molecular dipoles, can also be calculated.

A number of DFT methods and basis sets have been evaluated for their ability to calculate bond distances in hydrocarbons.[71] With the use of the B3LYP functionals, the commonly employed basis sets such as 6-31G* and 6-31G** gave excellent correlations with experimental values but overestimated C–H bond lengths by about 0.1 Å, while C–C bond lengths generally were within 0.01 Å. Because of the systematic variation, it is possible to apply a scaling factor that predicts C–H bond lengths with high accuracy. Ground state geometries have also been calculated (B3LYP) for molecules such as formaldehyde, acetaldehyde, and acetone.

69. A. D. Becke, *Phys. Rev. A*, **38**, 3098 (1988); A. D. Becke, *J. Chem. Phys.*, **96**, 2155 (1992); A. D. Becke, *J. Chem. Phys.*, **97**, 9173 (1992); A. D. Becke, *J. Chem. Phys.*, **98**, 5648 (1993).
70. C. Lee, W. Yang and R. G. Parr, *Phys. Rev. B*, **37**, 785 (1988).
71. A Neugebauer and G. Häflinger, *Theochem*, **578**, 229 (2002).

Bond Distances in Carbonyl Compounds

Basis set	CH_2=O		CH_3CH=O			$(CH_3)_2$C=O	
	C−H	C=O	C−H	C=O	C−C	C=O	C−C
Experiment	1.108	1.206	1.106	1.213	1.504	1.222	1.507
311++G** [a]	1.105	1.201	1.109	1.205	1.502	1.211	1.514
aug-CCPVDZ[b]	1.114	1.207					

a. W. O. George, B. F. Jones, R. Lewis, and J. M. Price, *J. Molec. Struct.*, **550/551**, 281 (2000).
b. B. J. Wang, B. G. Johnson, R. J. Boyd, and L. A. Eriksson, *J. Phys. Chem.*, **100**, 6317 (1996).

In Chapter 3, we compare the results of DFT calculations on the relative thermodynamic stability of hydrocarbons with those from MO methods. There is some indication that B3LYP calculations tend to underestimate the stability of hydrocarbons as the size of the molecule increases. For example, with the 6-311++G($3df$, $2p$) basis set, the error calculated for propane (−1.5 kcal/mol), hexane (−9.3), and octane (−14.0) increased systematically.[72] Similarly, when the effect of successive substitution of methyl groups on ethane on the C−C bond energy was examined, the error increased from 8.7 kcal/mol for ethane to 21.1 kcal/mol for 2,2,3,3-tetramethylbutane (addition of six methyl groups, B3LYP/6-311++G(d, p). The trend for the MP2/6-311++G (d, p) was in the same direction, but those were considerably closer to the experimental value.[73] The difficulty is attributed to underestimation of the C–C bond strength. As we study reactions, we will encounter a number of cases where DFT calculations have provided informative descriptions of both intermediates and transition structures.[74] In these cases, there is presumably cancellation of these kinds of systematic errors, because the comparisons that are made among reactants, intermediates, and product compare systems of similar size. Use of isodesmic reactions schemes should also address this problem.

DFT calculations have been used to compute the gas phase acidity of hydrocarbons and compare them with experimental values, as shown in Table 1.13. The

Table 1.13. Gas Phase Enthalpy of Ionization of Hydrocarbons in kcal/mol by B3LYP/6-311++G Computation**

Compound	ΔH_{calc}	ΔH_{exp}
CH_4[a]	416.8	416.7
C_2H_6[a]	419.4	420.1
$CH_3CH_2CH_3$ (*pri*)[a]	416.5	419.4
$CH_3CH_2CH_3$ (*sec*)[a]	414.4	415.6
$(CH_3)_3CH$ (*tert*)[a]	410.2	413.1
Cyclopropane[b]	411.5	411.5
Bicyclo[1.1.0]butane[b]	396.7	399.2
Bicyclo[1.1.1]pentane[b]	407.7	–
Cubane[b]	406.7	404.0
$CH_2=CH_2$[a]	405.8	407.5
HC≡CH[a]	375.4	378.8

a. P. Burk and K. Sillar, *Theochem*, **535**, 49 (2001).
b. I. Alkorta and J. Elguero, *Tetrahedron*, **53**, 9741 (1997).

72. L. A. Curtiss, K. Ragahavachari, P. C. Redfern and J. A. Pople, *J. Chem. Phys.*, **112**, 7374 (2000).
73. C. E. Check and T. M. Gilbert, *J. Org. Chem.*, **70**, 9828 (2005).
74. T. Ziegler, *Chem. Rev.*, **91**, 651 (1991).

Table 1.14. Gas Phase Ionization Energies in kcal/mol for Some Strong Acids[a]

Acid	DFT	Experimental		DFT
H_2SO_4	306	302.2	$ClSO_3H$	292.6
FSO_3H	295.9	299.8	$HClO_4$	298.5
CF_3SO_3H	297.7	299.5	HBF_4	293.1
CH_3SO_3H	317.0	315.0	$H_2S_2O_7$	280.2
CF_3CO_3H	316.0	316.3	$HSbF_6$	262.4

a. From B3LYP/6-311+G** computations. Ref. 75.

agreement with experimental values is quite good. The large differences associated with hydridization changes are well reproduced. The increased acidity of strained hydrocarbons such as cyclopropane, bicyclo[1.1.1]butane, and cubane is also reproduced. For acyclic alkanes, the acidity order is *tert*-H > *sec*-H > *pri*-H, but methane is more acidic than ethane. We discuss the issue of hydrocarbon acidity further in Topic 3.1.

DFT computations can be extended to considerably larger molecules than advanced ab initio methods and are being used extensively in the prediction and calculation of molecular properties. A recent study, for example, examined the energy required for ionization of very strong acids in the gas phase.[75] Good correlations with experimental values were observed and predictions were made for several cases that have not been measured experimentally, as shown in Table 1.14.

Apart from its computational application, the fundamental premises of DFT lead to a theoretical foundation for important chemical concepts such as electronegativity and hardness-softness. The electron density distribution should also be capable of describing the structure, properties, and reactivity of a molecule. We explore this aspect of DFT in Topic 1.5.

1.4. Representation of Electron Density Distribution

The total electron density distribution is a physical property of molecules. It can be approached experimentally by a number of methods. Electron density of solids can be derived from X-ray crystallographic data.[76] However, specialized high-precision measurements are needed to obtain information that is relevant to understanding chemical reactivity. Gas phase electron diffraction can also provide electron density data.[77] The electron density is usually depicted as a comparison of the observed electron density with that predicted by spherical models of the atoms and is called *deformation electron density*. For example, Figure 1.24 is the result of a high-precision determination of the electron density in the plane of the benzene ring.[78] It shows an accumulation of electron density in the region between adjacent atoms and depletion of electron density in the center and immediately outside of the ring. Figure 1.25

75. I. A. Koppel, P. Burk, I. Koppel, I. Leito, T. Sonoda, and M. Mishima, *J. Am. Chem. Soc.*, **122**, 5114 (2000).
76. P. Coppens, *X-ray Charge Densities and Chemical Bonding*, Oxford University Press, Oxford, 1997.
77. S. Shibata and F. Hirota, in *Stereochemical Applications of Gas-Phase Electron Diffraction,* I. Hargittai and M. Hargittai, eds., VCH Publishers, New York, 1988, Chap. 4.
78. H.-B. Burgi, S. C. Capelli, A. E. Goeta, J. A. K. Howard, M. A. Sparkman, and D. S. Yufit, *Chem. Eur. J.*, **8**, 3512 (2002).

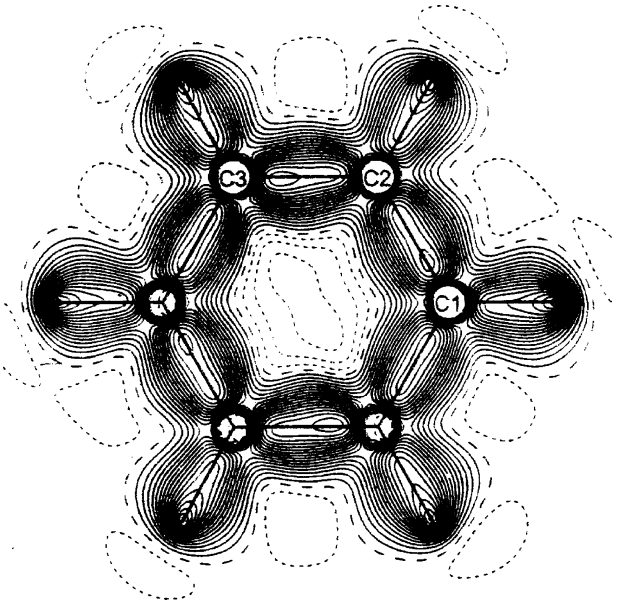

Fig. 1.24. Deformation electron density in the molecular plane of benzene. Contours at $0.05e\,\text{Å}^{-3}$ intervals. Positive contours are solid; negative contours are dashed. From *Chem. Eur. J.*, **8**, 3512 (2002).

shows electron density difference maps for benzene in and perpendicular to the molecular plane. The latter representation shows the ellipsoidal distribution owing to the π bond. These experimental electron density distributions are consistent with our concept of bonding. Electron density accumulates between the carbon-carbon and carbon-hydrogen bond pairs and constitutes both the σ and π bonds. The density above and below the ring is ellipsoid, owing to the π component of the bonding.

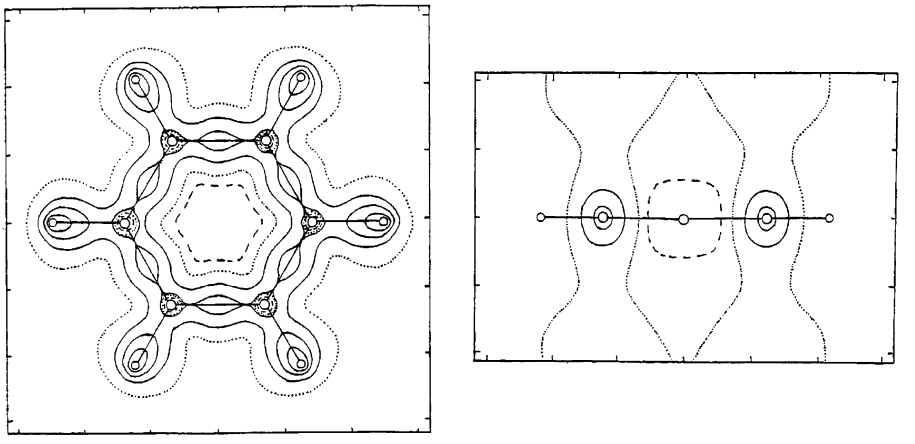

Fig. 1.25. Deformation electron density maps for benzene. (a) In the plane of the ring. (b) Perpendicular to the ring and intersecting a C−C bond. The positive contours (solid lines) are in steps of $0.2e\text{Å}^{-3}$ and negative contours (dashed lines) in steps of $0.1e\text{Å}^{-3}$. From S. Shibata and F. Hirota, in *Stereochemical Applications of Gas-Phase Electron Diffraction,* I. Hargittai and M. Hargittai, eds., VCH Publishers, Weinheim, 1988, Chap. 4.

Figure 1.26 presents data for formaldehyde. Panel (a) is the theoretical electron density in the molecular plane. It shows the expected higher electron density around oxygen. The hydrogen atoms are represented by the small peaks extending from the large carbon peak. The electron density associated with the C–H bonds is represented by the ridge connecting the hydrogens to carbon. Panels (b) and (c) are difference maps. Panel (b) shows the accumulation of electron density in the C–H bonding regions and that corresponding to the oxygen unshared electrons. Panel (c) shows the net accumulation of electron density between the carbon and oxygen atoms, corresponding to the σ and π bonds. The electron density is shifted toward the oxygen.

These experimental electron density distributions are in accord with the VB, MO, and DFT descriptions of chemical bonding, but are not easily applied to the determination of the relatively small differences caused by substituent effects that are of primary interest in interpreting reactivity. As a result, most efforts to describe electron density distribution rely on theoretical computations. The various computational approaches to molecular structure should all arrive at the same "correct" *total electron distribution*, although it might be partitioned among orbitals differently. The issue we discuss in this section is how to interpret information about electron density in a way that is chemically informative, which includes efforts to partition the total electron density among atoms. These efforts require a definition (model) of the atoms, since there is no inherent property of molecules that partitions the total electron density among individual atoms.

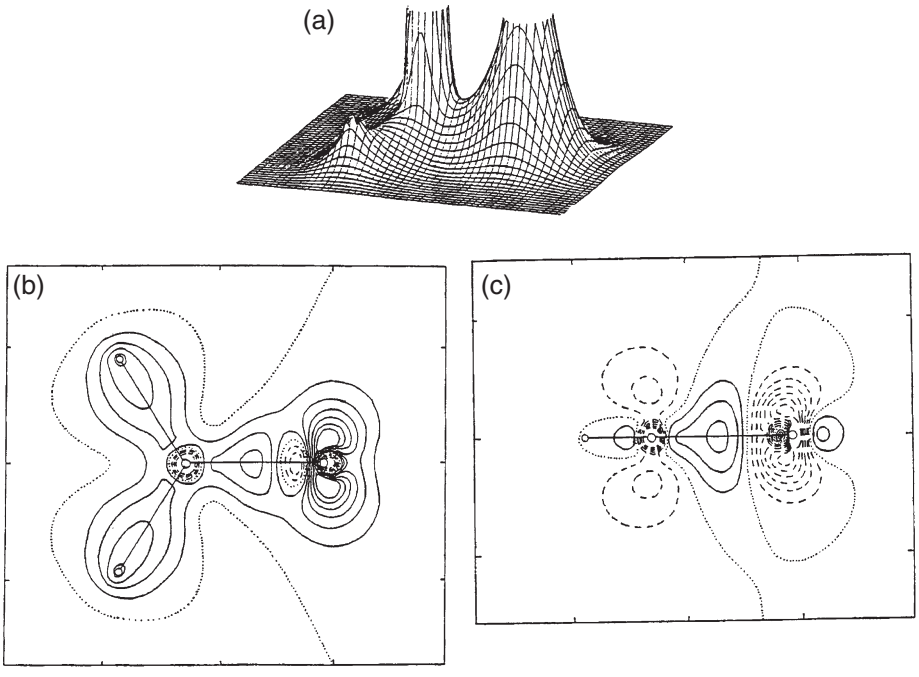

Fig. 1.26. Comparison of electron density of formaldehyde with a spherical atom model: (a) total electron density in the molecular plane; (b) the electron density difference in the molecular plane; (c) the electron density difference in a plane perpendicular to the molecular plane. The contours in (b) and (c) are in steps of $0.2e$Å^{-3}. The solid contours are positive and the dashed contours are negative. From S. Shibata and F. Hirota, in *Stereochemical Applications of Gas-Phase Electron Diffraction*, I. Hargittai and M. Hargittai, eds., VCH Publishers, Weinheim, 1988, Chap. 4.

Qualitative VB theory uses resonance structures and bond polarity relationships to arrive at an indication of relative charge distribution. For example, in propenal the combination of a preferred resonance structure and the higher electronegativity of oxygen relative to carbon leads to the expectation that there will be a net negative charge on oxygen and compensating positive charges on C(1) and C(3) (see p. 21). How much the hydrogen atoms might be affected is not clear. As a first approximation, they are unaffected, since they lie in the nodal plane of the conjugated π system, but because the electronegativity of the individual carbons is affected, there are second-order adjustments.

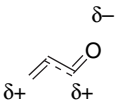

Numerical expression of atomic charge density in qualitative VB terminology can be obtained by use of the electronegativity equalization schemes discussed in Section 1.1.4. The results depend on assumptions made about relative electronegativity of the atoms and groups. The results are normally in agreement with chemical intuition, but not much use is made of such analyses at the present time. MO calculations give the total electron density distribution as the sum of the electrons in all the filled molecular orbitals. The charge distribution for individual atoms must be extracted from the numerical data. Several approaches to the goal of numerical representation of electron distribution have been developed.[79]

1.4.1. Mulliken Population Analysis

In MO calculations, the total electron density is represented as the sum of all populated MOs. The electron density at any atom can be obtained by summing the electron density associated with the basis set orbitals for each atom. Electron density shared by two or more atoms, as indicated by the overlap integral, is partitioned equally among them. This is called a *Mulliken population analysis*.[80]

$$P = 2 \sum_{\substack{\iota=1 \\ \mu\nu}}^{N_{\text{occ}}} c_{\iota\mu} c_{\iota\nu} X_\mu X_\nu \tag{1.21}$$

$$P_A = \sum c_{\iota\mu} c_{\iota\nu} X_\mu X_\nu \text{for } \mu_\iota \nu \text{ on } A \tag{1.22}$$

The Mulliken population analysis, and all other schemes, depend on the definition used to assign charges to atoms. For example, the π orbital in formaldehyde has two electrons, and according to HF/3-21G calculations they are assigned as shown at the left below. When all the basis set orbitals are considered, the charge distribution is as shown on the right.[81] Output from typical MO calculations can provide this kind of atomic charge distribution. No great significance can be attached to the specific numbers, since they are dependent on the particular basis set that is used. The qualitative trends in redistribution

79. S. M. Bachrach, *Rev. Comput. Chem.*, **5**, 171 (1994).
80. R. S. Mulliken, *J. Chem. Phys.*, **36**, 3428 (1962).
81. W. J. Hehre, L. Radom, P. v. R. Schleyer, and J. A. Pople, *Ab Initio Molecular Orbital Theory*, Wiley-Interscience, New York, 1986, pp. 118–121; A. Szabo and N. S. Ostlund, *Modern Quantum Chemistry: Introduction to Advanced Electronic Structure Theory*, Macmillan, New York, 1982.

of electron density are more meaningful. The charge distribution of formaldehyde is in accord with its fundamental chemical reactivity, that is, susceptibility to reactions with nucleophiles at carbon and with Lewis acids at oxygen.

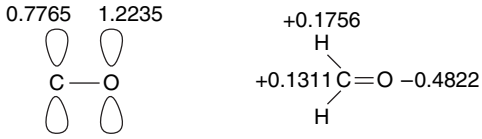

1.4.2. Natural Bond Orbitals and Natural Population Analysis

Another approach for assignment of atomic charges, known as the *natural population analysis* (NPA) method, developed by F. Weinhold and collaborators,[82] involves formulating a series of hybrid orbitals at each atom. *Natural bond orbitals* (NBO) describe the molecule by a series of localized bonding orbitals corresponding to a Lewis structure. Another set of orbitals describes combinations in which electron density is transferred from filled to antibonding orbitals. These interactions correspond to *hyperconjugation* in VB terminology. The total energy of the molecule is given by the sum of these two components:

$$E = E_{\sigma,\sigma} + E_{\sigma,\sigma^*} \tag{1.23}$$

Typically the E_{σ,σ^*} term accounts for only a small percentage of the total binding energy; however, as it represents a perturbation on the localized structure, it may be particularly informative at the level of chemical structure and reactivity. The charges found by NPA are illustrated below by the methyl derivatives of the second-row elements. Note that the hydrogens are assigned quite substantial positive charges ($\sim 0.2e$), even in methane and ethane. The total positive charge on the hydrogen *decreases* somewhat as the substituent becomes more electronegative. The carbon atom shows a greater shift of electron density to the substituent as electronegativity increases, but remains slightly negative, even for fluoromethane. The protocol for the NPA method is incorporated into MO computations and is used frequently to represent electron distribution.

NPA Populations for CH_3-X(6-31G*)[a]

X	δC	δH_3[b]	δX
H	−0.867	+0.650	+0.217
Li	−1.380	+0.576	+0.805
BeH	−1.429	+0.689	+0.740
BH_2	−1.045	+0.712	+0.333
CH_3	−0.634	+0.643	0.000
NH_2	−0.408	+0.586	−0.178
OH	−0.225	+0.547	−0.322
F	−0.086	+0.513	−0.427

a. From A. E. Reed, R. B. Weinstock and F. Weinhold, *J. Chem. Phys.*, **83**, 735 (1985).
b. Total charge on the three hydrogens of the methyl group.

82. A. E. Reed, R. B. Weinstock, and F. Weinhold, *J. Chem. Phys.*, **83**, 735 (1985); A. E. Reed, L. A. Curtiss, and F. Weinhold, *Chem. Rev.*, **88**, 899 (1988); F. Weinhold and J. Carpenter, in R. Naaman and Z Vager, eds., *The Structure of Small Molecules and Ions*, Plenum Press, New York, 1988.

Scheme 1.5. Relative Weight of NBO Resonance Structures[a]

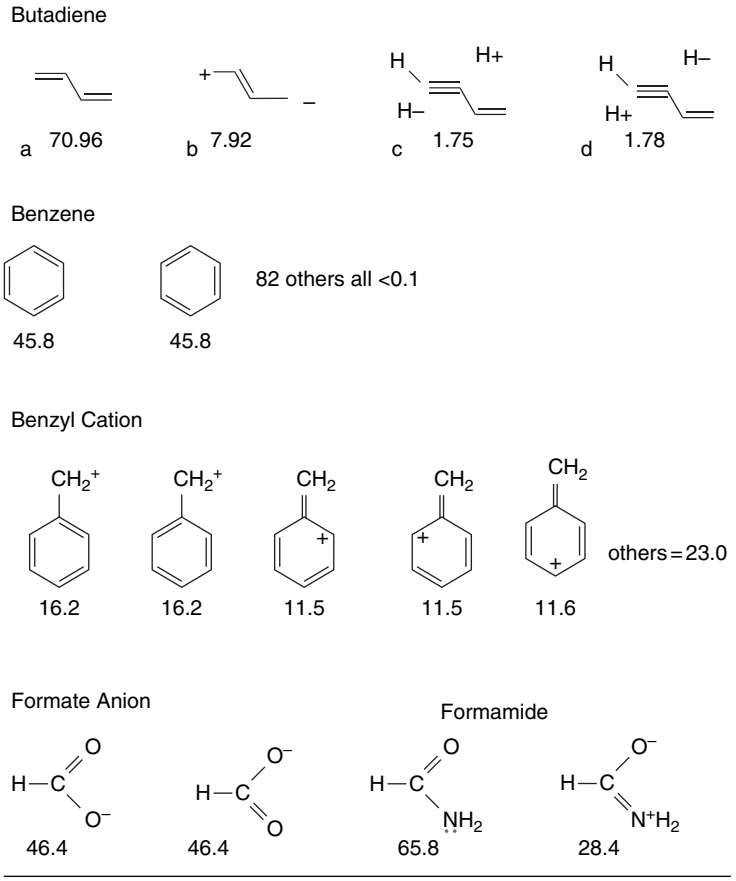

a. E. D. Glendening and F. Weinhold, *J. Comput. Chem.*, **19**, 593, 610 (1998).

The NPA electron distribution can be related to the VB concept of resonance structures. The orbitals corresponding to localized structures and those representing delocalization can be weighted. For example, Scheme 1.5 shows the relative weighting of the most important resonance structures for 1,3-butadiene, benzene, the benzyl cation, formamide, and the formate anion. These molecules are commonly used examples of the effect of conjugation and resonance on structure and reactivity.

Resonance structure **b** is commonly used to describe delocalization of π electrons in butadiene. Resonance structures **c** and **d** describe hyperconjugation. The structures represent electron transfer between *anti* hydrogens by σ-σ^* interactions. Note that the hydrogen atoms act as both electron donors and acceptors. As the two hydrogens are in very similar chemical environments, we expect little net transfer of charge, but the delocalization affects such properties as NMR spin coupling constants. We will see in Topic 1.1 that this kind of delocalization is also important for hydrogens bonded to sp^3 carbon atoms.

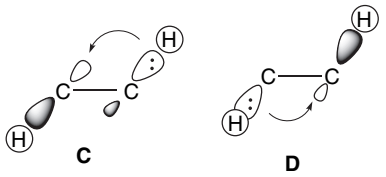

C D

The NBO resonance structures for benzyl cation reveals the importance of charge delocalization to the *ortho* and *para* positions. The resonance structures shown for formate ion and formamide represent the important cases of carboxylate anions and amides and coincide with the qualitative ideas about the relative importance of resonance structures discussed on pp. 19–20.

1.4.3. Atoms in Molecules

Chemists have long thought of a molecule as the sum of its constituent atoms and groups. The homologous hydrocarbons, for example, have closely related properties, many of which can be quantitatively expressed as the sum of contributions from the CH_3, CH_2, CH, and C groups in the molecule. The association of properties with constituent atoms is also inherent in the concept of functional groups and its implication that a particular combination of atoms, such as a hydroxy group, has properties that are largely independent of the remainder of the molecule. There is now a vast amount of both experimental and computational data on nuclear positions and electron distribution in molecules. The question is whether these data can be interpreted as being the sum of atomic properties and, if so, how one would go about "dividing" a molecule into its constituent atoms.

R. F. W. Bader and associates at Canada's McMaster University have derived a means of describing the electron distribution associated with specific atoms in a molecule, called the *atoms in molecules* (AIM) method.[83] The foundation of this approach is derived from quantum mechanics and principles of physics. It uses the methods of topology to identify atoms within molecules. The electron density of a molecule is depicted by a series of contours. *Bond paths* are the paths of maximum electron density between any two atoms. The *critical point* is a point on the bond path where the electron density is a maximum or a minimum with respect to dislocation in any direction. The bond critical point is defined by the equation

$$\overline{\nabla}\rho(\mathbf{r}).\ \overline{N}(\mathbf{r}) = 0 \tag{1.24}$$

The critical point is the point at which the gradient vector field for the charge density is zero, that is, either a maximum or minimum along $\overline{N}$. The condition $\overline{\nabla}\rho(\mathbf{r}) \cdot \overline{N}(\mathbf{r}) = 0$ applied to other paths between two atoms defines a unique surface that can represent the boundary of the atoms within the molecule. The electron density within these boundaries then gives the atomic charge. The combination of electron density contours, bond paths, and critical points defines the *molecular graph*. This analysis can be applied to electron density calculated by either MO or DFT methods. For a very simple molecule such as H_2, the bond path is a straight line between the nuclei. The

[83] R. F. W. Bader, *Atoms in Molecules: A Quantum Theory*, Oxford University Press, Oxford, 1990. For an introductory discussion of the AIM method for describing electron density, see C. F. Matta and R. J. Gillespie, *J. Chem. Ed.*, **79**, 1141 (2002).

electron density accumulates between the two nuclei, relative to electron distribution in spherical atoms, as indicated earlier in Figure 1.1. Although there is an electron *density minimum* on the bond path midway between the two hydrogens, this minimum is a *maximum* with respect to displacement perpendicular to the bond path.

Bond paths are generally *not* linear in more complex molecules. They are particularly strongly curved in strained molecules, such as those containing small rings. Figure 1.27 gives the molecular graphs for ethane, propane, butane, pentane, and hexane, showing subdivision of the molecule into methyl and methylene groups. Note that the CH_2 units become increasingly similar as the chain is lengthened. Bader's work gives a theoretical foundation to the concept that the properties of a molecule are the sum of the properties of the constituent atoms or groups.

The total electron density graphs for molecules such as methyl cation, ethane, and ethene show strong peaks around the nuclear positions. Figure 1.28a illustrates the electron density $\rho(\mathbf{r})$ for the methyl cation, and Figure 1.28b gives the corresponding gradients, showing the surfaces that partition the ion into C and H atoms. Note that there are peaks in the electron density corresponding to the nuclear positions. The existence of bonds is indicated by the ridge of electron density between the C and H atoms. The arrow in Figure 1.28a indicates the location of the bond critical point, which occurs at a *saddle point*, that is, the electron density is at a minimum along the bond path, but a maximum with respect to any other direction. Figure 1.28b shows the gradient and the zero flux surface that divides the ion into C and H atoms. The dots show the location of the bond critical points.

The electron density can also be characterized by its *ellipticity*, the extent to which it deviates from cylindrical symmetry, reflecting the contribution of π orbitals. While the C≡C bond in ethyne is cylindrically symmetrical, the C–C bonds in ethene and benzene have greater extension in the direction of the π component.[84] Ellipticity is defined by

$$E = \lambda_1/\lambda_2 - 1 \tag{1.25}$$

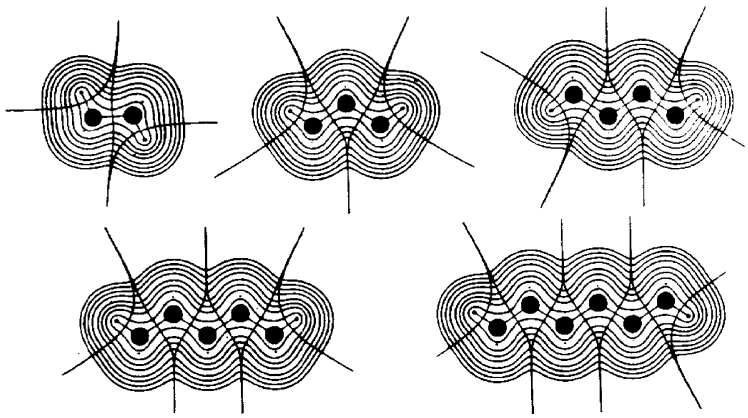

Fig. 1.27. Molecular graphs for ethane, propane, butane, pentane, and hexane. Reproduced with permission from R. F. W. Bader, in *The Chemistry of Alkanes and Cycloalkanes*, S. Patai and Z. Rappoport, eds., John Wiley & Sons, New York, 1992, Chap. 1.

84. R. F. W. Bader, T. S. Slee, D. Cremer, and E. Kraka, *J. Am. Chem. Soc.*, **105**, 5061 (1983); D. Cremer and E. Kraka, *J. Am. Chem. Soc.*, **107**, 3800 (1985).

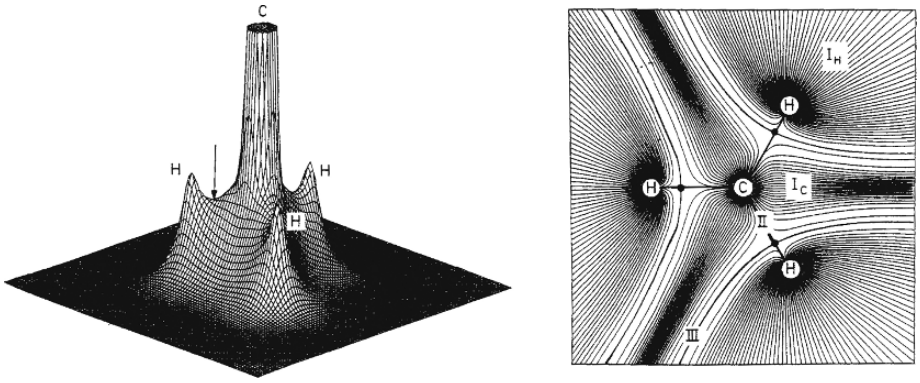

Fig. 1.28. (a) Electron density of the methyl cation in the plane of the atoms (truncated at C); (b) gradient vector field $\overline{\nabla}\rho(\mathbf{r})$ of the electron density distribution terminating at H (I_H), C (I_C); the bond path and critical point (II); and the zero flux surfaces (III) partitioning the ion into C and H atoms. From E. Kraka and D. Cremer, in *Theoretical Models of Chemical Bonding*, Part 2, Z. B. Maksic, ed., Springer Verlag, Berlin, 1990, pp. 459, 461.

where λ_1 and λ_2 are vectors to a specified electron density in the two dimensions perpendicular to the bond path at the bond critical point.

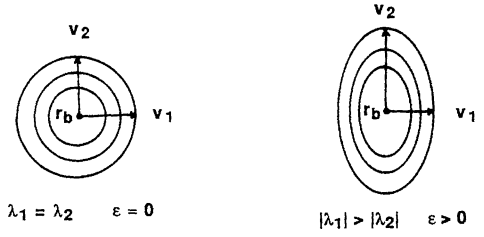

The ellipticity of the electron density in benzene is 0.23, while that in ethene is 0.45 using HF/6-31G* electron density. Ellipticity can provide structural insight as an indicator of π character. For example, the ellipticity of the C(2)–C(3) bond in 1,3-butadiene is about one-seventh that of the 1,2-bond, indicating a modest contribution from the π bond. Bond ellipticity can also indicate delocalization through hyperconjugation. For example, the C(2)–C(3) bond in propene has an ellipticity of 0.03, reflecting the $\sigma - \pi^*$ interactions in the molecule (see pp. 22–23).

We would expect the electron density to respond to the electronegativity of the atoms forming the bond. This relationship has been examined for the hydrogen compounds of the second-row elements. Table 1.15 gives the AIM radius for each of the second-row elements in its compound with hydrogen. Note that the bond critical point moves closer to the hydrogen as the other element becomes more electronegative. That is, the *hydrogen gets smaller* as electron density shifts to the more electronegative element. The charge density at the bond critical point, $\rho_{(c)}$, rises rapidly at first, but then levels off going toward the right in the periodic table. The initial increase reflects the increasing covalent character of the bond. The bonds to Li and Be are largely ionic in character, whereas the other bonds have increasing covalent character.

These relationships are depicted in Figure 1.29. Note that the hydrogen changes from hydridelike character in LiH to the much diminished electron density in H–F. There is steadily greater sharing of electron density from Li to C, as indicated by the

Table 1.15. Charge Density and Its Location at Bond Critical Points for Hydrogen Compounds of the Second-Row Elements (6-31G)[a]**

Compound	*r*X (au)	rH (au)	$\rho_{(c)}$
LiH	1.358	1.656	0.0369
BeH_2	1.069	1.416	0.0978
BH_3	0.946	1.275	0.1871
CH_4	1.252	0.801	0.2842
NH_3	1.421	0.492	0.3495
OH_2	1.460	0.352	0.3759
FH	1.454	0.279	0.3779

a. K. E. Edgecombe and R. J. Boyd, *Int. J. Quantum Chem.*, **29**, 959 (1986).

increased prominence of the nonspherical valence (shared) electron density. Beginning at N, the electron density associated with unshared electron pairs becomes a prominent feature.

Although not so dramatic in character, the same trends can be seen in carbon atoms of different hybridization. The "size" of hydrogen shrinks as the electronegativity of carbon increases in the sequence $sp^3 < sp^2 < sp$ (Figure 1.30).

Wiberg and co-workers looked at how electron density changes as substituents on methane change from very electropositive (e.g., lithium) to very electronegative (e.g., fluorine).[85] This is a question of fundamental relevance to reactivity, since we know that compounds such as methyllithium are powerful bases and nucleophiles, whereas the methyl halides are electrophilic in character. The results illustrate how fundamental characteristics of reactivity can be related to electron density. Table 1.16 Gives the methyl group "radius" and $\rho_{(c)}$, the electron density at the bond critical point for several substituted methanes.

Going across the second row, X = Li, BeH, CH_3, F, we see that the bond critical point moves closer to C as the C "shrinks" in response to the more electronegative substituents. This is particularly evident in the value of *R*, which gives the ratio of the

Table 1.16. Bond Critical Points, Charge Density, and Bond Angles for Substituted Methanes[a]

X	*r*C	*r*X	*R*	$\rho_{(c)}$C–X	∠H–C–X°
Li	1.2988	0.7025	0.541	0.0422	112.6
BeH	1.1421	0.5566	0.487	0.1030	112.1
CH_3	0.7637	0.7637	1.000	0.2528	111.2
H	0.6605	0.4233	1.560	0.2855	109.5
CN	0.6263	0.8421	1.344	0.2685	109.8
O^-	0.4417	0.8781	1.988	0.3343	116.5
O–Li	0.4425	0.9181	2.075	0.2872	112.5
F	0.4316	0.9331	2.162	0.2371	109.1
CF_3	0.6708	0.8286	1.235	0.2871	109.4
NH_3^+	0.4793	1.0278	2.144	0.2210	108.1
N_2^+	0.4574	1.0522	2.301	0.1720	105.0

NOTE: *r*C and *r*X are distances to bond critical point in Å. *R* is the ratio at these distances. $\rho_{(c)}$ is the electron density at the bond critical point and ∠H–C–X is the bond angle.
a. K. B. Wiberg and C. M. Breneman, *J. Am. Chem. Soc.*, **112**, 8765 (1990).

85. K. B. Wiberg and C. M. Breneman, *J. Am. Chen. soc*., **112**, 8765 (1990).

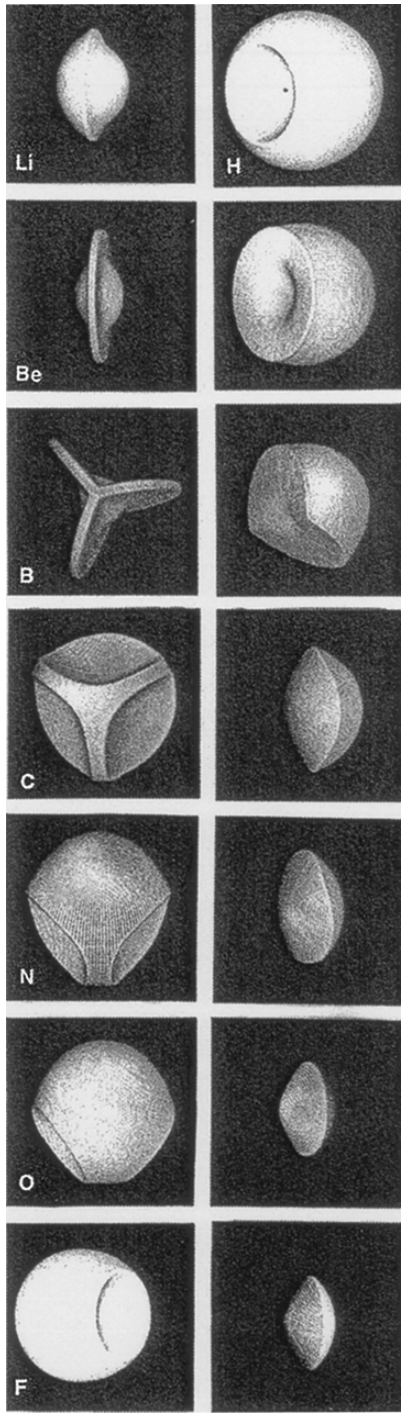

Fig. 1.29. Representation of the atoms in the second-row hydrides. The hydrides of Li, Be, and B consist primarily of a core of decreasing radius and a small, but increasing, shared density. The form of the atoms changes markedly at methane. No core is visible on the C atom, and the H atoms are reduced in size and lie on the convex interatomic surface. The increasing polarity of the remaining molecules is reflected in the decreasing size of the H atom and the increasing convexity of the interatomic surface. Reproduced from R. F. W. Bader, *Angew. Chem. Int. Ed. Engl.*, **33**, 620 (1994), by permission of Wiley-VCH.

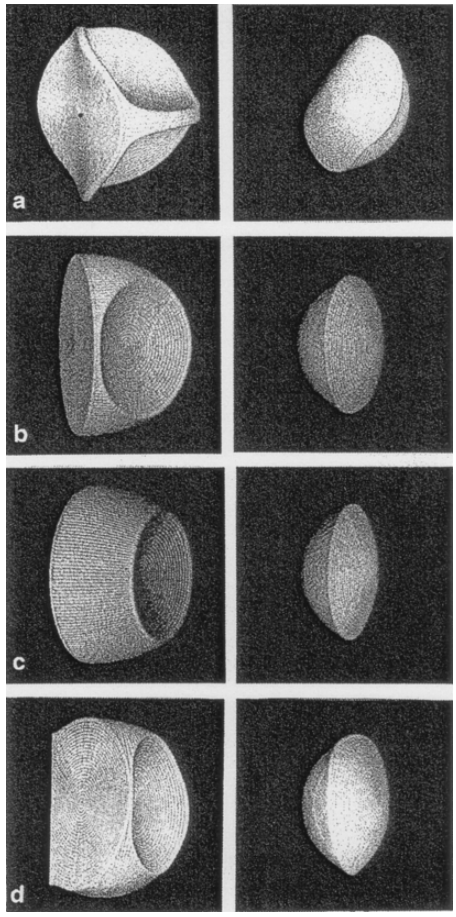

Fig. 1.30. The carbon and hydrogen atoms in: (a) ethane, (b) ethene, (c) ethyne, and (d) benzene. Note that the hydrogen is largest in ethane and smallest in ethyne. Reproduced from *Angew. Chem. Int. Ed. Engl.*, **33**, 620 (1994), by permission of Wiley-VCH.

C radius to the radius of the substituent X in the C−X bond. The charge density $\rho_{(c)}$ is very low for the largely ionic C−Li bond. It is also worth noting that there is a trend in bond angles: they become smaller as the substituent becomes more electronegative. This can be attributed to the C−X bond having more *p* character as the substituent becomes more electronegative. The net atomic charges are shown in Table 1.17.

The methyldiazonium ion $[CH_3–N{\equiv}N]^+$ is interesting. Later (Section 4.1.5) we will learn that N≡N is a very reactive leaving group and indeed it is the best there is, at least of those routinely used in solution chemistry. The computed structure of $[CH_3–N{\equiv}N]^+$ shows a weak bond (low value of ρ) and a high net positive charge (+0.840) on the methyl group. This structural information suggests that $[CH_3–N{\equiv}N]^+$ is a methyl cation weakly bound to N_2, and poised to release N_2.

$$\overset{\delta^+}{CH_3}\text{----}N{\equiv}N$$

There is a remarkable difference in the stability of methyl and ethyldiazonium ions.[86] The affinity of CH_3^+ for N_2 (C–N bond strength) based on thermodynamic data is 45 ± 7 kcal/mol. Computational results give values of 43.5 ± 1 kcal/mol. The ethyldiazonium ion is much less stable and the computed bond strength is only 11.5 kcal/mol, some 32 kcal/mol less that for methyldiazonium ion. Two aspects of this comparison are worth remembering for future reference: (1) The very unstable methyldiazonium ion is the *most stable* of the alkyl diazonium ions by a considerable margin. Later (Section 11.2.1, Part B) we will examine aryldiazonium ions and find that they are substantially more stable. (2) The indication that because it is better able to disperse the positive charge, an ethyl group binds nitrogen even more weakly than a methyl group presages the major differences in carbocation stability (methyl < *pri* < *sec* < *tert*) that we explore in Chapters 3 and 4.

The methoxide ion CH_3O^- is another important and familiar reagent. We know it to be a strong base and a good nucleophile. These characteristics are consistent with the high charge density on oxygen. Less well appreciated is the reactivity of methoxide as a hydride donor. We see that potential chemical reactivity reflected in the high negative charge on hydrogen in the methoxide ion given in Table 1.17.

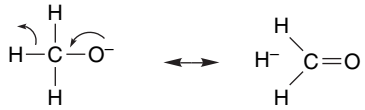

The AIM method provides a means of visualizing the subdivision of molecules into atoms. However, its definition of atoms differs from that used for the MPA and NPA methods, and it gives distinctly different numerical values for atomic charges. The distortion of charge toward the more electronegative atom is greater than in the MPA and NPA methods. The magnitude of these charge distributions often overwhelm resonance contributions in the opposite direction. Another feature of AIM charges is that they assign small negative charge to hydrogen and positive charge to carbon in hydrocarbons. This is the reverse of the case for MPA and NPA charges and is also counter to the electronegativity scales, which assign slightly greater electronegativity to carbon than hydrogen.

Table 1.17. Net AIM Charges for Methyl Derivatives

X	δC	δX	δH_3[a]
Li	−0.506	+0.903	−0.397
BeH	−0.669	+0.876	−0.207
CH_3	+0.237	0	−0.237
CN	+0.343	−0.362	+0.018
O^-	+1.206	−1.475	−0.732
F	+0.867	−0.743	−0.123
NH_3^+	+0.504	+0.337	+0.159
N_2^+	+0.390	+0.160	+0.450

[a] δC = total electron density for carbon in the methyl group; δX = total electron density for substituent X; δH = net electron density on the three hydrogens in the methyl group. From K. B. Wiberg and C. M. Breneman, *J. Am. Chem. Soc.*, **112**, 8765 (1990).

[86] R. Glaser, G. S.-C. Choy, and M. K. Hall, *J. Am. Chem. Soc.*, **113**, 1109 (1991).

1.4.4. Comparison and Interpretation of Atomic Charge Calculations

While the total electron density is a real physical property that can be measured or calculated, atomic charge distribution is not a physically observable quantity. Rather, the values depend on the definition and procedures used to define atoms and assign charges. Moreover, with some methods, the charge found is dependent on the basis set orbitals that are used. For these reasons, the actual numerical values of charge should not be taken literally, but useful information about the trends in electron distribution within a molecule and qualitative comparisons can be made.[87] For example, Table 1.18 gives the total charge on carbon and oxygen in formaldehyde using several different basis sets by the MPA, NPA, and AIM methods. Each of the methods shows the expected shift of electron density from carbon to oxygen, but the shift is considerably more pronounced for the AIM analysis.

Atomic charges have been used to analyze the nature of the interaction between the nitrogen and carbon groups in amides. In VB language this interaction is described in terms of resonance. These resonance structures account for the most characteristic properties of amides. Amides are quite polar and react with protons and Lewis acids at oxygen, but not at nitrogen. The partial C=N double bond character also accounts for the observed rotational barrier of about 18 kcal/mol.

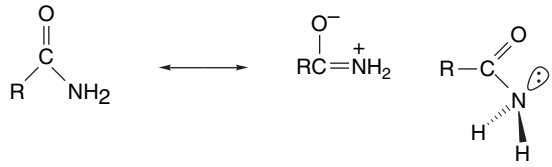

There has been a NPA analysis of the delocalization in amides.[88] Both the planar and rotated forms of formamide and its =S, =Se, and =Te analogs were studied by NPA and natural resonance theory. HF/6-31+G*, MP2/6-31+G*, and B3LYP/6-31+G* calculations were employed. At the MP2/6-31+G* level, the transfer of charge noted on going from the planar to rotated form of formamide was +0.105 at N, −0.088 at O, and −0.033 at C. This charge transfer is consistent with the resonance formulation. The shifts were in the same direction but somewhat larger for the heavier elements,

Table 1.18. Atomic Populations in Formaldehyde Calculated Using Various Methods and Basis Sets[a]

Basis set	Oxygen population			Carbon population		
	MPA	NPA	AIM	MPA	NPA	AIM
STO-3G	8.188	8.187	8.935	5.925	5.833	4.999
4-31G	8.485	8.534	8.994	5.824	5.778	5.069
3-21G	8.482	8.496	8.935	5.869	5.782	5.124
6-31G*	8.416	8.578	9.295	5.865	5.668	4.742
6-31G**	8.432	8.577	9.270	5.755	5.676	4.701
6-311+G**	8.298	8.563	9.240	5.892	5.606	4.755

[a] From S. M. Bachrach, *Rev. Comp. Chem.*, **5**, 171 (1994).

87. S. M. Bachrach, *Rev. Comp. Chem.*, **5**, 171 (1994).
88. E. D. Glendening and J. A. Hrabal, II, *J. Am. Chem. Soc.*, **119**, 12940 (1997).

Table 1.19. AIM Charge Distribution and Bond Order in Planar and 90° Formamide[a]

A. Charge Distribution

	Planar			90°		
	σ	π	Total	σ	π	Total
O	5.682	1.710	9.394	5.736	1.604	9.344
N	4.626	1.850	8.476	4.852	1.370	8.222
C	1.632	1.710	4.020	1.854	0.390	4.240

B. Bond Order

	Planar			90°		
C=O	0.668	0.458	1.127	0.677	0.571	1.248
C–N	0.655	0.229	0.884	0.844	0.046	0.891

[a] K. B. Wiberg and K. E. Laidig, *J. Am. Chem. Soc.*, **109**, 5935 (1987). K. B. Wiberg and C. M. Breneman, *J. Am. Chem. Soc.*, **114**, 831 (1992).

evidently reflecting the increasing ability of S, Se, and Te to accept electron density by *polarization*. As indicated earlier in Scheme 1.3, formamide shows a considerable contribution from the dipolar resonance structure when analyzed by natural resonance theory. At the MP2/6-31G+* level, the weightings of the two dominant structures are 58.6 and 28.6%. The C=N bond order is 1.34 and the C=O bond order is 1.72. The specific numbers depend on the computational method, but this analysis corresponds closely to the traditional description of amide resonance.

An AIM electron distribution analysis was also performed by comparing the planar structure with a 90° rotated structure that would preclude resonance. The charges, π, and total bond orders are given in Table 1.19. Although the O charge does not change much, the C–N bond order does, consistent with the resonance formulation. The charge buildup on oxygen suggested by the dipolar resonance structure is largely neutralized by a compensating shift of σ electron density from carbon to nitrogen.

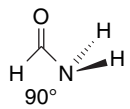

Table 1.20 gives data by which we can compare the output of several methods of charge assignment for substituted ethenes. If we compare ethene and ethenamine as an example of a double bond with an electron-releasing group (ERG) substituent, we see evidence of the conjugation (resonance) effects discussed on p. 22. The MPA and NPA methods show an increase in negative charge at the terminal CH_2 group, as indicated by resonance. There is a smaller, although still negative, charge on this carbon in the compounds with electron-withdrawing groups (EWG), e.g., CH=O, CF_3, CN, and NO_2. The AIM charges present a quite different picture, with *inductive effects* resulting from differences in electronegativity playing a dominant role. The shift of electron density to more electronegative atoms overwhelms other factors. Compare, for example, the fluoro, hydroxy, amino, cyano, and methyl substituents. The dominant factor in the charge distribution here is accumulation of negative charge on the more electronegative atoms. Note that the calculated charge at the terminal C is the same for NH_2 and CN substituents, which have opposing influences on reactivity.

Table 1.20. Calculated Atomic Charges for Substituted Alkenes[a]

1 2 3
$CH_2=CH-XY_n$

	MPA						NPA						AIM					
XY_n	C(1)	H(1)	C(2)	H(2)	X(3)	Y(3)	C(1)	H(1)	C(2)	H(2)	X(3)	Y(3)	C(1)	H(1)	C(2)	H(2)	X(3)	Y(3)
H	−0.25	+0.12					−0.42	+0.21					+0.08	−0.04				
CH_3	−0.29	+0.12	−0.09	+0.13	−0.36	+0.12	−0.44	+0.20	−0.20	+0.21	−0.67	+0.22	+0.08	−0.05	+0.02	−0.06	+0.24	−0.06
CF_3	−0.25	+0.16	−0.26	+0.17	+1.11	−0.37	−0.35	+0.23	−0.36	+0.23	+1.27	−0.42	+0.12	0.00	+0.07	0.00	+2.04	−0.75
CH=O	−0.26	+0.16	−0.19	+0.17	+0.37		−0.34	+0.22	−0.35	+0.24	+0.48		+0.05	0.00	+0.05	+0.02	+1.30	
CN	−0.23	+0.16	−0.12	+0.19	+0.27	−0.45	−0.31	+0.23	−0.35	+0.26	+0.30	−0.35	+0.15	+0.01	+0.17	+0.02	+1.15	−1.50
NO_2	−0.24	+0.19	+0.03	+0.25	+0.55	−0.46	−0.32	+0.24	−0.14	+0.25	+0.64	−0.46	+0.17	+0.04	+0.38	+0.06	+0.41	−0.54
NH_2	−0.36	+0.12	+0.14	+0.14	−0.71	+0.28	−0.56	+0.21	+0.04	+0.21	−0.91	+0.40	+0.15	−0.05	+0.51	−0.04	−1.33	+0.40
OH	−0.39	+0.12	+0.26	+0.20	−0.61	+0.35	−0.59	+0.22	+0.22	+0.20	−0.77	+0.50	+0.18	−0.04	+0.57	0.00	−1.30	+0.63
F	−0.36	+0.14	+0.30	+0.14	−0.37		−0.55	+0.23	+0.31	+0.19	−0.40		+0.29	−0.01	+0.48	+0.01	−0.7	

a. M. A. McAllister and T. T. Tidwell, *J.Org.Chem.*, **59**, 4506 (1994). The calculations are at the HF6-31G** level. Hydrogens at each carbon atom are averaged.

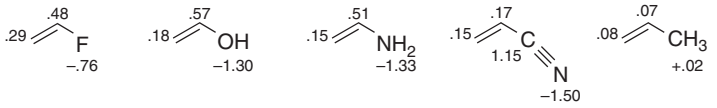

AIM charges on substituted ethenes.

There are, as indicated at the beginning of this section, not necessarily "right" and "wrong" charge densities, since they are determined by the definitions of the models that are used, not by a physical measurement. That circumstance should be kept in mind when using atomic charge densities in evaluating structural and reactivity features. We encounter all three (MPA, NPA, AIM) of the methods for charge assignment in specific circumstances. The MPA and NPA methods, which are based on orbital occupancy partitions, seem to parallel qualitative VB conceptions more closely. In Table 1.20, for example, C(1) is less negative with the EWG cyano and nitro groups than with propene. For the ERG amino and hydroxy, the carbon is more negative. The AIM charges minimize these resonance effects by compensating adjustments in the σ electron distribution. The tendency of the AIM charges to emphasize polar effects can be seen in nitroethene and cyanoethene. The AIM charges are more positive at C(2) than at C(1). These characteristic shifts of charge toward the more electronegative element are due, at least in part, to an inherent tendency of the AIM analysis to derive larger sizes for the more electronegative elements.[89]

1.4.5. Electrostatic Potential Surfaces

While atomic charges must be assigned on the basis of definitions that depend on the method, the *electrostatic potential surface* (EPS) of a molecule is both a theoretically meaningful and an experimentally determinable quantity. The mathematical operation in constructing the electronic potential surface involves sampling a number of points external to the van der Waals radii of atoms in the molecule. A positive charge is attracted to regions of high electron density (negative potential) and repelled in regions of low electron density (positive potential) The calculations then give a contour map or color representation of the molecule's charge distribution. Several approaches have been developed, one of which is called CHELPG.[90]

Figure 1.31 shows electrostatic potential maps for the planar (conjugated) forms butadiene, ethenamine, and propenal.[91] The diagrams on the left are in the plane of the molecule, and those on the right are perpendicular to the plane of the molecule and depict effects on the π orbital. Solid and dashed lines represent positive and negative potentials, respectively. The electrostatic potential for butadiene is positive at all locations in the plane of the molecule. For propenal (b) the potential becomes negative in the area of the oxygen unshared electron pairs. For ethenamine there is a negative potential external to the CH_2 group. There are regions of negative potential above and below the molecular plane in butadiene, reflecting the π electron density. This area is greatly diminished and shifted toward oxygen in propenal. For ethenamine the negative potential is expanded on C(2) and also includes the plane of the molecule. This is consistent with an increase in the electron density at C(2). Table 1.21 gives

89. C. L. Perrin, *J. Am. Chem. Soc.*, **113**, 2865 (1991).
90. A. C. M. Breneman and K. B. Wiberg, *J. Comput. Chem.*, **11**, 361 (1990).
91. K. B. Wiberg, R. E. Rosenberg, and P. R. Rablen, *J. Am. Chem. Soc.*, **113**, 2890 (1991).

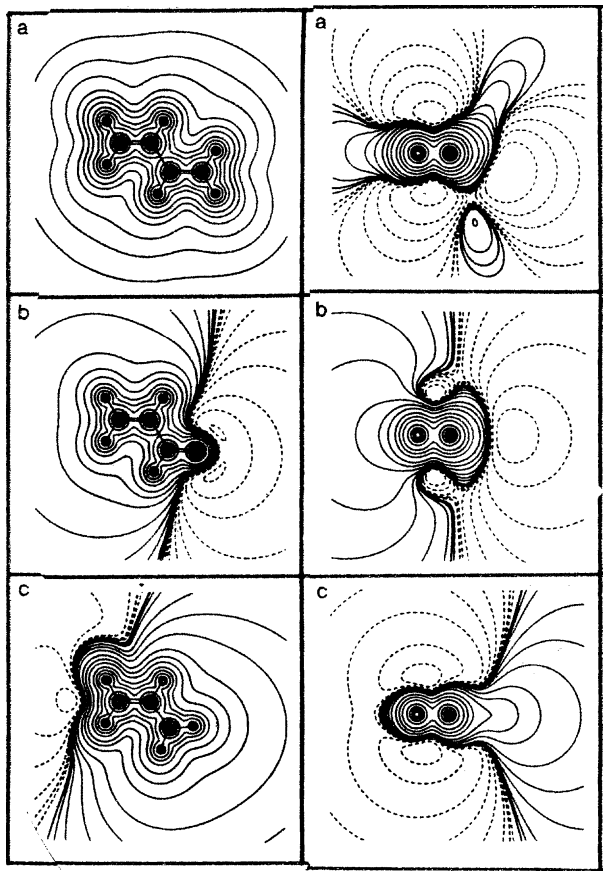

Fig. 1.31. Electrostatic potential contours for: (a) butadiene, (b) propenal, and (c) ethenamine. Solid lines are positive potential and dashed lines are negative. Left. In the plane of the molecule. Right. In the plane of the π electrons. Reproduced from *J. Am. Chem. Soc.*, **113**, 2890 (1991), by permission of the American Chemical Society.

the effective atomic charges derived from electrostatic potential at the CH_2, CH, and a substituent group comparable to propenal.

These charges are in accord with the resonance (pp. 20–22) and qualitative MO (pp. 46–48) descriptions of electron density in these molecules. The CH_2=CH− bond in ethenamine is seen to be strongly polarized, with the π-donor effect of the nitrogen unshared pair increasing electron density at C(2), while the polar effect makes C(1) substantially positive. The effects on the double bond in propenal are much less

Table 1.21. Atomic Charges for Butadiene, Propenal, and Ethenamine Derived from Electrostatic Potentials

X	CH_2	CH	X	
−CH=CH_2	−0.097	+0.097	CH + 0.097	CH_2 − 0.097
−CH=O	+0.024	−0.065	CH + 0.579	O − 0.538
−NH_2	−0.292	+0.438	N − 0.950	H + 0.178

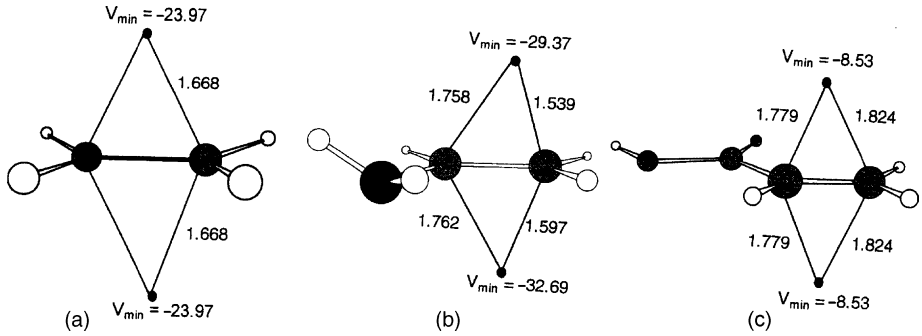

Fig. 1.32. Location and magnitude of points of most negative potential for: (a) ethene, (b) ethenamine, and (c) propenoic acid. Potentials are in kcal/mol. From *J. Org. Chem.*, **66**, 6883 (2001).

dramatic. Most of the charge separation is in the formyl group. However, the charge at the terminal CH_2 changes from slightly negative to slightly positive.

The effect of substituents on ethene on the location and magnitude of the most negative potential has been calculated (HF/6-31G**).[92] Figure 1.32 compares the position and magnitude for ethene, ethenamine, and propenoic acid, which has an electron-withdrawing carbonyl group comparable to propenal. Table 1.22 gives the same data for several other substituted ethenes.

The V_{neg} data give an order of $NH_2 > OH$, $OCH_3 > CH_3 > CH_2{=}CH > HC{\equiv}C > F > CO_2H > CH{=}O > NO_2$. This corresponds well with substituent effects that are discussed in Chapter 3. Note that the order $CH_3 > CH_2{=}CH > HC{\equiv}C$ reflects the electronegativity differences of the carbon substituents. The location of the point of most negative potential (cp) also shifts with substituents. It is closer to the terminal carbon C(2) for electron-releasing groups, but slightly closer to C(1) for electron-withdrawing groups. The cp is closer to the molecular plane for electron-releasing groups. This information can be translated into predictions about reactivity toward electrophiles. Donor substituents both increase the negative potential and move it toward C(2), consistent with preferred attack by the electrophile at the more electron-rich carbon (Markovnikov's rule, see Chapter 5). Electron-withdrawing groups such

Table 1.22. Magnitude and Location of Most Negative Potential in Substituted Ethenes

Substituent	V_{neg}	C(1)-cp	C(2)-cp
NH_2	−33.07	1.758	1.539
OH	−26.54	1.795	1.606
CH_3O	−25.98	1.790	1.628
CH_3	−25.04	1.696	1.618
H	−23.97	1.668	1.669
$CH_2{=}CH$	−21.90	1.724	1.682
$HC{\equiv}C$	−15.94	1.769	1.773
F	−13.99	1.850	1.689
HO_2C	−8.53	1.779	1.824
HC=O	−5.08	1.790	1.839
O_2N	+5.90	2.205	2.223

92. C. H. Suresh, N. Koga, and S. R Gadre, *J. Org. Chem.*, **66,** 6883 (2001).

as CH=O and NO_2 decrease the negative potential (in fact it is positive for NO_2) and increase the distance from the double bond. This results in a weaker attraction to the approaching electrophile and reduced reactivity.

1.4.6. Relationships between Electron Density and Bond Order

We would expect there to be a relationship between the electron density among nuclei and the bond length. There is a correlation between bond length and bond order. Bonds get shorter as bond order increases. Pauling defined an empirical relationship for bond order in terms of bond length for C–C, C=C, and C≡C bond lengths.[93] For carbon, the parameter a is 0.3:

$$n_{\mathrm{BOND}} = \exp\left(\frac{r_0 - r}{a}\right) \tag{1.26}$$

The concept of a bond order or bond index can be particularly useful in the description of transition structures, where bonds are being broken and formed and the bond order can provide a measure of the extent of reaction at different bonds. It has been suggested that the parameter in the Pauling relationship (1.26) should be 0.6 for bond orders < 1.[94]

MO calculations can define bond order in terms of atomic populations. Mayer developed a relationship for the bond order that is related to the Mulliken population analysis[95]:

$$B_{AB} = \sum_{\lambda \in A} \sum_{\omega \in B} (PS)_{\omega\lambda} (PS)_{\lambda\omega} \tag{1.27}$$

Wiberg applied a similar expression to CNDO calculations, where $\mathbf{S} = 1$, to give the bond index, BI[96]:

$$\mathrm{BI}_{AB} = \sum_{\lambda \in A} \sum_{\omega \in B} P_{\omega\lambda} P_{\lambda\omega} \tag{1.28}$$

In these treatments, the sum of the bond order for the second-row elements closely approximates the valence number, 4 for carbon, 3 for nitrogen, and 2 for oxygen. As with the Mulliken population analysis, the Mayer-Wiberg bond orders are basis-set dependent.

The NPA orbital method of Weinhold (Section 1.4.2) lends itself to a description of the bond order. When the NPAs have occupancy near 2.0, they correspond to single bonds, but when delocalization is present, the occupancy (and bond order) deviates, reflecting the other contributing resonance structures. There have also been efforts to define bond orders in the context of AIM. There is a nearly linear relationship between the $\rho_{(c)}$, and the bond length for the four characteristic bond orders for carbon 1, 1.5 (aromatic), 2, and 3.[97]

93. L. Pauling, *J. Am. Chem. Soc.*, **69**, 542 (1947).
94. Ref. 30 in K. N. Houk, S. N. Gustafson, and K. A. Black, *J. Am. Chem. Soc.*, **114**, 8565 (1992).
95. I. Mayer, *Chem. Phys. Lett.*, **97**, 270 (1983).
96. K. B. Wiberg, *Tetrahedron*, **24**, 1083 (1968).
97. R. F. W. Bader, T. T. Nguyen-Dang, and Y. Tal, *Rep. Prog. Phys.*, **44**, 893 (1981); For 6-31G* values see X. Fadera, M. A. Austen, and R. F. W. Bader, *J. Phys. Chem. A*, **103**, 304 (1999).

	r (au)	ρ (au)
C_2H_6	2.906	0.241
C_6H_6	2.646	0.291
C_2H_4	2.468	0.329
C_2H_2	2.207	0.368

This linear relationship exists for a variety of other C−C bonds, including those in strained ring molecules and even in carbocations.[98] There is also a high-precision correlation ($r = -0.998$) for a series of bond lengths in aromatic compounds having differing bond orders,[99] but it does not appear to hold for C–O or C–N bonds.[100]

Bond order in the AIM context has also been defined as:[101]

$$\rho_{AB} = 2\sum_i \langle i/i\rangle_A \langle i/i\rangle_B \tag{1.29}$$

For hydrocarbons, this treatment gives bond orders closely corresponding to the Lewis structures, but there is a reduction of the bond order for polar bonds, owing to the ionic portion of the bond.

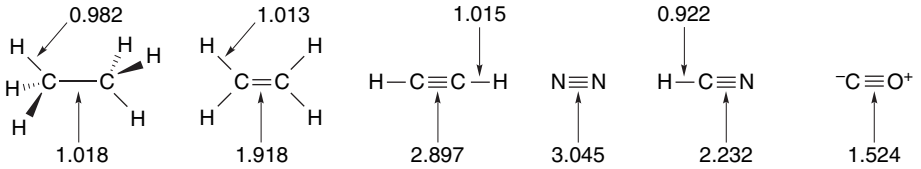

Chapter Summary

In this chapter we have reviewed the basic concepts of chemical bonding and their relationship to molecular structure. We have also introduced the two major computational approaches based on both molecular orbital (MO) and density functional theory (DFT) methods. These computational methods are powerful complements to experimental methods for describing molecular structure and properties. The orbital and electron density representations these computations provide can help interpret structure, properties, and reactivity. We must, however, remember to distinguish between the parts of this information that represent physically measurable properties (e.g., molecular dimensions and total electron distribution) and those that depend on definition (e.g., individual orbital shapes, atomic charge assignments). Our goal is to grasp the fundamental structural consequences of nuclear positions and electron distribution. Three key concepts, *electronegativity*, *delocalization*, and *polarizability*, allow us to make qualitative judgments about structure and translate them into a first approximation of expected properties and reactivity.

98. R. F. W. Bader, T. H. Tang, Y. Tal, and F. W. Biegler-König, *J. Am. Chem. Soc.*, **104**, 946 (1982).
99. S. T. Howard and T. M. Krygowski, *Can. J. Chem.*, **75**, 1174 (1997).
100. S. T. Howard and O. Lamarcke, *J. Phys. Org. Chem.*, **16**, 133 (2003).
101. J. Cioslowski and S. T. Mixon, *J. Am. Chem. Soc.*, **113**, 4142 (1991).

Topic 1.1. The Origin of the Rotational (Torsional) Barrier in Ethane and Other Small Molecules

One of the most general structural features of saturated hydrocarbons is the preference for staggered versus eclipsed conformations. This preference is seen with the simplest hydrocarbon with a carbon-carbon bond—ethane. The staggered conformation is more stable than the eclipsed by 2.9 kcal/mol, as shown in Figure 1.33.[102]

The preference for the staggered conformation continues in larger acyclic and also cyclic hydrocarbons, and is a fundamental factor in the conformation of saturated hydrocarbons (see Section 2.2.1). The origin of this important structural feature has been the subject of ongoing analysis.[103] We consider here the structural origin of the energy barrier. A first step in doing so is to decide if the barrier is the result of a destabilizing factor(s) in the eclipsed conformation or a stabilizing factor(s) in the staggered one. One destabilizing factor that can be ruled out is van der Waals repulsions. The van der Waals radii of the hydrogens are too small to make contact, even in the eclipsed conformation. However, there is a repulsion between the bonding electrons. This includes both electrostatic and quantum mechanical effects (exchange repulsion) resulting from the Pauli exclusion principle, which requires that occupied orbitals maintain maximum separation (see Section 1.1.2). There is also a contribution from nuclear-nuclear repulsion, since the hydrogen nuclei are closer together in the eclipsed conformation. The main candidate for a stabilizing interaction is σ delocalization (hyperconjugation). The staggered conformation optimizes the alignment of the σ and σ* orbitals on adjacent carbon atoms.

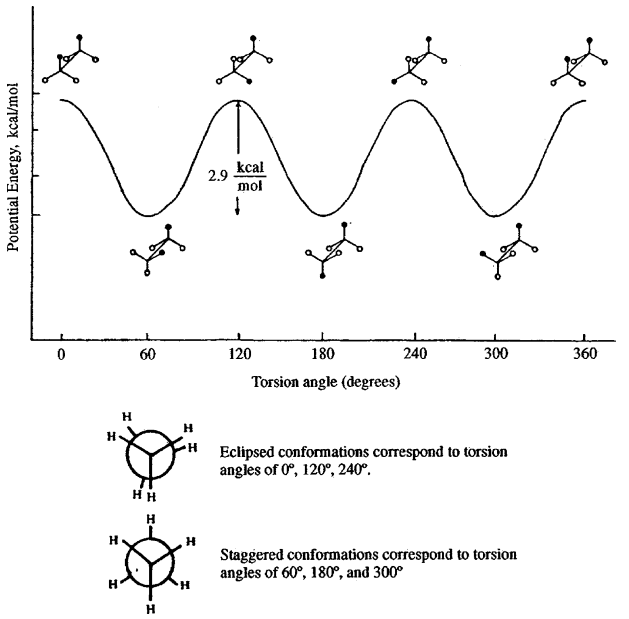

Fig. 1.33. Potential energy as a function of rotation angle for ethane.

[102] K. S. Pitzer, *Disc. Faraday Soc.*, **10**, 66 (1951); S. Weiss and G. E. Leroi, *J. Chem. Phys.*, **48,** 962 (1968); E. Hirota, S. Saito, and Y. Endo, *J. Chem. Phys.*, **71**, 1183 (1979).

[103] R. M. Pitzer, *Acc. Chem. Res.*, **16**, 207 (1983).

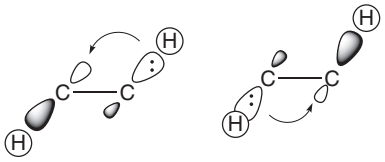

The repulsive electronic interactions were emphasized in early efforts to understand the origin of the rotational barrier.[104] In particular the π character of the π_z, π_y, π'_z, and π'_y (see Figure 1.34) was emphasized.[105] The repulsive interactions among these orbitals are maximized in the eclipsed conformation.

Efforts have been made to dissect the contributing factors within an MO framework. The NPA method was applied to ethane. Hyperconjugation was found to contribute nearly 5 kcal/mol of stabilization to the staggered conformation, whereas electron-electron repulsion destabilized the eclipsed conformation by 2 kcal/mol.[106] These two factors, which favor the staggered conformation, are partially canceled by other effects. The problem is complicated by adjustments in bond lengths and bond angles that minimize repulsive interactions. These deformations affect the shapes and energies of the orbitals. When the effects of molecular relaxation are incorporated into

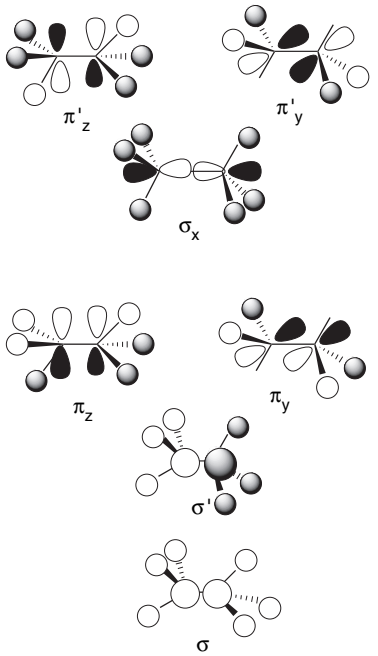

Fig. 1.34. Molecular orbitals of ethane revealing π character of π_z, π_y, π'_z, and π'_y orbitals. Only filled orbitals are shown.

104. J. P. Lowe, *J. Am. Chem. Soc.*, **92**, 3799 (1970); J. P. Lowe, *Science*, **179**, 527 (1973).
105. E. T. Knight and L. C. Allen, *J. Am. Chem. Soc.*, **117**, 4401 (1995).
106. J. K. Badenhoop and F. Weinhold, *Int. J. Quantum Chem.*, **72**, 269 (1999).

the analysis, the conclusion reached is that delocalization (hyperconjugation) is the principal factor favoring the staggered conformation.[107]

When methyl groups are added, as in butane, two additional conformations are possible. There are two staggered conformations, called *anti* and *gauche*, and two eclipsed conformations, one with methyl-methyl eclipsing and the other with two hydrogen-methyl alignments. In the methyl-methyl eclipsed conformation, van der Waals repulsions come into play. The barrier for this conformation increases to about 6 kcal/mol, as shown in Figure 1.35. We pursue the conformation of hydrocarbons further in Section 2.2.1.

Changing the atom bound to a methyl group from carbon to nitrogen to oxygen, as in going from ethane to methylamine to methanol, which results in shorter bonds, produces a regular *decrease* in the rotational barrier from 2.9 to 2.0 to 1.1 kcal/mol, respectively. The NPA analysis was applied to a dissection of these barriers.[108] The contributions to differences in energy between the eclipsed and staggered conformations were calculated for four factors. These are effects on the localized bonds (E_{Lewis}), hyperconjugation (E_{deloc}), van der Waals repulsions (E_{steric}), and exchange ($E_{2\times2}$). The dominant stabilizing terms are the ΔE_{deloc} and $\Delta E_{2\times2}$, representing hyperconjugation and exchange, respectively, but

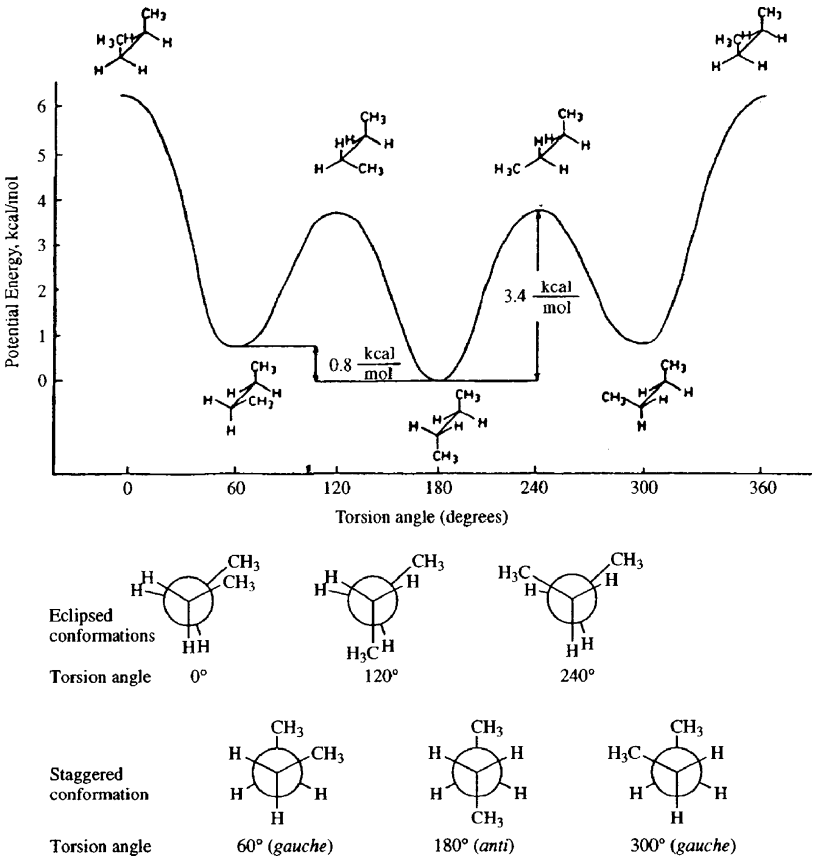

Fig. 1.35. Potential energy diagram for rotation about the C(2)−C(3) bond in butane.

[107] V. Pophristic and L. Goodman, *Nature*, **411**, 565 (2001); F. Weinhold, *Angew. Chem. Int. Ed. Engl.*, **42**, 4188 (2003).

[108] J. K. Badenhoop and F. Weinhold, *Int. J. Quantum Chem.*, **72**, 269 (1999).

this analysis indicates that the overall barrier results from compensating trends in the four components. These results pertain to a fixed geometry and do not take into account bond angle and bond length adjustments in response to rotation.

	CH_3CH_3	CH_3NH_2	CH_3OH
ΔE_{Lewis}	−1.423	−0.766	−0.440
ΔE_{deloc}	+4.953	+2.920	+1.467
ΔE_{steric}	−0.827	−0.488	−1.287
$\Delta E_{2\times2}$	+2.009	+1.483	+0.475
ΔE_{total}	+4.712	+3.149	+0.215

The methanol rotational barrier was further explored, using the approach described above for ethane.[109] The effect of changes in molecular structure that accompany rotation were included. The approach taken was to systematically compare the effect on the rotational barrier of each specific interaction, e.g., hyperconjugation and exchange repulsion, and to determine the effect on molecular geometry, i.e., bond lengths and angles. The analysis of electrostatic forces (nuclear-nuclear, electron-electron, and nuclear-electron) showed that it was the nuclear-electron forces that are most important in favoring the staggered conformation, whereas the other two actually favor the eclipsed conformation. The structural response to the eclipsed conformation is to lengthen the C−O bond, destabilizing the molecule. The more favorable nuclear-electron interaction in the staggered conformation is primarily a manifestation of hyperconjugation. In comparison with ethane, a major difference is the number of hyperconjugative interactions. The oxygen atom does not have any antibonding orbitals associated with its unshared electron pairs and these orbitals cannot act as acceptors. The oxygen unshared electrons function only as donors to the adjacent *anti* C–H bonds The total number of hyperconjugative interactions is reduced from six in ethane to two in methanol.

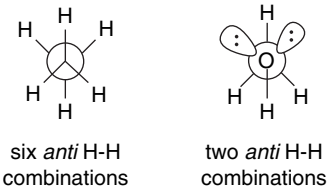

Topic 1.2. Heteroatom Hyperconjugation (Anomeric Effect) in Acyclic Molecules

It is expected that hyperconjugation would be enhanced in certain systems containing heteroatoms. If one atom with an unshared electron pair is a particularly good electron donor and another a good σ* acceptor, the $n \rightarrow \sigma^*$ contribution should be enhanced. This is represented by a charged, "no-bond" resonance structure.

[109] V. Pophristic and L. Goodman, *J. Phys. Chem. A*, **106**, 1642 (2002).

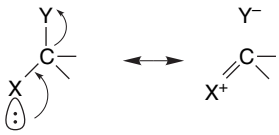

Heteroatom hyperconjugation can also be expressed in MO terms. The *n*, σ, and σ* orbitals are involved, as depicted below. If the **A** atom is the donor and **C** the acceptor, the MO perturbation indicates a stabilization of the **A** *n* orbital by partial population of the **B**–**C** σ* orbital.

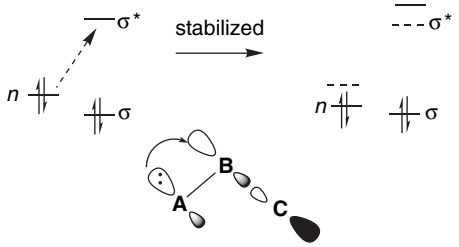

This stereoelectronic interaction has a preference for an *anti* relationship between the donor electron pair and the acceptor σ* orbital. Such interactions were first recognized in carbohydrate chemistry, where the term *anomeric effect* originated. We use the more general term *heteroatom hyperconjugation* in the discussion here. The $n \rightarrow \sigma^*$ interaction should be quite general, applying to all carbon atoms having two heteroatom substituents. Such compounds are generally found to be stabilized, as indicated by the results from an HF/3-21G level calculations given in Table 1.23.

A study of the extent of hyperconjugation in disubstituted methanes using B3LYP/6-31G** calculations and NPA analysis found that σ* acceptor capacity increases with electronegativity, i.e., in the order C < N < O < F for the second row.[110] However, acceptor σ* capacity also increases going down the periodic table for the halogens, F < Cl < Br < I. The electronegativity trend is readily understood, but the trend with size had not been widely recognized. The effect is attributed to the lower energy of the σ* orbitals with the heavier elements. Donor ability also appears to increase going down the periodic table. This trend indicates that *softness* (polarizability) is a factor in hyperconjugation. The stabilizations for substituted methylamines according to these B3LYP/6-31G** calculations are as follows:

Table 1.23. Calculated Stabilization in kcal/mol for Disubstituted Methanes[a]

	Y(acceptor)		
X(donor)	NH_2	OH	F
NH_2	10.6	12.7	17.6
OH		17.4	16.2
F			13.9

a. P. v. R. Schleyer, E. D. Jemmis, and G. W. Spitznagel, *J.Am. Chem. Soc*., **107**, 6393 (1985).

110. I. V. Alabugin and T. A. Zeidan, *J. Am. Chem. Soc.*, **124**, 3175 (2002).

$H_2N{-}CH_2{-}X \leftrightarrow H_2N^+{=}CH_2\ X^-$

X	kcal/mol
H	8.07
F	20.49
Cl	22.55
Br	29.87

Heteroatom hyperconjugation favors the *anti* alignment of the interacting orbitals. One way to estimate the magnitude of the stabilization is to compare the conformations of individual molecules that are or are not properly aligned for hyperconjugation. Hyperconjugative stabilization is expected to have at least three interrelated consequences: (1) altered bond lengths; (2) enhanced polarity, as represented by the charged resonance structure; and (3) an energetic preference for the conformation that optimizes hyperconjugation. These issues have been examined for many small molecules, and we illustrate the analysis by considering a few, such as dimethoxymethane, fluoromethanol, fluoromethylamine, and diaminomethane.

Dimethoxymethane prefers a conformation that allows alignment of an unshared pair on each oxygen (donor) with a C–O σ* orbital on the other. This condition is met in the conformation labeled *gauche*, *gauche*. In contrast, the extended hydrocarbon-like *anti*, *anti* conformation does not permit this alignment.

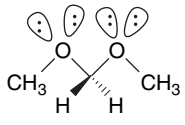

anti, anti

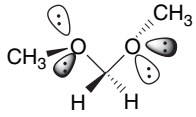

gauche, gauche

Calculations using the 6-31* basis set found the *gauche*, *gauche* conformation to be about 5 kcal/mol more stable than the *anti*, *anti*.[111] Later MP2/6-311++G** and B3LYP/6-31G** calculations found the *gauche*, *gauche* arrangement to be about 7 kcal/mol more stable than *anti*, *anti*. There are two other conformations that have intermediate (3–4 kcal/mol) energies.[112] Dissecting these conformational preferences to give an energy for the anomeric effect is complicated, but there is general agreement that in the case of dimethoxymethane it accounts for several kcal/mol of stabilization.

Fluoromethanol also shows a preference for the *gauche* conformation. At the HF/6-31G** level it is 4.8 kcal/mol more stable than the *anti* conformation and 2.4 kcal/mol more stable than the eclipsed conformation.[113] Only the *gauche* conformation aligns an unshared pair *anti* to the C–F bond.

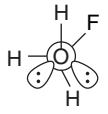

eclipsed

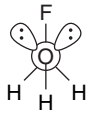

anti

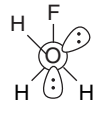

gauche

NPA analysis was used to isolate the $n \rightarrow \sigma^*$ component and placed a value of 18 kcal/mol on the heteroatom hyperconjugation. This is about 11 kcal/mol higher than

111. K. B. Wiberg and M. A. Murcko, *J. Am. Chem. Soc.*, **111**, 4821 (1989).
112. J. R. Kneisler and N. L. Allinger, *J. Comput. Chem.* **17**, 757 (1996).
113. U. Salzner and P. v. R. Schleyer, *J. Am. Chem. Soc.*, **115**, 10231 (1993).

the same component in the *anti* and eclipsed conformations, so other factors must contribute to reducing the total energy difference.

Another molecule that has received attention is fluoromethylamine. From MP2/6-31G** calculations the *anti* arrangement of the nitrogen unshared pair and the C–F bond is found to be the most stable conformation by 7.5 kcal/mol.[114] Some of the structural effects expected for hyperconjugation, such as lengthening of the C–F bond are seen, but are not dramatic.[115]

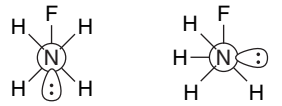

Experimental structural data (electron diffraction) is available for *N*-fluoromethyl-*N*,*N*-dimethylamine.[116] The only conformation observed is the *anti* arrangement of the unshared pair and C–F bond. MP2/6-311G(2*d*,*p*) calculations suggest that the *gauche* alignment is about 5 kcal/mol less stable.

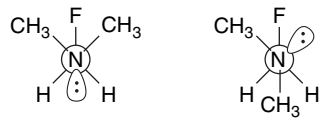

Diaminomethane would also be expected to be stabilized by an anomeric effect. Overall, there is a rather small preference for the *gauche*, *gauche* conformation, but NPA analysis suggests that there is an $n \rightarrow \sigma^*$ component of 5–6 kcal/mol that is offset by other factors.[117]

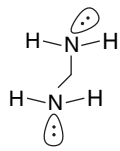

preferred *gauche* conformation for diaminomethane

We should conclude by emphasizing that the *stabilization of these compounds does not mean that they are unreactive.* In fact, α-halo ethers and α-halo amines are highly reactive toward solvolysis. The hyperconjugation that is manifested in net stabilization *weakens* the carbon-halogen bond and the molecules dissociate readily in polar solvents. Methoxymethyl chloride is at least 10^{14} times as reactive a methyl

114. J. J. Irwin, T. K. Ha, and J. Dunitz, *Helv. Chim. Acta*, **73**, 1805 (1990).
115. K. B. Wiberg and P. R. Rablen, *J. Am. Chem. Soc.*, **115**, 614 (1993).
116. D. Christen, H. G. Mack, S. Rudiger, and H. Oberhammer, *J. Am. Chem. Soc.*, **118**, 3720 (1996).
117. L. Carballeira and I. Perez-Juste, *J. Comput. Chem.* **22**, 135 (2001).

chloride toward solvolysis in ethanol,[118] owing to the fact that the cationic intermediate is stabilized even more, 57.6 kcal/mol, according to the computational results on p. 22.

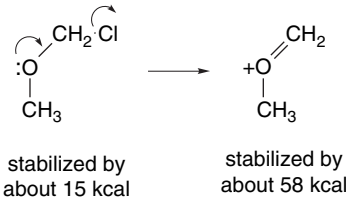

As indicated at the beginning of this section, heteroatom hyperconjugation was first recognized in carbohydrates. The anomeric effect has been particularly well studied in cyclic systems, such as found in carbohydrates. We return to the anomeric effect in cyclic systems in Topic 2.3.

Topic 1.3. Bonding in Cyclopropane and Other Small Ring Compounds

Molecules such as cyclopropane that are forced by geometry to have nonideal bond angles are said to be *strained*. This means that the bonds are not as strong as those in comparable molecules having ideal bond angles and results in both lower thermodynamic stability and increased reactivity. The increased reactivity has at least two components. (1) Typically, reactions lead to a less strained product and partial relief of strain lowers the energy barrier. (2) Strained molecules require orbital rehybridization, which results in electrons being in higher energy orbitals, so they are more reactive.[119] There have been many experimental and computational studies aimed at understanding how strain affects structure and reactivity.

The simplest VB description of cyclopropane is in terms of bent bonds. If the carbons are considered to be sp^3 hybrid, in accordance with their tetravalent character, the bonding orbitals are not directed along the internuclear axis. The overlap is poorer and the bonds are "bent" and weaker.

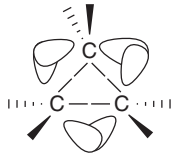

The overlap can be improved somewhat by adjustment of hybridization. Increased *p* character in the C−C bonds reduces the interorbital angle and improves overlap, which means that the C–H bonds must have increased *s* character. Compared to ethane or propane, cyclopropane has slightly shorter C−C and C–H distances and an open CH_2 bond angle,[120] which is consistent with rehybridization. The C–H bonds in cyclopropane are significantly stronger than those in unstrained hydrocarbons, owing

118. P. Ballinger, P. B. de la Mare, G. Kohnstam, and B. M. Prestt, *J. Chem. Soc.*, 3641 (1955).
119. A. Sella, H. Basch, and S. Hoz, *J. Am. Chem. Soc.*, **118**, 416 (1996).
120. J. Gauss, D. Cremer, and J. F. Stanton, *J. Phys. Chem. A*, **104**, 1319 (2000).

to the greater *s* character in the carbon orbital. Proponents of VB description argue that the properties of cyclopropane are well described by the bent bond idea and that no other special characteristics are needed to explain bonding in cyclopropane.[121] There is, however, an unresolved issue. Cyclopropane has a total strain energy of 27.5 kcal/mol. This is only slightly greater than that for cyclobutane (26.5 kcal/mol), which suggests that there might be some special stabilizing feature present in cyclopropane.

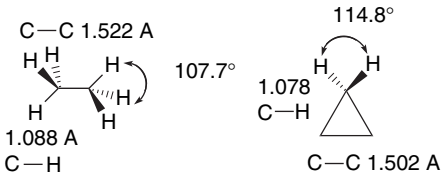

In MO terms, cyclopropane can be described as being formed from three sp^2-hybridized methylene groups. The carbon-carbon bonds in the plane of the ring are then considered to be derived from six unhybridized carbon 2*p* orbitals. This leads to a delocalized molecular orbital with maximum overlap *inside* the ring and two other degenerate orbitals that have maximum density *outside* the ring. According to this picture, the orbital derived from lobes pointing to the center of the ring should be particularly stable, since it provides for delocalization of the electrons in this orbital.

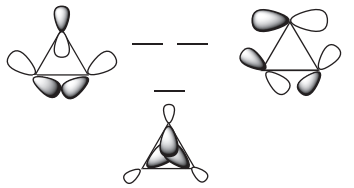

MOs for cyclopropane derived from C 2*p* orbitals

Schleyer and co-workers made an effort to dissect the total bonding energy of cyclopropane into its stabilizing and destabilizing components.[122] Using C–H bond energies to estimate the strain in the three-membered ring relative to cyclohexane, they arrived at a value of 40.4 kcal/mol for total strain. The stronger C–H bonds (108 kcal/mol), contribute 8.0 kcal/mol of stabilization, relative to cyclohexane. Using estimates of other components of the strain, such as eclipsing, they arrived at a value of 11.3 kcal/mol as the stabilization owing to σ delocalization. The concept of σ delocalization is also supported by the NMR spectrum and other molecular properties that are indicative of a ring current. (See Section 8.1.3 for a discussion of ring current as an indicator of electron delocalization.) The Laplacian representation (see Topic 1.4) of the electron density for cyclopropane shown in Figure 1.36 shows a peak at the center of the ring that is not seen in cyclobutane.[123] The larger cross-ring distances in cyclobutane would be expected to reduce overlap of orbitals directed toward the center of the ring.

[121] J. G. Hamilton and W. E. Palke, *J. Am. Chem. Soc.*, **115**, 4159 (1993); P. Karadakov, J. Gerratt, D. L. Cooper, and M. Raimondi, *J. Am. Chem. Soc.*, **116**, 7714 (1994); P. B. Karadakov, J. Gerratt, D. L. Cooper, and M. Raimondi, *Theochem*, **341**, 13 (1995).

[122] K. Exner and P. v. R. Schleyer, *J. Phys. Chem. A*, **105**, 3407 (2001).

[123] D. Cremer and J. Gauss, *J. Am. Chem. Soc.*, **108**, 7467 (1986).

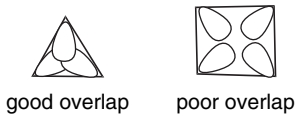

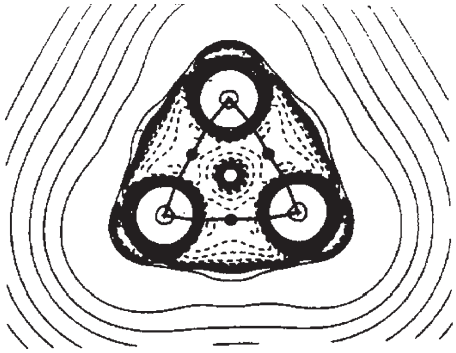

Fig. 1.36. Contours of the Laplacian for cyclopropane in the plane of the rings. Dots are bond critical points. Reproduced with permission from R. F. W. Bader, in *Chemistry of Alkanes and Cycloalkanes*, S. Patai and Z. Rappoport, eds., John Wiley & Sons, New York, 1992, Chap. 1.

Bicyclo[1.1.0]butane, bicyclo[1.1.1]pentane, [1.1.1]propellane, and spiro[2.2]pentane are other molecules where strain and rehybridization affect molecular properties. The molecules show enhanced reactivity that can be attributed to characteristics of the rehybridized orbitals. The structures are shown in Scheme 1.6, which also shows calculated AIM charge distributions and strain energy.

The strain in bicyclo[1.1.0]butane results in decreased stability and enhanced reactivity.[124] The strain energy is 63.9 kcal/mol; the central bond is nearly pure *p* in character,[125] and it is associated with a relatively high HOMO.[126] These structural features are reflected in enhanced reactivity toward electrophiles. In acid-catalyzed reactions, protonation gives the bicyclobutonium cation (see Section 4.4.5) and leads to a characteristic set of products.

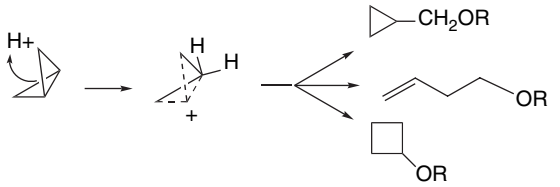

124. S. Hoz, in *The Chemistry of the Cyclopropyl Group*, Part 2, S. Patai and Z. Rappoport, eds., Wiley, Chichester,. 1987, pp 1121–1192; M. Christl, *Adv. Strain Org. Chem.*, **4**, 163 (1995).
125. J. M. Schulman and G. J. Fisanick, *J. Am. Chem. Soc.*, **92**, 6653 (1970); R. D. Bertrand, D. M. Grant, E. L. Allred, J. C. Hinshaw, and A. B. Strong, *J. Am. Chem. Soc.*, **94**, 997 (1972); D. R. Whitman and J. F. Chiang, *J. Am. Chem. Soc.*, **94**, 1126 (1972); H. Finkelmeier and W. Lüttke, *J. Am. Chem. Soc.*, **100**, 6261 (1978).
126. K. B. Wiberg, G. B. Ellison, and K. S. Peters, *J. Am. Chem. Soc.*, **99**, 3941 (1977).

Scheme 1.6. AIM Charge Distribution and Strain Energy (kcal/mol) for Cyclic Hydrocarbons

Monocyclic

Charge:	C −0.010 H +0.005	C +0.06 H −0.03	C +0.08 H −0.04	C +0.08 H −0.04
Strain:	27.5	26.5	6.2	0

Bicyclic

C(2) +0.072
H(2) −0.002
C(1) −0.12
H(1) +0.054
63.9

C(5) −0.03
H(5) +0.002

C(1) −0.043
H(1) +0.011
54.7

C(2) +0.082
H(2) −0/025

C(2) −0.059
H(2) −0.030

C(1) +0.030
H(1) −0.028
51.8

C(2) +0.043
H(2) −0.030
C(1) +0.036
H(1) −0.011
68.0

C(7) 0.036
H(7) −0.034
C(2) +0.058
H(2) −0.036

C(1) +0.074
H(1) −0.033
14.4

C(2) +0.061
H(2) −0.40
C(1) +0.101
H(1) −0.044
7.4

Propellanes

C(2) +0.026
H(2) +0.023
C(1) −0.107
98

C(5) +0.036
H(5) +0.019
C(2) 0.0103
H(2) −0.014

C(1) −0.149
104

C(7) +0.042
H(7) +0.013

C(2) +0.099
H(2) −0.020
C(1) −0.152
105

C(2) +0.051
H(2) −0.023
C(1) =−0.016
89

Others

C(2) = +0.003
H(2) = +0.007
C(1) =−0.072
63.2

C(1) =−0.111
H(1) = +0.111
140

C(1) = +0.003
H(1) =−0.003
154.7

a. R. F. W. Bader in *The Chemistry of Alkanes and Cycloalkanes*, S. Patai and Z. Rappoport, eds., John Wiley & Sons, New York, 1992, p. 51.

Bicyclo[1.1.0]butane also reacts with the halogens. With I_2, the main product is 1,3-diiodocyclobutane (5:1 *cis:trans*). With Br_2 and Cl_2, cyclopropylcarbinyl and butenyl products are also formed.[127] The initial attack occurs from the *endo* face of the molecule and the precise character of the intermediate appears to be dependent on the halogen.

127. K. B. Wiberg, G. M. Lampman, R. P. Ciula, D. S. Connor, P. Schertler, and J. Lavanish, *Tetrahedron*, **21**, 2749 (1968); K. B. Wiberg and G. J. Szeimies, *J. Am. Chem. Soc.*, **92**, 571 (1970).

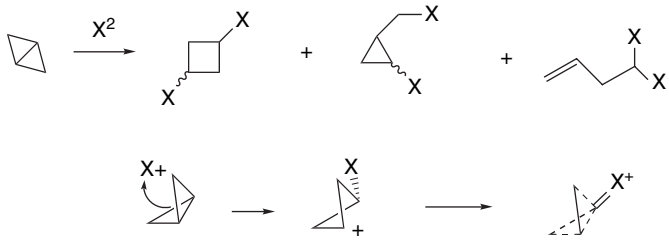

The bridgehead C–H bond in tricyclo[1.1.1]pentane is not quite as strong as the C–H bond in cyclopropane. A value of 104.4 kcal/mol is calculated at the MP3/6-31G* level.[128] The total strain energy is 68 kcal/mol.

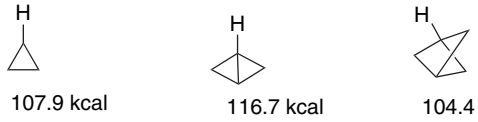

C-H bond strengths at MP3/6-311G* level

The alignment of the two bridgehead bonds is such that there is strong interaction between them. As a result of this interaction, there is hyperconjugation between the two bridgehead substituents. For example, the ^{19}F chemical shifts are effected by $\sigma \rightarrow \sigma^*$ donation to the C–F σ^* orbital.[129]

[1.1.1]Propellane has a very unusual shape. All four bonds at the bridgehead carbons are directed toward the same side of the nucleus.[130] There have been many computational studies of the [1.1.1]propellane molecule. One of the main objectives has been to understand the nature of the bridgehead-bridgehead bond and the extension of the orbital external to the molecule. The distance between the bridgehead carbons in [1.1.1]propellane is calculated to be 1.59 Å. The molecule has been subjected to AIM analysis. The $\rho_{(c)}$ value for the bridgehead-bridgehead bond is $0.173a_o^3$, which indicates a bond order of about 0.7.[131] There is a low-temperature X-ray crystal structure of [1.1.1]propellane. Although it is not of high resolution, it does confirm the length of the bridgehead bond as 1.60 Å.[132] Higher-resolution structures of related tetracyclic compounds give a similar distance and also show electron density external to the bridgehead carbons.[133]

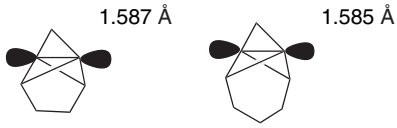

128. K. B. Wiberg, C. M. Hadad, S. Sieber, and P. v. R. Schleyer, *J. Am. Chem. Soc.*, **114**, 5820 (1992).
129. W. Adcock and A. N. Abeywickrema, *J. Org. Chem.*, **47**, 2957 (1982); J. A. Koppel, M. Mishima, L. M. Stock, R. W. Taft, and R. D. Topsom, *J. Phys. Org. Chem.*, **6**, 685 (1993).
130. L. Hedberg and K. Hedberg, *J. Am. Chem. Soc.*, **107**, 7257 (1985).
131. K. B. Wiberg, R. F. W. Bader, and C. D. H. Lau, *J. Am. Chem. Soc.*, **109**, 985 (1987); W. Adcock, M. J. Brunger, C. I. Clark, I. E. McCarthy, M. T. Michalewicz, W. von Niessen, E. Weigold, and D. A. Winkler, *J. Am. Chem. Soc.*, **119**, 2896 (1997).
132. P. Seiler, *Helv. Chim. Acta*, **73**, 1574 (1990).
133. P. Seiler, J. Belzner, U. Bunz, and G. Szeimies, *Helv. Chim. Acta*, **71**, 2100 (1988).

Surprisingly, [1.1.1]propellane is somewhat more stable to thermal decomposition than the next larger propellane, [2.1.1]propellane, indicating a reversal in the trend of increased reactivity with increased strain. To understand this observation, it is important to recognized that the energy of *both the reactant and intermediat*e influence the rate of unimolecular reactions that lead to decomposition. In the case of propellanes, homolytic rupture of the central bond is expected to be the initial step in decomposition. This bond rupture is very endothermic for [1.1.1]propellane. Because relatively less strain is released in the case of [1.1.1]propellane than in the [2.1.1]- and [2.2.1]-homologs, [1.1.1]propellane is kinetically most stable.[134]

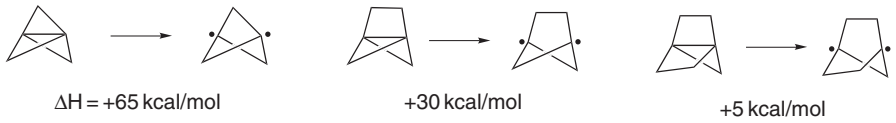

Another manifestation of the relatively small release of strain associated with breaking the central bond comes from MP4/6-31G* calculations on the energy of the reverse ring closure.[135]

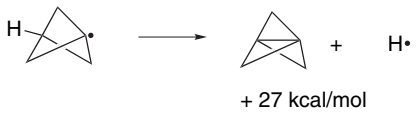

The thermal decomposition of [1.1.1]propellane has been studied both experimentally and by computation.[136] The initial product is 1,2-dimethylenecyclopropane, and the E_a is 39.7 kcal/mol. The mechanism of the reactions has been studied using both MO and DFT calculations. The process appears to be close to a concerted process, which is represented in Figure 1.37. DFT computations suggest that structure **A** is an intermediate,[137] slightly more stable than **TS1** and **TS2**. The corresponding MO calculations [CCSD(T)/6-311G(2*d*,*p*)] do not find a minimum. However, both methods agree that **A**, **TS1**, and **TS2** are all close in energy. Note that this reaction is *heterolytic* and that the diradical is not an intermediate. This implies that there is a smaller barrier for the observed reaction than for homolytic rupture of the central bond. The calculated E_a is substantially less than the bond energy assigned to the bridgehead bond, which implies that bond making proceeds concurrently with bond breaking, as expected for a concerted process.

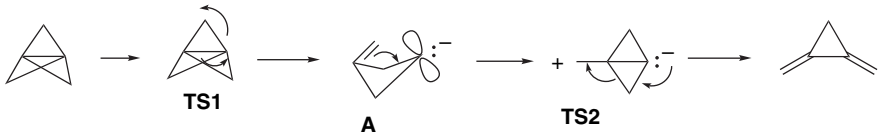

Visual models, additional information and exercises on Thermal Rearrangement of [1.1.1]Propellane can be found in the Digital Resource available at: Springer.com/carey-sundberg.

134. K. B. Wiberg, *Angew. Chem. Int. Ed. Engl.*, **25**, 312 (1985).
135. W. Adcock, G. T. Binmore, A. R. Krstic, J. C. Walton and J. Wilkie, *J. Am. Chem. Soc.*, **117**, 2758 (1995).
136. O. Jarosch, R. Walsh, and G. Szeimies, *J. Am. Chem. Soc.*, **122**, 8490 (2000).
137. . Both B3LYP/6-311G(d,p) and B3PW91/D95(*d*,*p*) computations were done and the latter were in closer agreement with the CCSD(T)/6-311G(2*d*,*p*) results.

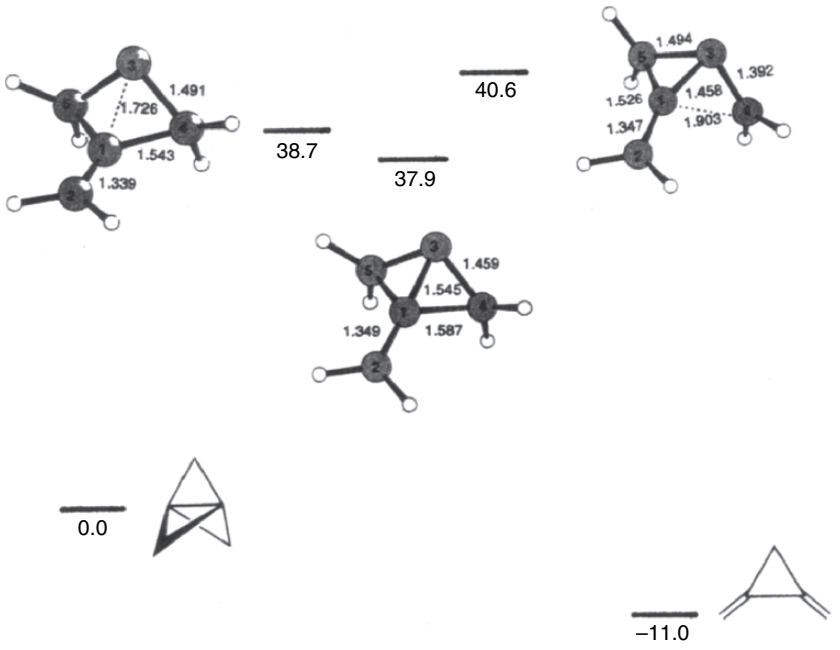

Fig. 1.37. DFT (B3PW91/D95(*d*,*p*) representation of the thermal isomerization of [1.1.1]propellane to 1,2-dimethylenecyclopropane. Adapted from O. Jarosch, R. Walsh, and G. Szeimies, *J. Am. Chem. Soc.*, **122**, 8490 (2000).

Both radicals and electrophiles react at the bridgehead bond of [1.1.1]propellane. The reactivity toward radicals is comparable to that of alkenes, with rates in the range of 10^6 to 10^8 $M^{-1}\,s^{-1}$, depending on the particular radical.[138] For example, [1.1.1]propellane reacts with thiophenol at room temperature.[139]

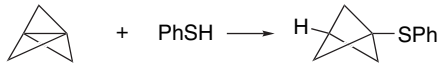

Reaction with the halogens breaks the bridgehead bond and leads to 1,3-dihalobicyclo[1.1.1]butanes. When halide salts are included, mixed dihalides are formed, suggesting an ionic mechanism.[140]

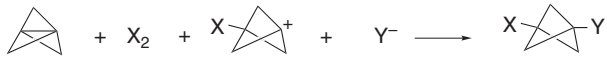

[1.1.1]Propellane and maleic anhydride copolymerize to an alternating copolymer.[141]

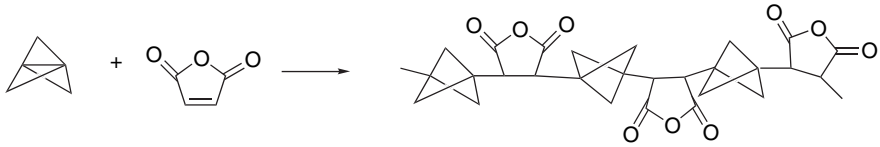

Each of these reactions indicates the high reactivity of the bridgehead-bridgehead bond.

138. P. F. McGarry and J. C. Scaiano, *Can. J. Chem.* **76**, 1474 (1998).
139. K. B. Wiberg and S. T. Waddell, *J. Am. Chem. Soc.*, **112**, 2194 (1990).
140. I. R. Milne and D. K. Taylor, *J. Org. Chem.*, **63**, 3769 (1998).
141. J. M. Gosau and A.-D. Schlüter, *Chem. Ber.*, **123**, 2449 (1990).

Topic 1.4. Representation of Electron Density by the Laplacian Function

Electron distribution in molecules can be usefully represented by the *Laplacian* of the electron density. The Laplacian is defined by the equation

$$\nabla^2\rho = \frac{\partial^2\rho}{\partial x^2} + \frac{\partial^2\rho}{\partial y^2} + \frac{\partial^2\rho}{\partial z^2} \tag{1.30}$$

which is a measure of the curvature of the electron density. The negative of $\nabla^2\rho$, called L, depicts regions of electron concentration as maxima and regions of electron depletion as minima. The Laplacian function can distinguish these regions more easily than the total electron density contours. It also depicts the concentric shells corresponding to the principal quantum numbers. Figure 1.38 shows the L functions for water, ammonia, and methane. The diagrams show concentration of valence shell electron density in the region of bonds. The water and ammonia molecules also show maxima corresponding to the nonbonding electrons.

Figure 1.39 shows L for ethane, ethene, and ethyne.[142] Note the regions of bonding associated with the two shells of carbon between the two carbons and between carbon and hydrogen. Figure 1.40 shows a perspective view of ethene indicating the saddle point between the carbon atoms. The ridge with a saddle point corresponds to electron density in the nodal plane of the π bond.

Figure 1.41 compares the Laplacian of the experimental electron density from a low-temperature crystallographic study of ethane with the computed L using the 6-311G** basis set.[143] This serves to make a connection between computed and experimental electron density.

The electron density for small molecules corresponds to expectations based on electronegativity. Figure 1.42 gives $L(\mathbf{r})$ for N_2 (a), CO (b), and $H_2C{=}O$ (c, d). The diagram for nitrogen shows the concentric shells and accumulation of electron density between the nitrogen nuclei. The distribution, of course, is symmetrical. For $C{\equiv}O$ there is a substantial shift of electron density toward carbon, reflecting the polar character of the $C{\equiv}O$ bond. Figure 1.42c is $L(\mathbf{r})$ in the molecular plane of formaldehyde. In

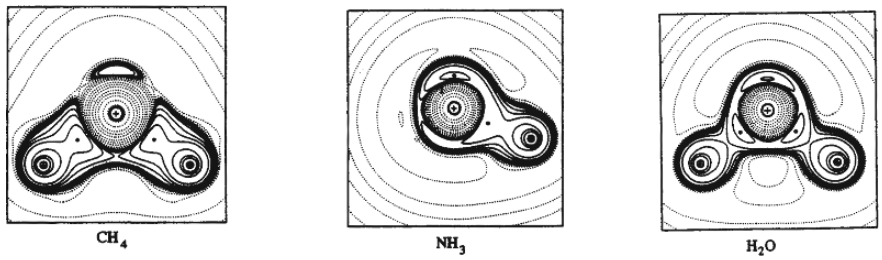

Fig. 1.38. Contour maps of L for methane, ammonia, and water. For water, the contours are in the plane of the molecule. For ammonia and methane the contours are in the plane that bisects the molecule with a hydrogen above and below the plane. Reproduced with permission from R. J. Gillespie and P. L. A. Popelier, *Chemical Bonding and Molecular Geometry*, Oxford University Press, Oxford, 2001, p. 172.

142. R. F. W. Bader, S. Johnson, T.-H. Tang and P. L. A. Popelier *J. Phys. Chem.*, **100**, 15398 (1996).
143. V. G. Tsirelson, *Can. J. Chem.*, **74**, 1171 (1996).

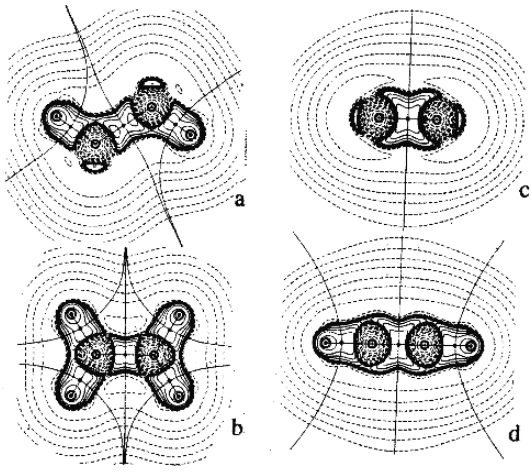

Fig. 1.39. Contour maps of $L(r)$ for: (a) ethane in a plane bisecting *anti*-hydrogens; (b) ethene in the molecular plane; (c) ethene perpendicular to the molecular plane, and (d) ethyne. The solid lines depict the zero-flux surfaces of the C and H atoms. From *J. Phys. Chem.* **100**, 15398 (1996).

addition to the C–H bonds, the contours indicate the electron density associated with the unshared pairs on oxygen. Figure 1.42d, shows L perpendicular to the plane of the molecule and is influenced by the π component of the C=O bond. It shows greater electron density around oxygen, which is consistent with the expectation that carbon would have a partial positive change.

These diagrams can help to visualize the electron density associated with these prototypical molecules. We see that most electron density is closely associated with

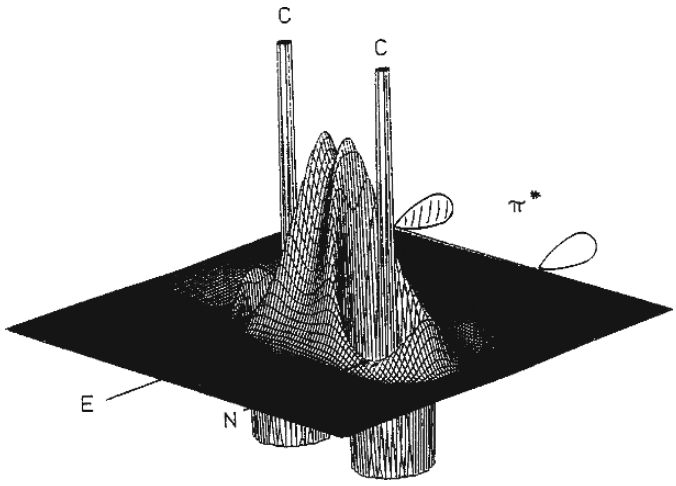

Fig. 1.40. Perspective of Laplacian $-\nabla^2\rho_c\mathbf{r}$ of ethene in a plane perpendicular to the molecular plane. From E. Kraka and D. Cremer in *The Concept of the Chemical Bond*, Z. B. Maksic, ed., Springer-Verlag 1990, p. 533.

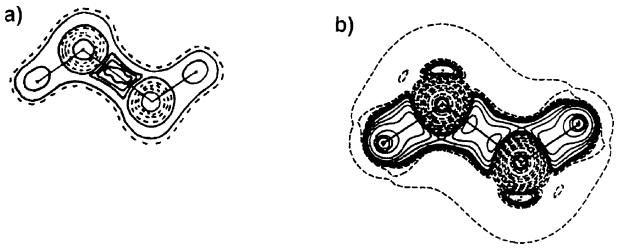

Fig. 1.41. Comparison of experimental (a) and theoretical (b) Laplacian of the electron density of ethane. From *Can. J. Chem.*, **74**, 1171 (1996).

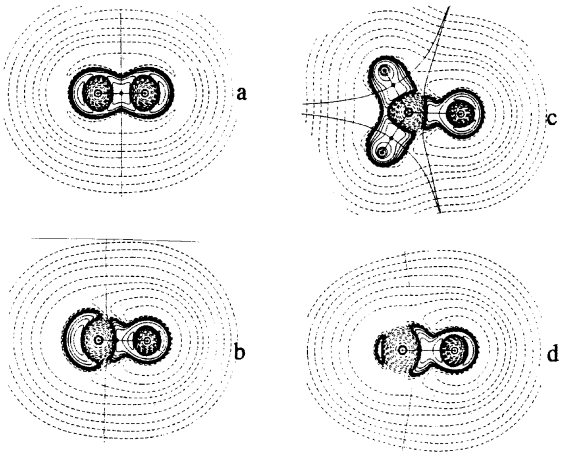

Fig. 1.42. Contour plots of $L(\mathbf{r})$ for N_2 (a), CO (b), and $H_2C{=}O$ in (c) and perpendicular to (d) the plane of the molecule. From *J. Phys. Chem.*, **100**, 15398 (1996).

the nuclei, but that regions of increased electron density corresponding to chemical bonds can be recognized. Most of the electron density diagrams that are available are the results of computation. Where experimental data are available, there is excellent correspondence with the computational data.

Topic 1.5. Application of Density Functional Theory to Chemical Properties and Reactivity

The qualitative ideas of valence bond (VB) theory provide a basis for understanding the relationships between structure and reactivity. Molecular orbital (MO) theory offers insight into the origin of the stability associated with delocalization and also the importance of symmetry. As a central premise of density functional theory (DFT) is that the electron density distribution determines molecular properties, there has be an effort to apply DFT to numerical evaluation of the qualitative concepts such as electronegativity, polarizability, hardness, and softness. The sections that follow explore the relationship of these concepts to the description of electron density provided by DFT.

T.1.5.1. DFT Formulation of Chemical Potential, Electronegativity, Hardness and Softness, and Covalent and van der Waal Radii

DFT suggests quantitative expressions and interrelation of certain properties such as electronegativity and polarizability, and the related concepts of hardness and softness introduced in Sections 1.1.3 through 1.1.6.[144] DFT calls the escaping tendency of an electron from a particular field its *chemical potential*,[145] μ, defined by

$$\mu = (\partial E/\partial N)_v \tag{1.31}$$

which is the slope of a curve for the energy of the system as a function of the change in the number or electrons.

A stable system, such as a molecule, attains a common chemical potential among its components. That is, there is no net force to transfer electron density from one point to another. The idea that chemical potential is equivalent throughout a molecule, and specifically between bonded atoms, accords with the concept of *electronegativity equalization* (see Section 1.1.4).[146] Chemical potential is related to electrophilicity and nucleophilicity. A system with an attraction toward electrons is electrophilic, whereas a system that can donate electrons is nucleophilic. Chemical potential is considered to be the opposite of absolute (Mulliken) electronegativity and can be approximated by

$$\mu = -\frac{\text{IP} + \text{EA}}{2} \tag{1.32}$$

which is negative of the Mulliken absolute electronegativity:

$$\chi = \frac{\text{IP} + \text{EA}}{2} \tag{1.33}$$

Since μ is the slope of electronic energy as a function of the change in the number of electrons, the Mulliken equation gives the energy for the $+1$ (IP) and -1 (EA) ionization states. This is illustrated in Figure 1.43, which shows that $(\text{IP}+\text{EA})/2$ is the average slope over the three points and should approximate the slope at the midpoint, where $N = 0$.[147]

The Luo-Benson expression for electronegativity[148]

$$V = n/r \tag{1.34}$$

which relates electronegativity to the number of valence shell electrons n and the atomic radius r is both theoretically related[149] and empirically correlated[150] with the Mulliken

144. P. W. Chattaraj and R. G. Parr, *Structure and Bonding*, **80**, 11 (1993); G.-H. Liu and R. G. Parr, *J. Am. Chem. Soc.*, **117**, 3179 (1995).
145. R. G. Parr, R. A. Donnelly, M. Levy, and W. E. Palke, *J. Chem. Phys.*, **68**, 3801 (1978).
146. R. T. Sanderson, *J. Am. Chem. Soc.*, **105**, 2259 (1983); R. T. Sanderson, *Polar Covalence*, Academic Press, New York, 1983.
147. R. G. Pearson, *Chemical Hardness*, Wiley-VCH, Weinheim, 1977, p. 33; see also R. P. Iczkowski and J. L. Margrave, *J. Am. Chem. Soc.*, **83**, 3547 (1961).
148. Y. R. Luo and S. W. Benson, *J. Phys. Chem.*, **92**, 5255 (1988); Y.-R. Luo and S. W. Benson, *J. Am. Chem. Soc.*, **111**, 2480 (1989); Y. R. Luo and S. W. Benson, *J. Phys. Chem.*, **94**, 914 (1990); Y. R. Luo and S. W. Benson, *Acc. Chem. Res.*, **25**, 375 (1992).
149. P. Politzer, R. G. Parr, and D. R. Murphy, *J. Chem. Phys.*, **79**, 3859 (1983).
150. Y. R. Luo and P. D. Pacey, *J. Am. Chem. Soc.*, **113**, 1465 (1991).

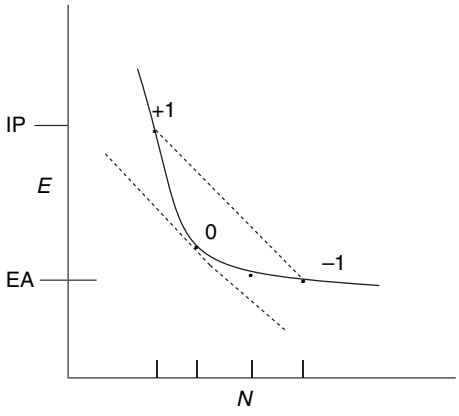

Fig. 1.43. Diagram showing that $(EA + IP)/2$ provides an approximation of the slope of E for the neutral atoms. Adapted from R. G. Pearson, *Chemical Hardness*, Wiley-VCH, Weinheim, 1997, p. 33.

absolute electronegativity $(IP+EA)/2$. The principle of maximum hardness[151] (p. 16) can be derived as a consequence of DFT, as can the concepts of hardness and softness.[152]

In DFT, hardness is defined as

$$2\eta = (\partial\mu/\partial N)_v \tag{1.35}$$

which is the curvature of the plot of E versus N and is approximated by

$$\eta \cong (IP - EA)/2 \tag{1.36}$$

and softness, $S = 1/\eta$ is

$$(\partial N/\partial\mu)_v \cong 2/(IP - EA) \tag{1.37}$$

There is a linear correlation between the empirical electronegativity (Pauling scale) and hardness and the absolute electronegativity (Mulliken electronegativity) for the nontransition metals[153]:

$$\chi = 0.44\eta + 0.044\chi_{abs} + 0.04 \tag{1.38}$$

This correlation is illustrated in Figure 1.44. Polarizability is related to softness. Expressed as $\alpha^{1/3}$, it is proportional to softness, approximated by $2/(IP - EA)$.[154]

DFT also suggests explicit definitions of covalent and van der Waals radii. The covalent radius in the AIM context is defined by the location of the bond critical point

151. R. G. Parr and P. K. Chattaraj, *J. Am. Chem. Soc.*, **113**, 1854 (1991); T. K. Ghanty and S. K. Ghosh, *J. Phys. Chem.*, **100**, 12295 (1996).
152. P. K. Chattaraj, H. Lee, and R. G. Parr, *J. Am .Chem. Soc.*, **113**, 1855 (1991).
153. R. G. Pearson, *Chemical Hardness*, Wiley-VCH, Weinheim, Germany, 1997, p. 44; J. K. Nagle, *J. Am. Chem. Soc.*, **112**, 4741 (1990).
154. T. K. Ghanty and S. K. Ghosh, *J. Phys. Chem.*, **97**, 4951 (1993); S. Hati and D. Datta, *J. Phys. Chem.*, **98**, 10451 (1994).

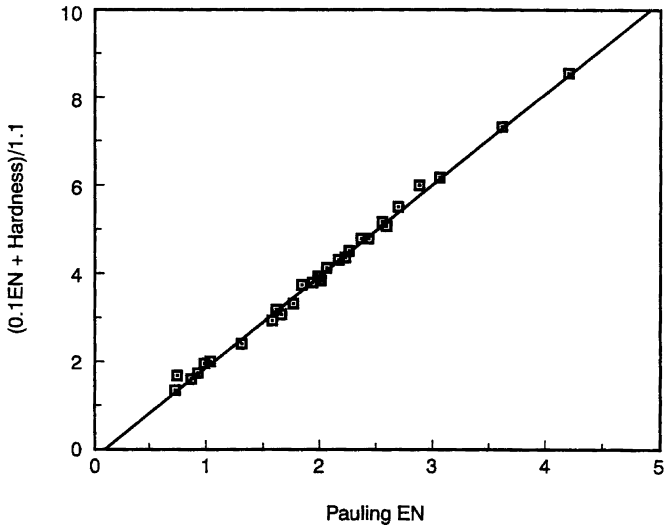

Fig. 1.44. Correlation between empirical (Pauling) electronegativity, (χ_{Pauling}), hardness (η), and absolute (Mulliken) electronegativity (χ_{abs}). From R. G. Pearson, *Chemical Hardness*, Wiley-VCH, Weinheim, 1997, p. 54.

and depends on the other element in the bond. The covalent radii of atoms can also be defined theoretically within DFT,[155] and are equated with the distance at which the chemical potential equals the total electrostatic potential calculated for the atom. This is the point at which the electrostatic potential crosses from negative to positive and where the sum of the kinetic energy and exchange and correlation functionals is zero. Using the approximation $-(\text{IP}+\text{EA})/2 = \mu$, one finds φ_r, the distance at which this equality holds[156]:

$$\text{at } r_c \; V_c = \mu \cong -\frac{\text{IP}+\text{EA}}{2} \tag{1.39}$$

The values derived in this way are shown in Table 1.24.

The AIM treatment defines van der Waals radii in terms of a particular electron density contour. It has been suggested that the 0.002 au contour provides a good representative of the van der Waals dimension of a molecule.[157]

T.1.5.2. DFT Formulation of Reactivity—The Fukui Function

The electron density $\rho(\mathbf{r})$ can provide information about the *reactivity* of a molecule. MO theory can assess reactivity in terms of frontier orbitals and, in particular, the energy, atomic distribution and symmetry of the HOMO and LUMO. DFT provides a representation of total electron distribution and extracts indicators of reactivity. The

155. P. Ganguly, *J. Am. Chem. Soc.*, **115**, 9287 (1993).
156. P. Politzer, R. G. Parr, and D. R. Murphy, *J. Chem. Phys.*, **79**, 3859 (1983).
157. R. F. W. Bader, W. H. Henneker, and P. D. Cade, *J. Chem. Phys.* **46**, 3341 (1967); R. F. W. Bader and H. J. T. Preston, *Theor. Chim. Acta*, **17**, 384 (1970).

Table 1.24. Covalent Radii from DFT

Atom	Covalent radius (au)[a]
Li	1.357
B	1.091
C	0.912
N	0.814
O	0.765
F	0.671
Na	1.463
Al	1.487
Si	1.296
P	1.185
S	1.120
Cl	0.999
Se	1.209
Br	1.116
I	1.299

a. P. Politzer, R. G. Parr, and D. R. Murphy, *J. Chem. Phys.*, **79**, 3859 (1983); M. K. Harbola, R. G. Parr, and C. Lee, *J. Chem. Phys.*, **94**, 6055 (1991).

responsiveness of this electron distribution to a perturbing external field, e.g., an approaching reagent, must be evaluated. This responsiveness is described by the *Fukui function*,[158] which is a reactivity indicator is defined by

$$f(\mathrm{r}) = [n(\mathrm{r})/N]\left[\frac{\delta\mu}{\delta\nu(\mathbf{r})}\right]_{\mathrm{N}} = \left(\frac{\partial\rho(\mathrm{r})}{\partial N}\right)_{\nu(\mathrm{r})} \tag{1.40}$$

where N is the change in the number of electrons in the system.

Fukui functions are defined for electrophilic (f^-), nucleophilic (f^+), and radical (f°) reactions by comparing the electron density $\rho(\mathbf{r})$, with one fewer electron, one more electron, and the average of the two[159]:

$$f^-(\mathbf{r}) = \rho_N(\mathbf{r}) - \rho_{N-1}(\mathbf{r}) \tag{1.41}$$

$$f^+(\mathbf{r}) = \rho_{N+1}(\mathbf{r}) - \rho_N(\mathbf{r}) \tag{1.42}$$

$$f^\circ(\mathbf{r}) = \frac{\rho_{\mathrm{N}+1}(\mathbf{r}) - \rho_{\mathrm{N}-1}(\mathbf{r})}{2} \tag{1.43}$$

The Fukui function describes interactions between two molecules in terms of the electron transfer between them. The extent of electron transfer is related to chemical potential (and electronegativity) and hardness (and polarizability).

$$\Delta\mathrm{N} = \frac{|\mu_{\mathrm{B}}^\circ - \mu_{\mathrm{A}}^\circ|}{\eta_{\mathrm{B}}^\circ + \eta_{\mathrm{A}}^\circ} \tag{1.44}$$

The responsiveness of the electron density to interaction with another field is nonuniform over the molecule. The electron density can be further partitioned among

158. R. G. Parr and W. Yang, *J. Am. Chem. Soc.*, **106**, 4049 (1984).
159. C. Lee, W. Yang, and R. G. Parr, *Theochem*, **40**, 305 (1988).

the atoms of a molecule by *condensed Fukui* functions. These calculations must use a scheme, such as Mulliken population analysis (see Section 1.4.1) for dividing the electron density among the atoms. The condensed Fukui functions identify regions of space that are electron-rich (f^-) and electron-poor (f^+).[160] Reactivity at individual atoms can also be expressed as *local softness*, which is the product of the Fukui function and global softness S.[161] As with the Fukui function, these are defined for electrophilic, nucleophilic, and radical reactants.

$$s^- = [\rho_{(N)} - \rho_{(N-1)}]S \tag{1.45}$$

$$s^+ = [\rho_{(N+1)} - \rho_{(N)}]S \tag{1.46}$$

and

$$s^\circ = \tfrac{1}{2}[\rho_{(N+1)} - \rho_{(N-1)}]S \tag{1.47}$$

The idea that *frontier orbitals* control reactivity introduced in the context of MO theory has an equivalent in DFT. The electron density distribution should have regions of differing susceptibility to approach by nucleophiles and electrophiles. Reactivity should correspond to the ease of distortion of electron density by approaching reagents. This response to changes in electron distribution is expressed in terms of the Fukui function, which describes the ease of displacement of electron density in response to a shift in the external field. Since the electron distribution should respond differently to interaction with electron acceptors (electrophiles) or electron donors (nucleophiles), there should be separate f^+ and f^- functions. Reaction is most likely to occur at locations where there is the best match (overlap) of the f^+ function of the electrophile and the f^- function of the nucleophile.[162] For example, the f^+ and f^- functions for formaldehyde have been calculated and are shown in Figure 1.45.[163] The f^+ function, describing interaction with a nucleophile, has a shape similar to the π^* MO. It has a higher concentration on carbon than on oxygen and the maximum value is perpendicular to the molecular plane. The f^- function is similar in distribution to the nonbonding (n) electron pairs of oxygen. This treatment, then, leads to predictions about the reactivity toward nucleophiles and electrophiles that are parallel to those developed from MO theory (see p. 45). A distinction to be made is that in the MO formulation the result arises on the basis of a particular orbital combination—the HOMO and LUMO. The DFT formulation, in contrast, comes from the total electron density. Methods are now being developed to compute Fukui functions and other descriptors of reactivity derived from total electron density.

DFT can evaluate properties and mutual reactivity from the electron distribution. These relationships between qualitative concepts in chemistry, such as electronegativity and polarizability, suggest that DFT does incorporate fundamental relationships between molecular properties and structure. At this point, we want to emphasize the conceptual relationships between the electron density and electronegativity and polarizability. We can expect electrophiles to attack positions with relatively high electron density and polarizability. Nucleophiles should attack positions of relatively

160. Y. Li and J. N. S. Evans, *J. Am. Chem. Soc.*, **117**, 7756 (1995).
161. W. Yang and W. J. Mortier, *J. Am. Chem. Soc.*, **108**, 5708 (1986).
162. R. F. Nalewajski, *Top. Catal.*, **11/12**, 469 (2000).
163. A. Michalak, F. De Proft, P. Geerlings, and R. F. Nalewajski, *J. Phys. Chem. A*, **103**, 762 (1999); F. Gilardoni, J. Weber, H. Chermette, and T. R. Ward, *J. Phys. Chem. A*, **102**, 3607 (1998).

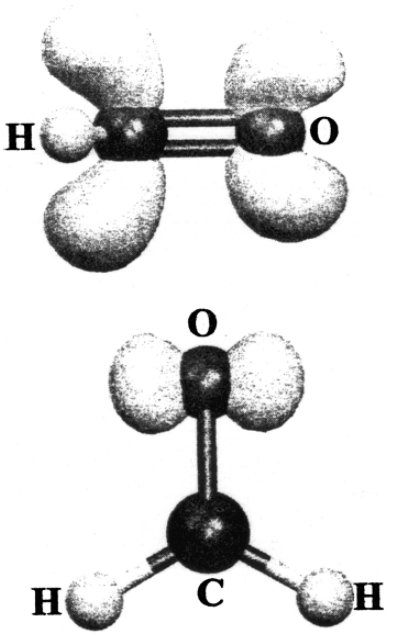

Fig. 1.45. Fukui function f^+ and f^- isosurfaces for CH_2=O (0.001 au). Reproduced with permission from F. Gilardoni, J. Weber, H. Chermette, and T. R. Ward, *J. Phys. Chem. A*, **102**, 3607 (1998).

low electron density. The hard-soft concept also states that *reactant and reagent should match* with respect to these properties. The methods for exploiting this potential are currently under development.

T.1.5.3. DFT Concepts of Substituent Groups Effects

The interpretation and correlation of information about organic compounds depends on the concept of *substituent effects*, which is the idea that a particular group of atoms will affect structure and reactivity in a predictable way. This is a long-standing and fundamental concept in organic chemistry. Recent developments, particularly in DFT, have provided new theoretical foundations and interpretations. Substituents groups can be classified as electron-releasing (ERG) or electron-withdrawing (EWG). There is an approximate ordering of such groups that is related in a general way to electronegativity. We discuss substituent effects in detail in Chapter 3, but here we want to introduce some broad concepts concerning the ways that substituents affect structure and reactivity.

Traditionally, the focus has been on polar and resonance effects, based on VB ideas about structure, and the emphasis is on partial charges arising from polar bonds and resonance/hyperconjugation. However, in MO theory, we use the idea of *perturbations*. The question asked is, "How does a substituent affect the energy and shapes of the orbitals, with particular attention to the HOMO and LUMO, the *frontier orbitals*. Ultimately, substituents affect structure and reactivity by changing the electron density distribution. From the concept of electronegativity, we know that bonds have dipoles,

which influence interactions with approaching reagents and thus affect reactivity. We also discussed the concept of *polarizability*, which refers to the ease of distortion of the electron density distribution of an atom or an ion and can be described as *hardness* or *softness*. Since chemical reactions involve the reorganization of electrons by breaking and forming bonds, polarizability also has a major influence on reactivity.

There have been a number of efforts to assign numerical values to electronegativity of substituent groups, analogous to the numbers assigned to atoms (see Section 1.1.3). These have been based on structural parameters, charge distribution, thermodynamic relationships and on MO computations.[164] More recently, DFT descriptions of electron density have developed and these, too, have been applied to organic functional groups. DFT suggests quantitative expressions of some of the qualitative concepts such as electronegativity, polarizability, hardness, and softness.[165] DFT describes a molecule as an electron density distribution, in which the nuclei are embedded, that is subject to interaction with external electrical fields, such as that of an approaching reagent. Several methods are currently being explored to find correlations and predictions based on DFT concepts that were introduced in Section 1.3.

De Proft, Langenaeker, and Geerlings applied the DFT definitions of electronegativity, hardness, and softness to calculate group values, which are shown in Table 1.25. These values reveal some interesting comparisons. The electronegativity values calculated for C_2H_5, $CH_2{=}CH$, and $HC{\equiv}C$ are in accord with the relationship with hybridization discussed in Section 1.1.5. The methyl group is significantly more electronegative and harder than the ethyl group. This is consistent with the difference noted between methyl and ethyl diazonium ions in Section 1.4.3. Typical EWGs such as $CH{=}O$, $C{\equiv}N$, and NO_2 show high electronegativity. Hardness values are more difficult to relate to familiar substituent effects. The acetyl, carboxamide, and nitro groups, for example, are among the softer substituents. This presumably reflects the electron density of the unshared electron pairs on oxygen in these groups.

AIM results from methyl compounds were also used to develop a group electronegativity scale. Boyd and Edgecombe defined a quantity F_A in terms of r_H, the location of the bond critical point to hydrogen, N_A the number of valence electrons of the atom A, and $\rho_{(c)}$, the electron density at the bond critical point[166]:

$$F_n = r_H / N_A \rho(r_c) r_{AH} \tag{1.48}$$

These were than scaled to give numerical comparability with the Pauling electronegativity scale.[167] In another approach, the charge on the methyl group was taken as the indicator of the electronegativity of the group X and the results were scaled to the Pauling atomic electronegativity scale.[168] It was also noted that the electronegativity value correlated with the position of the bond critical point relative to the bond length:

$$r_c/R = 0.785 - 0.042\chi^0_x \tag{1.49}$$

As the group becomes more electronegative, the critical point shifts toward the substituent. Table 1.26 compares two of the traditional empirical electronegativity

164. A. R. Cherkasov, V. I. Galkin, E. M. Zueva, and R. A. Cherkasov, *Russian Chem. Rev.* (Engl. Transl.), **67**, 375 (1998).
165. P. W. Chattaraj and R. G. Parr, *Struct. Bonding*, **80** 11 (1993); G.-H. Liu and R. G. Parr, *J. Am. Chem. Soc.*, **117**, 3179 (1995).
166. R. J. Boyd and K. E. Edgecombe, *J. Am. Chem. Soc.*, **110**, 4182 (1988).
167. R. J. Boyd and S. L. Boyd, *J. Am. Chem. Soc.*, **114**, 1652 (1992).
168. S. Hati and D. Datta, *J. Comput. Chem.*, **13**, 912 (1992).

Table 1.25. Properties of Substituent Groups[a]

Group	χ(eV)	η(eV)	$S(10^{-2}\,eV^{-1})$
CH_3	5.12	5.34	9.36
CH_3CH_2	4.42	4.96	10.07
$CH_2{=}CH$	5.18	4.96	10.07
$HC{\equiv}C$	8.21	5.77	8.67
$HC{=}O$	4.55	4.88	10.25
$CH_3C{=}O$	4.29	4.34	11.51
CO_2H	5.86	4.71	10.61
CO_2CH_3	5.48		
$CONH_2$	4.67	4.42	11.32
CN	8.63	5.07	9.86
NH_2	6.16	6.04	8.28
NO_2	7.84	4.89	10.22
OH	6.95	5.69	8.79
CH_3O	5.73	4.39	10.28
F	10.01	7.00	7.14
CH_2F	4.97	5.31	9.41
CHF_2	5.25	5.42	9.22
CF_3	6.30	5.53	9.05
SH	5.69	3.96	12.62
CH_3S	4.99	3.71	13.49
Cl	7.65	4.59	10.89
CH_2Cl	4.89	4.71	10.61
$CHCl_2$	5.12	4.38	11.42
CCl_3	5.53	4.10	12.21

a. F. De Proft, W. Langemaeker, and P.Geerlings, *J. Phys. Chem.*, **97**, 1826 (1993).

scales with these two sets calculated on a theoretical basis. Figure 1.46 is a plot that provides an indication of the scatter in the numerical values in comparison with an empirical scale.

The broad significance of the correlation shown in Figure 1.46 is to cross-validate the theoretical and empirical views of functional groups that have developed in organic chemistry. The two theoretical scales are based entirely on measures of electron density. As to more specific insights, with reference to Table 1.26, we see the orders $CCl_3 > CHCl_2 > CH_2Cl$ in electronegativity. This accords with the expectation for cumulative effects and is consistent with polar effects, as observed, for example, in the acidities of the corresponding carboxylic acids shown in Table 1.27. Note from Table 1.25 that the hardness and softness of the fluoro and chloro groups differ. Each additional fluoro substituent makes the group harder, but each chlorine makes it softer. This difference reflects the greater polarizability of the chlorine atoms.

If we compare the F, NO_2, CN, and CF_3 substituents, representing familiar EWGs, we see that they are in the upper range of group electronegativity in Table 1.25 (10.01, 7.84, 8.63, and 6.30, respectively). With the exception of F, however, these substituents are not particularly hard.

The values for ethyl, vinyl, and ethynyl are noteworthy. Quite high electronegativity and hardness are assigned to the ethynyl group. This is in reasonable accord with the empirical values in Table 1.25. The methyl group also deserves notice. We will see in other contexts that the methyl group is harder than other primary alkyl groups. The theoretical treatments suggest this to be the case. It is not clear that the empirical scales reflect much difference between a methyl and ethyl group. This may be because

Table 1.26. Empirical and Theoretical Electronegativity Scales for Some Functional Groups

Group	Wells[a]	Inamoto and Masuda[b]	Boyd and Boyd[c]	Hati and Datta[d]
CH_3	2.3	2.47	2.55	2.09
CH_2Cl	2.75	2.54	2.61	
$CHCl_2$	2.8	2.60	2.66	
CCl_3	3.0	2.67	2.70	
CF_3	3.35	2.99	2.71	2.49
$CH_2 = CH$	3.0	2.79	2.58	2.18
$HC{\equiv}C$	3.3	3.07	2.66	2.56
Ph	3.0	2.72	2.58	
$N{\equiv}C$	3.3	3.21	2.69	3.61
H	2.28	2.18		2.20
NH_2	3.35	2.99	3.12	2.96
N^+H_3	3.8	3.71	3.21	3.52
$N{\equiv}N^+$		3.71		4.06
NO_2	3.4	3.42	3.22	3.44
OH	3.7	3.47	3.55	3.49
F	3.95		3.95	3.75
Cl	3.03		3.05	2.68
Br	2.80		2.75	
I	2.28			

a. P. R. Wells, *Prog. Phys. Org. Chem.*, **6**, 111 (1968).
b. N. Inamoto and S. Masuda, *Chem. Lett.*, 1003 (1982).
c. R. J. Boyd and S. L. Boyd, *J. Am. Chem. Soc.*, **114**, 1652 (1992).
d. S. Hati and D. Datta, *J. Comput. Chem.*, **13**, 912 (1992).

the theoretical results pertain to isolated molecules, whereas the empirical values are derived from measurements in solution. The smaller size of the methyl group makes it less polarizable than larger alkyl groups. This difference is maximized in the gas phase, where there are no compensating solvent effects.

Let us now consider a few simple but important systems that can illustrate the application of these ideas. We know that the acidity of the hydrides of the second-row elements increases sharply going to the right in the periodic table. The same trend is true for the third row and in each case the third-row compound is more acidic than its second-row counterpart. This is illustrated by the gas phase ionization enthalpy data in Table 1.28.

The gas phase data from both the second- and third-row compounds can be correlated by an expression that contains terms both for electronegativity (χ) and hardness (μ). The sign is negative for hardness:

$$\Delta G_{\text{acid}} = 311.805 - 18.118\chi + 33.771\mu \tag{1.50}$$

Table 1.27. Gas Phase and Aqueous pK_a Values

	pK_a		pK_a
FCH_2CO_2H	2.59	$ClCH_2CO_2H$	2.87
CHF_2CO_2H	NA	$CHCl_2CO_2H$	1.35
CF_3CO_2H	0.52	CCl_3CO_2H	0.66

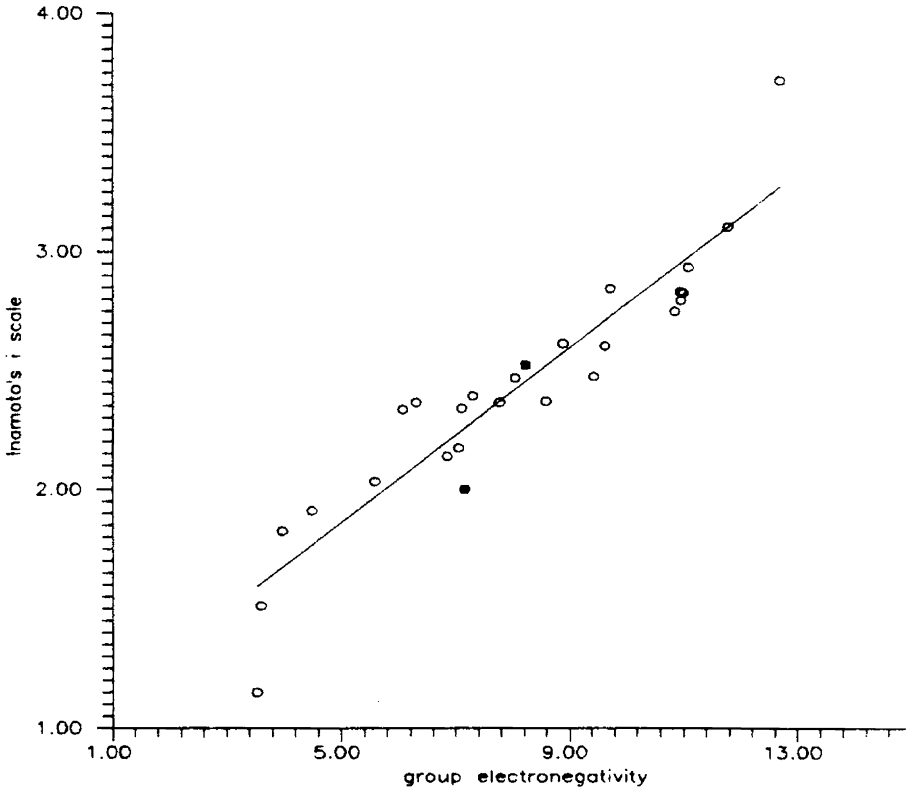

Fig. 1.46. Correlation between AIM electronegativity χ (in eV) with Inamoto *i* empirical group electronegativity scale. Correlation coefficient is 0.938. Reproduced with permission from S. Hati and D. Datta, *J. Comput. Chem.*, **13**, 912 (1992).

The implication is that both increased electronegativity and polarizability (or softness) contribute to acidity. The increasing acidity can be interpreted in terms of the ability of the anion to accommodate the negative charge left by the removal of a proton. The more electronegative and the more polarizable (softer) the anion, the better it can accept the additional charge. There is a related trend going down the periodic table, i.e., HI > HBr > HCl > HF. The order reflects the increasing bond strength from HI to HF, which is probably due to a combination of overlap and electronegativity effects.

Turning to an analogous group of organic compounds, we know that the order of acidity of alcohols in aqueous media is $CH_3OH > CH_3CH_2OH > (CH_3)_2CHOH >$

Table 1.28. Gas Phase and Aqueous p*K* Values[a]

Second row	ΔH	p*K*	Third row	ΔH	p*K*
CH_4	416.8	48	SiH_4	372.4	
NH_3	403.7	38	PH_3	369.0	29
H_2O	390.8	15.7	H_2S	351.3	7.0
HF	371.4	3.2	HCl	333.4	−7

a. F. De Proft, W. Langenaeker, and P. Geerlings, *Int J. Quantum Chem.*, **55**, 459 (1995).

$(CH_3)_3COH$, but the order is exactly the opposite in the gas phase.[169] The reverse order in the gas phase attracted a good deal of interest when it was discovered, since it is contrary to the general expectation that more highly substituted alkyl groups are better electron donors than methyl and primary groups. Both qualitative[170] and quantitative[171] treatments have identified polarizability, the ability to accept additional charge, as the major factor in the gas phase order. Note also that the order is predicted by the HSAB relationship since the softer (more substituted) alkoxides should bind a hard proton more weakly than the harder primary alkoxides.

Another study examined the acidity of some halogenated alcohols. The gas phase acidity order is $ClCH_2OH > BrCH_2OH > FCH_2OH > CH_3OH$. The same Cl > Br > F order also holds for the di- and trihalogenated alcohols.[172] The order reflects competing effects of electronegativity and polarizability. The electronegativity order F > Cl > Br is reflected in the size of the bond dipole. The polarizability order Br > Cl > F indicates the ability to disperse the negative charge. The overall trend is largely dominated by the polarizability order. These results focus attention on the importance of polarizability, especially in the gas phase, where there is no solvation to stabilize the anion. The intrinsic ability of the substituent group to accommodate negative charge becomes very important.

The role of substituents has been investigated especially thoroughly for substituted acetic and benzoic acids. Quantitative data are readily available from pK_a measurements in aqueous solution. Considerable data on gas phase acidity are also available.[173] EWG substituents increase both solution and gas phase acidity. In the gas phase, branched alkyl groups slightly enhance acidity. In aqueous solution, there is a weak trend in the opposite direction, which is believed to be due to poorer solvation of the more branched anions. Geerling and co-workers have applied DFT concepts to substituent effects on acetic acids.[174] The Fukui functions and softness descriptors were calculated using electron density and Mulliken population analysis (see Topic 1.5.2). The relative correlation of these quantities with both solution and gas phase acidity was then examined. In both cases, the best correlations were with the Mulliken charge. In the case of gas phase data, the correlations were improved somewhat by inclusion of a second parameter for group softness. The picture that emerges is consistent with the qualitative concepts of HSAB. The reactions in question are hard-hard interactions, the transfer of a proton (hard) to an oxygen base (also hard). The reactions are largely controlled by electrostatic relationships, as modeled by the Mulliken charges. The involvement of softness in the gas phase analysis suggests that polarizability makes a secondary contribution to anionic stability in the gas phase.

169. J. I. Brauman and L. K. Blair, *J. Am. Chem. Soc.*, **92**, 5986 (1976).
170. W. M. Schubert, R. B. Murphy, and J. Robins, *Tetrahedron*, **17**, 199 (1962); J. E. Huheey, *J. Org. Chem.*, **36**, 204 (1971).
171. F. De Proft, W. Langenaeker, and P. Geerlings, *Tetrahedron*, **51**, 4021 (1995); P. Pérez, *J. Phys. Chem. A*, **105**, 6182 (2001).
172. S. Damoun, W. Langenaeker, G. Van de Woude, and P. Geerlings, *J. Phys. Chem.*, **99**, 12151 (1995).
173. C. Jinfeng, R. D. Topsom, A. D. Headley, I. Koppel, M. Mishima, R. W. Taft, and S. Veji, *Theochem*, **45**, 141 (1988).
174. F. De Proft, S. Amira, K. Choho, and P. Geerlings, *J. Phys. Chem.*, **98**, 5227 (1994).

General References

T. A. Albright, J. K. Burdett, and M. H. Whangbo, *Orbital Interactions in Chemistry*, John Wiley & Sons, New York, 1985.

R. F. W. Bader, *Atoms in Molecules: A Quantum Theory*, Clarendon Press, Oxford, 1990.

W. T. Borden, *Modern Molecular Orbital Theory for Organic Chemists*, Prentice-Hall, Englewood Cliffs, NY, 1975.

I. Fleming, *Frontier Orbital and Organic Chemical Reactions*, John Wiley & Sons, New York, 1976.

W. J. Hehre, L. Radom, P. v. R. Schleyer, and J. Pople, *Ab Initio Molecular Orbital Theory*, Wiley-Interscience, New York, 1986.

F. Jensen, *Introduction to Computational Chemistry*, John Wiley & Sons, Chichester, 1999.

W. Koch and M. C. Holthausen, *A Chemist's Guide to Density Functional Theory*, Wiley-VCH, Chichester, 2000.

E. Lewars, *Computational Chemistry*, Kluwer Academic Publishers, Boston, 2003.

R. G. Parr and W. Yang, *Density Functional Theory of Atoms and Molecules*, Oxford University Press, Oxford, 1989.

L. Salem, *Electrons in Chemical Reactions*, John Wiley & Sons, New York, 1982.

P. v. R. Schleyer, ed., *Encyclopedia of Computational Chemistry*, John Wiley & Sons, New York, 1998.

H. E. Zimmerman, *Quantum Mechanics for Organic Chemists*, Academic Press, New York, 1975.

Problems

(*References for these problems will be found on page 1155.*)

1.1. Suggest an explanation for the following observations:

a. Although the hydrocarbon calicene has so far defied synthesis, but it has been estimated that it would have a dipole moment as large as 5.6 D.

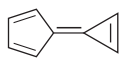

calicene

b. The measured dipole moment of 4-nitroaniline (6.2 D) is larger than the value calculated using standard group dipoles (5.2 D).

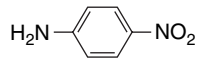

4-nitroaniline

c. The dipole moments of furan and pyrrole are in opposite directions.

furan

pyrrole

1.2. Predict the preferred site of protonation for each of the following molecules and explain the basis of your prediction.

a.

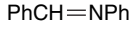

b.

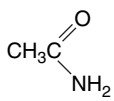

c.

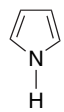

d.

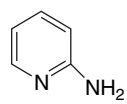

1.3. What physical properties, such as absorption spectra, bond lengths, dipole moment, etc., could be examined to obtain evidence of resonance interactions in the following molecules. What deviation from "normal" physical properties would you expect?

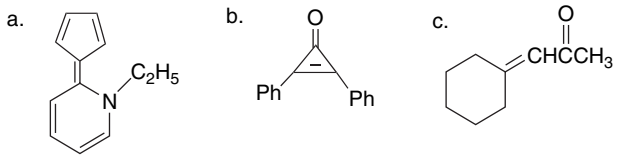

1.4. Consider each of the following physical characteristics of certain amides.

a. Carboxamides have rotational barriers on the order of 20 kcal/mol for the process:

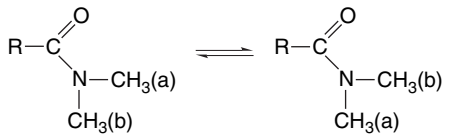

Develop a structural explanation for the barrier both in resonance and MO terminology.

b. The gas phase rotational barrier of *N*,*N*-dimethylformamide is about 19.4 kcal/mol, which is about 1.5 kcal/mol less than in solution. Is this change consistent with the explanation you presented in part (a)? Explain.

c. Account for the substantial differences in relative rates of alkaline hydrolysis for the following pairs of carboxamides.

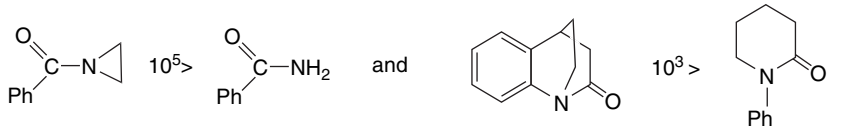

1.5. The AM1 semiempirical MO method was used to calculate structure, HOMO-LUMO orbital coefficients, and charge distribution for several substituted cyclopropenones. The results for 2-phenylcyclopropenone, 2-phenyl-3-methylcyclopropenone, and 2,3-diphenylcyclopropenone are given in Table 1.P5a. Based on this information, make predictions about the following reactions:

a. What will be the site of protonation of a cyclopropenone?

b. What will be the site of reaction of a cyclopropenone with a hard nucleophile, such as $^-$OH?

c. Is an alkyl or aryl substituent most effective in promoting reaction with a soft nucleophile?

Table 1.P5a. Orbital Coefficients and Energies

R	LUMO Coefficients				HOMO coefficients				Energy(kcal/mol)	
	C(1)	C(2)	C(3)	O	C(1)	C(2)	C(3)	O	HOMO	LUMO
C(2)=Ph C(3)=H	−0.088	0.445	−0.494	0.074	−0.058	−0.240	−0.444	0.275	−9.54	−0.82
C(2)=Ph C(3)=CH_3	−0.079	0.439	−0.501	0.066	0.071	−0.298	−0.436	0.290	−9.29	−0.76
C(2)=Ph C(3)=Ph	0.000	0.455	−0.455	0.000	−0.084	−0.348	−0.348	.270	−8.90	−1.14
Charges	C(1)	C(2)	C(3)	O						
C(2)=Ph C(3)=H	0.28	−0.11	−0.19	−0.27						
C(2)=Ph C(3)=CH_3	0.28	−0.11	−0.14	−0.27						
C(2)=Ph C(3)=Ph	0.28	−0.11	−0.11	−0.27						

1.6. It is observed that benzo[c] derivatives of furan, pyrrole, and thiophene are less stable and much more reactive than the corresponding benzo[b] derivatives. The differences are apparent for example in [4 + 2] cycloadditions, which are facile with the benzo[c] but not the benzo[b] derivatives. Some MO properties from AM1 calculations are given in Tables 1.P6a, 1.P6b and 1.P6c. What features of the results are in accord with the experimental observations? Do you find any features of the results than run counter to the observations.

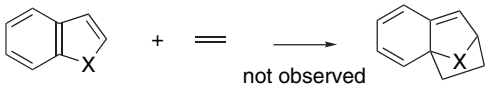

benzo[b]

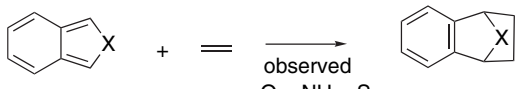

benzo[c]

Table 1.P6a. Enthalpy of Reactants and Transition Structures

	O	NH	S
ΔH_f (kcal/mol)			
Benzo[b]	20.8	55.2	42.4
Benzo[c]	27.9	61.7	49.4
ΔH_f for 4 + 2 TS			
Benzo[b]	75.7	115.3	110.8
Benzo[c]	64.5	104.8	102.4
$\Delta H^{\ddagger}$ for 4 + 2 TS			
Benzo[b]	38.4	43.6	51.9
Benzo[c]	20.1	26.6	36.5

Table 1.P6b. Bond Orders in Carbocyclic Rings

Benzo[b]heterocycles

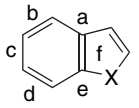

Benzo[c]heterocycles

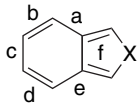

	O	NH	S		O	NH	S
a	1.34	1.30	1.30	a	1.12	1.16	1.15
b	1.46	1.50	1.51	b	1.71	1.66	1.67
c	1.37	1.33	1.32	c	1.15	1.19	1.18
d	1.45	1.50	1.51	d	1.71	1.66	1.67
e	1.45	1.28	1.30	e	1.12	1.16	1.15
f	1.30	1.27	1.32	f	1.14	1.20	1.20

Table 1.P6c. Orbital Energies in ev

	O	NH	S
HOMO:benzo[b]	−9.010	−8.403	−8.430
HOMO:benzo[c]	−8.263	−7.796	−8.340
LUMO:benzo[b]	−0.063	0.300	−0.166
LUMO:benzo[c]	−0.396	0.142	−0.592

1.7. The propellanes are highly reactive in comparison with unstrained hydrocarbons and readily undergo reactions that result in the rupture of the central bond. For example, it has been suggested that the polymerization of propellanes occurs by initial dissociation of the center bond. Perhaps surprisingly, it has been found that [1.1.1]propellane is considerably *less reactive* than either [2.2.1]propellane or [2.1.1]propellane. Use the computational enthalpy data below to estimate the energy required to break the center bond in each of the three propellanes. Assume that the bridgehead C–H bonds in each of the bicycloalkanes has a bond enthalpy of -104 kcal/mol. How might the results explain the relative reactivity of the propellanes.

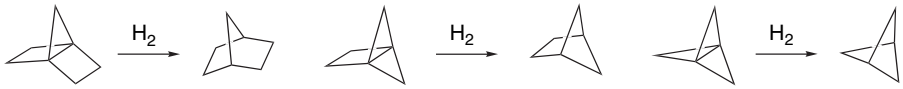

ΔH = –99 kcal/mol ΔH = –73 kcal/mol ΔH = –39 kcal/mol

1.8. Examine the heats of hydrogenation shown for unsaturated eight-membered ring hydrocarbons. (a) Discuss the differences among the different compounds in comparison with the standard ΔH_{H2} for an unstrained *cis* double bond, which is 27.4 kcal/mol. (b) Assigning a strain energy of 9.3 kcal/mol to cyclooctane, calculate the relative strain of each of the other compounds. (c) What role does conjugation play in relation to the observed ΔH_{H2}? (d) What conclusion do these data permit as to whether cyclooctatetraene is stabilized or destabilized by cyclic conjugation.

Compound	ΔH_{H2} (kcal/mol)
Z, *Z*, *Z*, *Z*-1,3,5,7-Cyclooctatetraene	97.06
Z, *Z*, *Z*-1,3,5-Cyclooctatriene	76.39
Z, *Z*, *Z*-1,3,6-Cyclooctatriene	79.91
Z, *Z*-1,3-Cyclooctadiene	48.96
Z, *Z*-1,4-Cyclooctadiene	52.09
Z, *Z*-1,5-Cyclooctadiene	53.68
Z-Cyclooctene	22.98
E-Cyclooctene	32.24

1.9. An isodesmic reaction suitable for calculating the resonance stabilization of benzene relative to cyclohexene is

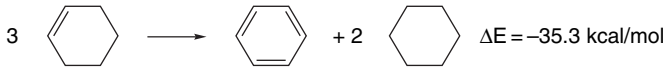

A similar calculation can be done with substituent groups in place. The results for several substituents by G3(MP2) computations are as follows:

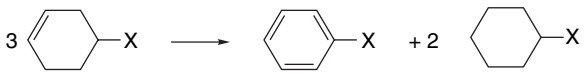

X	ΔE (kcal/mol)
H	−35.3
CH_3	−35.8
CH_3CH_2	−36.1
CH_2=CH	−38.1
HC≡C	−37.3
H_2N	−39.5

How do the calculated effects of substituents compare with the qualitative expectations on the basis of resonance concepts? How do the calculated stabilizations for the individual substituents compare with those calculated for double bonds and given on p. 52.

1.10. The explanation of substituent effects on the acidity of substituted carboxylic acids usually focuses on two factors: (a) The ability of the substituent to stabilize the negative charge; and (b) the effect of solvation on the anion. However, there will also be substituent effects on the stability and solvation of the undissociated acid. The studies described on p. XXX resulted in the following values for the gas phase energy (in hartrees) of the acids and anions and the resulting ΔG for gas phase ionization. Using this information and the solvation energies on p. 53,

analyze the relative importance of intrinsic anion stabilization and solvation on the observed acidity.

X	Acid, E_{gas}	Anion, E_{gas}	ΔG (kcal/mol)
H	−189.551612	−189.005818	342.49
CH_3	−228.792813	−228.241528	345.94
$ClCH_2$	−687.945725	−687.414262	333.50
$NCCH_2$	−320.909115	−320.386960	327.66
$(CH_3)_3C$	−346.481196	−345.936639	341.71

1.11. Cyclic amines such as piperidine and its derivatives show substantial differences in the properties of the axial C(2) and C(6) bonds. The axial C–H bonds are *weaker* than the equatorial C–H bonds, as indicated by a shifted C–H stretching frequency in the IR spectrum. The axial hydrogens also appear at higher field in ^{1}H-NMR spectra. Axial C(2) and C(6) methyl groups *lower* the ionization potential of the unshared pair of electrons on nitrogen more than equatorial C(2) and C(6) methyl groups. Discuss the structural basis of these effects in MO terminology.

1.12. Construct a qualitative MO diagram for the following systems and discuss how the π MOs are modified by addition of the substituent.

a. vinyl fluoride, compared to ethene
b. propenal, compared to ethene
c. acrylonitrile, compared to ethene
d. propene, compared to ethene
e. benzyl cation, compared to benzene
f. fluorobenzene, compared to benzene

1.13. Given below are the ΔE for some isodesmic reactions. Also given are the AIM and NPA charges at the carbon atoms of the double bond. Provide an explanation for these results in terms of both resonance structure and MO terminology.

a. Draw resonance structures and qualitative MO diagrams that indicate the stabilizing interaction.
b. Explain the order of stabilization N > O > F in both resonance and MO terminology.
c. Interpret the AIM and NPA charges in relationship to the ideas presented in (a) and (b).

$$CH_3CH_2X + CH_2{=}CH_2 \longrightarrow CH_3CH_3 + CH_2{=}CHX$$

X	ΔE	δC(1)[a]	δC(2)[a]	δC(1)[b]	δC(2)[b]
H	0	+0.08	+0.08	−0.25	−0.25
CH_3	−3.05	+0.02	+0.08	−0.09	−0.29
NH_2	−7.20	+0.51	+0.15	+0.14	−0.36
OH	−6.43	+0.58	+0.18	+0.26	−0.39
F	−0.99	+0.48	+0.29	+0.30	−0.36

a. AIM charges
b. NPA charges

1.14. In the Hückel MO treatment, orbitals on nonadjacent atoms are assumed to have no interaction. The concept of *homoconjugation* suggests that such orbitals may interact, especially in rigid structures in which the orbitals are directed toward one another. Consider, e.g, norbornadiene, (bicyclo[2.2.1]hepta-2,5-diene).

a. Construct an MO diagram according to HMO theory and assign orbital energies.
b. Construct the qualitative MO diagram that would result from significant overlap between the C(3) and C(5) and C(2) and C(6) orbitals.
c. The ionization potentials (IP) of some 2-substituted norbornadienes are given below. The two IP values pertain to the π system. Use PMO theory to analyze the effect these substituents have on the IP. Use a qualitative MO diagram to show how the substituents interact with the two double bonds and how this affects the IP. Discuss the effect the substituents have on the IP.

X	IP_1	IP_2
H	8.69	9.55
CH_3O	8.05	9.27
CN	9.26	10.12

1.15. a. Sketch the nodal properties of the Hückel HOMO orbital of the pentadienyl cation.
b. The orbital coefficients of two of the π MOs of pentadienyl are given below. Specify which is of lower energy; classify each orbital as bonding, nonbonding, or antibonding; and specify whether each orbital is *S* or *A* with respect to a plane bisecting the molecule perpendicular to the plane of the structure.

$$\psi_x = 0.50\varphi_1 + 0.50\varphi_2 - 0.50\varphi_4 - 0.50\phi_5$$
$$\psi_y = 0.58\varphi_1 - 0.58\varphi_3 + 0.58\varphi_5$$

1.16. There has been discussion as to whether unsaturated EWGs such as formyl or cyano stabilize or destabilize carbocations.

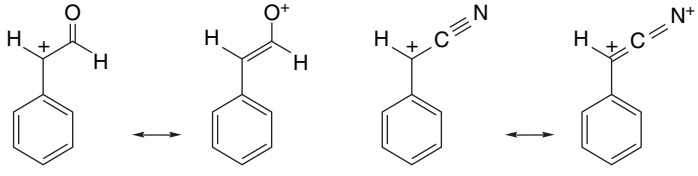

The diagrams below give STO-3G bond lengths and Mulliken charge densities for the benzyl cation and for its α-formyl and α-cyano derivatives. Analyze the effect of the substituents on the carbocation.

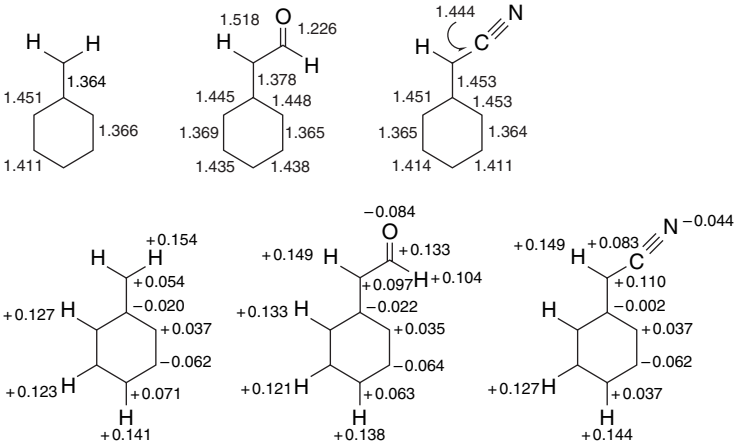

1.17 a. Calculate the HMO energy levels and atomic orbital coefficients for 1,3-butadiene.

b. Estimate the delocalization energy, in units of β, of the cyclobutadienyl dication $C_4H_4^{2+}$ from HMO theory.

c. Estimate, in units of β, the energy associated with the longest-wavelength UV-VIS absorption of 1,3,5,7-octatetraene. Does it appear at a longer or shorter wavelength than the corresponding absorption in 1,3,5-hexatriene?

1.18. Spiropentane has unusual strain and hybridization. Consider the following facets of its structure.

a. The strain energy of spiropentane (62.5 kcal/mol) is considerably more than twice that of cyclopropane (27.5 kcal/mol). Suggest an explanation.

b. The structure of spiropentane has been determined by X-ray crystallography. The endocyclic angles at the spiro carbon are about 62°, and the bond angles between C–C bonds in the adjacent rings are about 137°. How would you relate the strain to the hybridization of each carbon in spirocyclopentane based on these bond angles?

c. The fractional *s* character in a C–C bond can be estimated from ^{13}C–^{13}C coupling constants using the equation

$$J_{Ci-Cj} = K(s_i)(s_j)$$

where K is a constant = 550 Hz and s is the fractional s character of each atom. In spiropentane, the J for coupling between C(1) and C(3) is 20.2 Hz. The J between C(2) and C(3) is about 7.5 Hz. Calculate the s character of the C(1)–C(3) and C(2)–C(3) bonds.

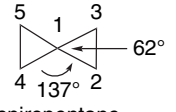

spiropentane

1.19. Predict whether the following gas phase reactions will be thermodynamically favorable or unfavorable. Explain your answer.

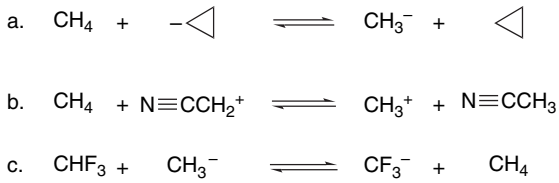

1.20. For each reaction, predict which compound would react faster (k) or give the more complete (K) reaction. Explain the basis for your prediction.

a.

b.

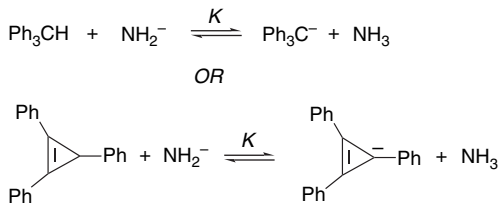

c.

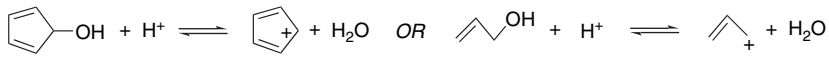

1.21. Computational comparison of the structures of the benzyl cation (**A**) and singlet phenyl carbene (**B**) indicate a much greater degree of double-bond character for the exocyclic bond in **A** than in **B**. Provide a rationale for this difference, both in VB and MO terminology.

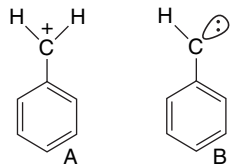

1.22. Interesting stability and structural trends have been found with MP2/6-31G* calculations on substituted imines. The data below give the ΔE for the isodesmic reaction:

$$YX-N=CH_2 + CH_3CH=CH_2 \longrightarrow CH_3N=CH_2 + YX-CH=CH_2$$

The data suggest that ΔE increases with χ_{XY}, the group electronegativity of the substituent. The X–N=CH_2 bond angle also decreases with χ_{AB}. The NPA

charges on the various atoms are given at the right of the table below. Discuss these trends, with particular attention to the interaction between the unshared electron pair on nitrogen and the C=N bond with the substituents.

Substituent	χ_{XY}	ΔE	XN = CH_2(°)	δ(X)[a]	δ(Y)[b]	δ(N)	δ(C)	δ(H)av
H	2.20	+4.1	110	+0.36	–	−0.66	−0.04	+0.17
CH_3	2.55	0.0	116	−0.44	+0.20$(H)_2$	−0.47	−0.06	+0.17
CH=O	2.66	−3.6	114	+0.65	−0.63 (=O)	−0.63	+0.07	+0.20
CN	2.69	−4.8	117	+0.47	−0.39 (N)	−0.55	+0.07	+0.20
CF_3	2.71	−4.7	118	+1.41	−0.42$(F)_3$	−0.59	+0.03	+0.20
NO_2	3.22	−10.0	111	+0.77	−0.44$(O)_2$	−0.38	+0.04	+0.22
NH_2[c]	3.12	−12.4	117	−0.71	+0.38$(H)_2$	−0.26	−0.15	+0.18
OH	3.55	−20.5	110	−0.64	+0.51 (H)	−0.14	−0.13	+0.20
F	4.00	−29.0	108	−0.31	–	0.00	−0.12	+0.22
H_3Si	1.90	+13.2	120	+1.29	−0.24$(H)_3$	−0.92	+0.03	+0.16

a. The charge on atom x.
b. The average charge on each atom Y.
c. The nitrogen in pyramidal in the lowest energy structure.

1.23. Table 1.P23a shows NPA charges for planar and twisted (C–N rotation) for formamide, 3-aminoacrolein and squaramide. Table 1.P23b gives computed ^{17}O chemical shifts for the planar and twisted forms. Figures 1.P23A–F are maps showing the potential for interaction with a particle of charge +0.5*e*. The barriers

Table 1.P23a. NPA Charges

	Planar	Twisted
Formamide		
O	−0.710	−0.620
C	+0.690	+0.695
N	−0.875	−0.929
NH_2	−0.080	−0.182
CH	+0.789	+0.812
3-Aminoacrolein		
O	−0.665	−0.625
C(1)	+0.512	+0.506
C(2)	−0.456	−0.351
C(3)	+0.198	+0.144
N	−0.832	−0.884
NH_2	−0.060	−0.149
Squaramide		
O(1)	−0.655	−0.609
C(1)	+0.519	+0.530
O(2)	−0.631	−0.626
C(2)	+0.554	+0.548
C(3)	+0.162	+0.088
C(4)	+0.258	+0.348
N(3)	−0.819	−0.851
NH_2	−0.001	−0.095
O(4)	−0.711	−0.687

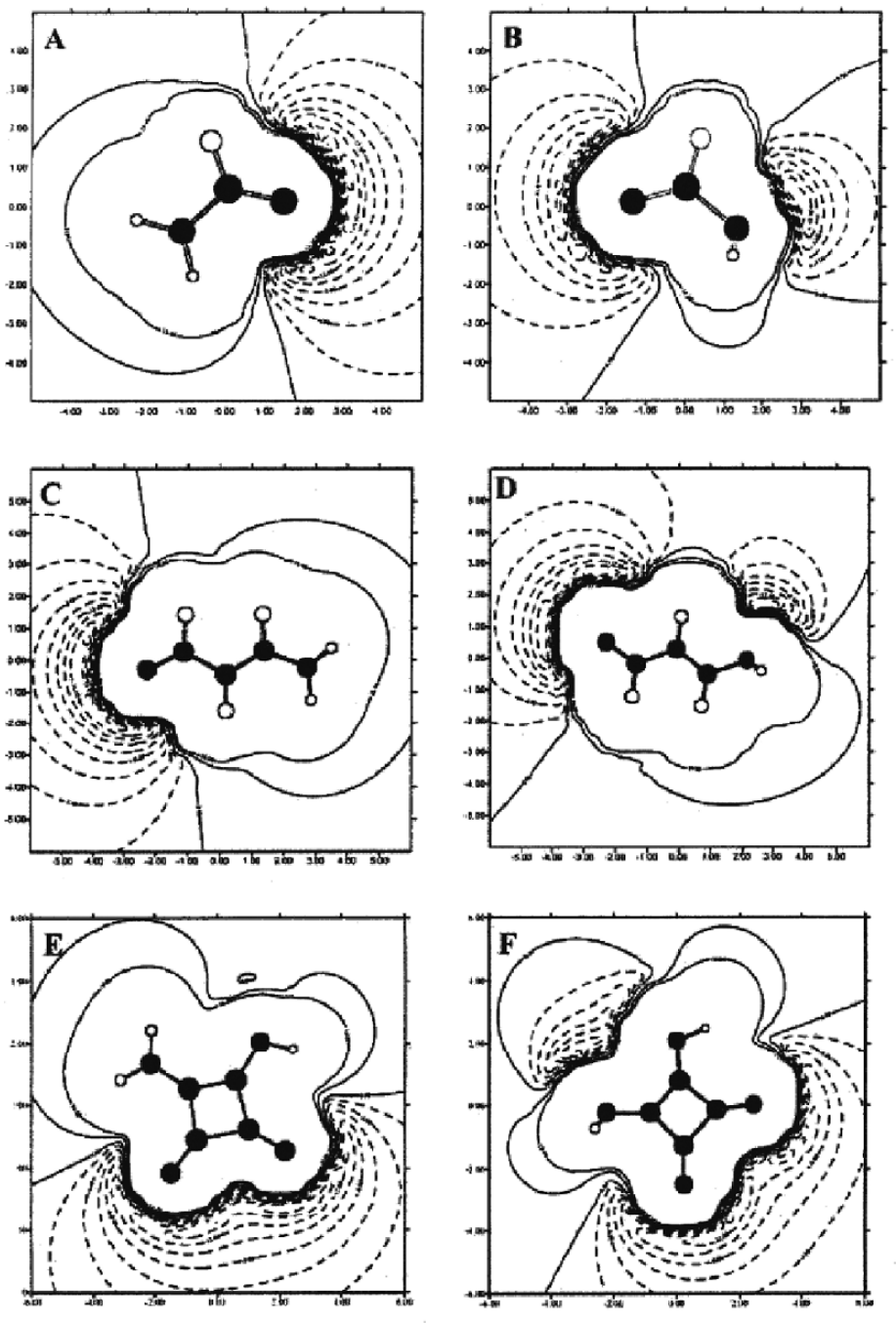

Fig. 1.P23. Molecular interaction potential maps for planar (left) and twisted (right)conformations of formamide, 3-aminoacrolein and squaramide.

Table 1.P23b. Calculated ^{17}O Chemical Shifts in ppm

	Planar	Twisted	Δ
Formamide	390	602	212
3-Aminoacrolein	568	630	62
Squaramide O(1)	446	526	80

to rotation of the three molecules are 14.9, 8.8, and 9.9 kcal/mol, respectively. On the basis of these data, discuss the extent of resonance interaction in each compound.